



Durham E-Theses

Enol intermediates derived from carboxylic acids, esters and amides

Eberlin, Alex R.

How to cite:

Eberlin, Alex R. (1995) *Enol intermediates derived from carboxylic acids, esters and amides*, Durham theses, Durham University. Available at Durham E-Theses Online: <http://etheses.dur.ac.uk/5282/>

Use policy

The full-text may be used and/or reproduced, and given to third parties in any format or medium, without prior permission or charge, for personal research or study, educational, or not-for-profit purposes provided that:

- a full bibliographic reference is made to the original source
- a [link](#) is made to the metadata record in Durham E-Theses
- the full-text is not changed in any way

The full-text must not be sold in any format or medium without the formal permission of the copyright holders.

Please consult the [full Durham E-Theses policy](#) for further details.

Enol Intermediates Derived From Carboxylic Acids, Esters And Amides

by

Alex.R.Eberlin, B.Sc. (Dunelm)

Graduate Society

The copyright of this thesis rests with the author.
No quotation from it should be published without
his prior written consent and information derived
from it should be acknowledged.

A thesis submitted for the degree of Doctor of Philosophy in the
Department of Chemistry, University of Durham

October 1995



- 6 DEC 1995

Enol intermediates derived from carboxylic acids esters and amides

by Alex.R.Eberlin

A thesis submitted for the degree of Doctor of Philosophy in the Department of Chemistry, University of Durham, October 1995

ABSTRACT

A kinetic investigation into the enolisation mechanism and enol contents of simple carboxylic acids, esters and amides has been undertaken. Measurement of the enolisation rate constants for malonic acid, ethylhydrogenmalonate and 2-carboxyacetamide were obtained. The halogenation reactions were carried out under conditions where the rate determining step was the enolisation and the reactions were zero order in halogen. The measurements were carried out using u.v./visible spectrophotometry. Results obtained for malonic acid and ethylhydrogenmalonate support the idea of an intramolecular acid catalysed mechanism involving a hydrogen bonded six membered transition state. The enolisation mechanisms were investigated in a number of buffer solutions and were found to be catalysed by general bases. Catalytic coefficients for the following bases were calculated, $\text{HO}_2\text{CCH}_2\text{CO}_2^-$, $\text{EtO}_2\text{CCH}_2\text{CO}_2^-$, $\text{ClCH}_2\text{CO}_2^-$, and H_2O .

Deuterium exchange reactions were monitored using ^1H N.M.R. and enolisation rate constants for cyano-containing esters and amides were calculated. The results show that the enolisation of amides occurs via an acid catalysed process whereas the enolisation of carboxylic acids and esters proceeds by an intramolecular acid catalysed or a general base catalysed mechanism.

Enol contents for simple carboxylic acid derivatives were determined from their reactions with halogens under conditions where the reaction of the halogen with the enol is rate limiting and the reaction is found to be first order in the halogen. It was demonstrated that chlorine, bromine and iodine react with carboxylic ester enols at or very close to the diffusion controlled limit (*ca* $5 \times 10^9 \text{ l mol}^{-1} \text{ sec}^{-1}$). The enol contents measured were found to be greater than expected, with the enol content of malonic acid very similar to that of acetone. An estimate of the acidity of carboxylic acid enols has shown them to be strong acids with pK_a values in the region 2-5.

ACKNOWLEDGEMENTS

I would like to thank my supervisor, Prof. D.L.H. Williams for all his guidance, support and encouragement he has given me throughout my period of study.

I am exceedingly grateful to all my co-workers; Simon, Andy, Ian, Helen, Sahab, Gaynor, Rachel, John, Jonathan, Tim, Jav, Ling, and Ana who have made the last three years so enjoyable. Special thanks to Colin Greenhalgh for all his help in maintaining the machines.

Finally I would like to thank EPSRC for funding this work.

DECLARATION

The material submitted in this thesis is the result of research carried out in the department of chemistry, University of Durham between October 1992 and October 1995. It has not been submitted for any other degree and is the authors own work, except where acknowledged by references.

STATEMENT OF COPYRIGHT

The copyright of this thesis lies with the author. No quotation from it should be published without his prior written consent and information derived from it should be acknowledged.

CONTENTS

	page
Chapter1: Introduction	1
1.1 Simple enols	2
1.1.1 Structure	2
1.1.2 Geometry of simple enols	5
1.1.3 Enol contents of simple carbonyl compounds	8
1.2 Stable and isolable enols	14
1.2.1 β -Dicarbonyl compounds	14
1.2.2 Fusons enols	16
1.2.3 Fluorine stabilised enols	20
1.3 Enolisation and ketonisation mechanisms	21
1.3.1 Acid catalysis	21
1.3.2 Base catalysis	25
1.3.3 Concerted catalysis	28
1.4 Reactions of enols	29
1.4.1 Halogenation	30
1.4.2 Nitrosation	31
1.5 Enols of carboxylic acids and derivatives	32
References	38
CHAPTER 2: Halogenation of malonic acid	45
2.1 Introduction	46
2.2 Zero order kinetics	47

	page
2.3 Base catalysis	62
2.4 First order halogenation	70
references	77
CHAPTER 3 Halogenation and deuterium exchange	
studies of α-cyanoethylacetate:	78
3.1 Introduction	79
3.2 Halogenation of α -cyanoethylacetate	80
3.3 Discussion	94
3.4 Deuterium exchange in α -cyanoethylacetate	99
3.4.1 Introduction	99
3.4.2 Results	100
references	112
CHAPTER 4 Halogenation of ethylhydrogenmalonate	113
4.1 Introduction	114
4.2 Results	115
4.2.1 Zero order kinetics	115
4.2.2 First order kinetics	127
4.3 Discussion	132
references	136

	Page
CHAPTER 5 Enolisation studies of amides	137
5.1 Introduction	138
5.2 Halogenation of cyanoacetamide	140
5.2.1 First order kinetics	141
5.2.2 Zero order kinetics	148
5.2.3 deuterium exchange	152
5.3 Enolisation of malonamide	161
5.3.1 Iodination in chloroacetic acid buffers	161
5.3.2 Metal ion catalysis	165
5.4 Enolisation of malonamic acid	167
5.4.1 Kinetic results	167
5.5 Discussion and results summary	173
references	182
CHAPTER 6 Experimental details	184
6.1 U.V./Visible spectrophotometry	185
6.2 Stopped flow spectrophotometry	186
6.3 Kinetic analysis	188
6.3.1 First order kinetics	188
6.3.2 Zero order kinetics	190
6.3.3 Sequential kinetics	192
6.4 N.M.R. spectroscopy	194

	Page
6.5 pH measurements	195
6.6 Diffusion controlled reactions	196
6.7 Synthesis of malonamic acid	197
Appendix	200
A.1 First year induction course	201
A.2 Research colloquia, seminars and lectures	202
A.3 Conferences attended	208

Chapter 1

Introduction

1.1 Simple Enols

1.1.1 Structure.

Simple enols are commonly defined as "substances in which the enol is the only functional group in the molecule, and the keto tautomer is a mono carbonyl compound". This definition is widely used in the literature to discriminate between the large number of other enols which are stabilised by special features (see section 1.2).

The simplest enol known is that formed from acetaldehyde. see Fig 1.



Figure 1

Vinyl alcohol

Vinyl alcohol was first proposed as a reactive intermediate over a hundred years ago by Erlenmeyer¹ who studied the hydrolysis of propenyl halides², and the dehydration of vic- glycols (1,2- diols). The instability (relative to the keto form) of vinyl alcohol ensured that it was only identified experimentally in the seventies by the photolysis of acetoin^{3,4} (3-hydroxy-2-butanone). See Fig 2.

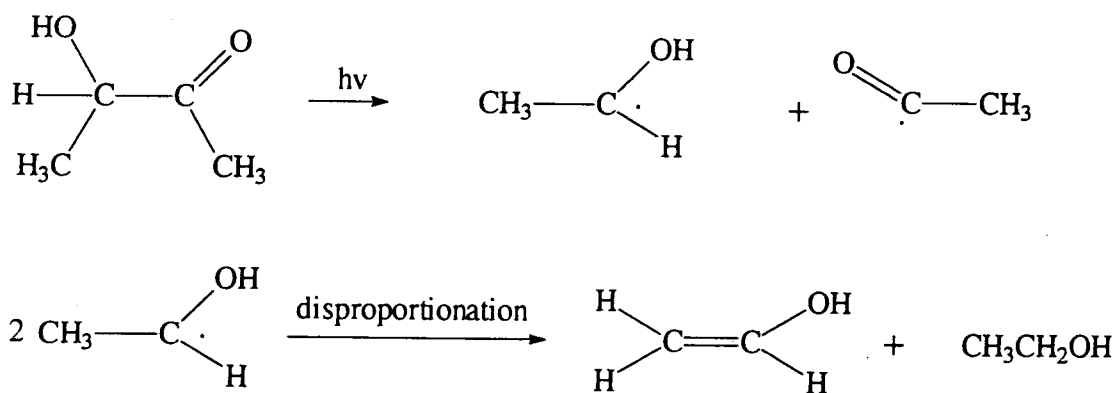


Figure 2

Vinyl alcohol is the simplest enol possible, and consequently has been the starting point for many theoretical investigations^{7,8,9} into enol stability. Heinrich⁵ *et al* have investigated the effect of a wide range of substituents on the carbonyl and enol moieties and have calculated keto/enol energy differences in many compounds. see Fig 3.

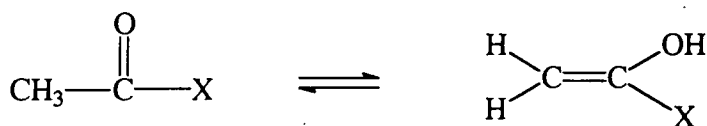
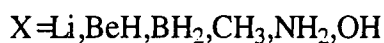


Figure 3



Ventura⁶ *et al* have carried out theoretical studies on the gas phase and solution phase mechanisms of ketonisation of vinyl alcohol (see section 1.3).

The structure of vinyl alcohol has been calculated many times. The most recent calculation (using the most extensive basis sets) is that carried out by Apeloig, Arad and Rappoport¹⁰. Vinyl alcohol is essentially a planar molecule and the most stable conformation is the syn conformation with the OH eclipsing the double bond.

See Fig 4.

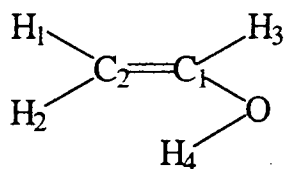


Figure 4

Table 1 shows the optimised geometries obtained from the latest calculations using the most extensive basis set.

Table 1

Bond	Bond distance (Å)	Bond angle	bond angle (deg)
C1=C2	1.335	C1—C2—H1	119.9
C1—O	1.365	C1—C2—H2	122.1
C2—H1	1.076	C2—C1—H3	122.7
C2—H2	1.082	C2—C1—O	126.8
C1—H3	1.080	H4—O—C1	108.1
O—H4	0.966		

The structure of vinyl alcohol has also been determined by microwave spectroscopy^{11,12}. The results obtained are very similar to the theoretical calculations and concur with the general features of planar geometry and a stable syn conformation.

Theoretical calculations on more complicated enols are restricted to alkyl substitution. A large number of ab-initio and empirical calculations have been carried out on the enol formed from acetone^{8,10,13,14} (propen-2-ol), again the results are very similar to those of vinyl alcohol, an essentially planar geometry with a stable syn conformation. Apeloig and co-workers¹⁰ have made an extensive study of a series of alkyl substituted enols, see Fig 5, and have investigated the relative stabilities of the cis and trans forms.

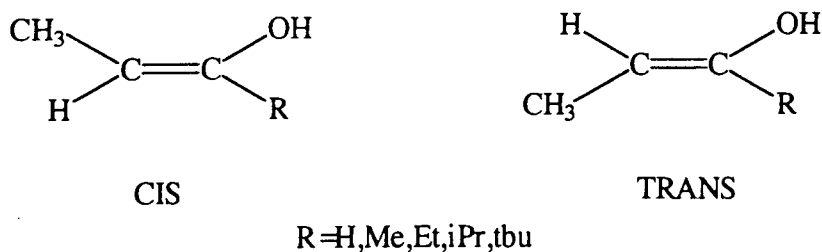


Figure 5

1.1.2 Generation of simple enols

Theoretical^{15,16} and experimental^{3,4} studies have shown that in the gas phase the intramolecular rearrangement of vinyl alcohol to acetaldehyde is very slow, and consequently simple enols generated in the gas phase don't rapidly tautomerise to the keto form. Vinyl alcohol can be generated in the gas phase^{4,12} by the pyrolysis of ethylene glycol ((1,2-ethanediol) at 700°C–1000°C and 0.02 -0.04 torr. See Fig 6.

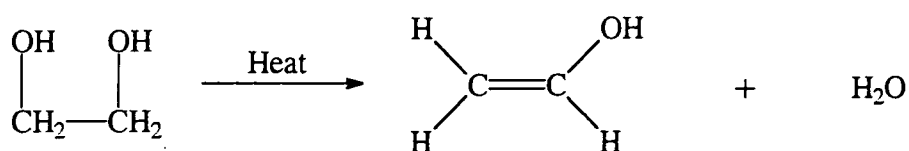


Figure 6

Vinyl alcohol can also be generated from cyclobutanol^{18,19} under similar conditions. See Fig 7.

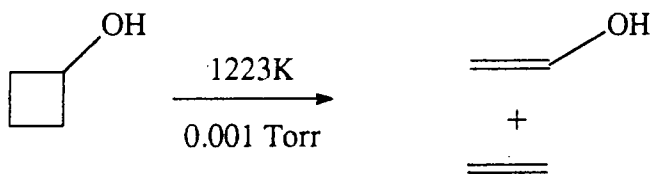


Figure 7

Under these conditions the half life of vinyl alcohol is approximately 20 secs.

More recently Turecek²⁰⁻²⁷ has developed a method of generating enols from the pyrolysis of Diels Alder adducts. See Fig 8.

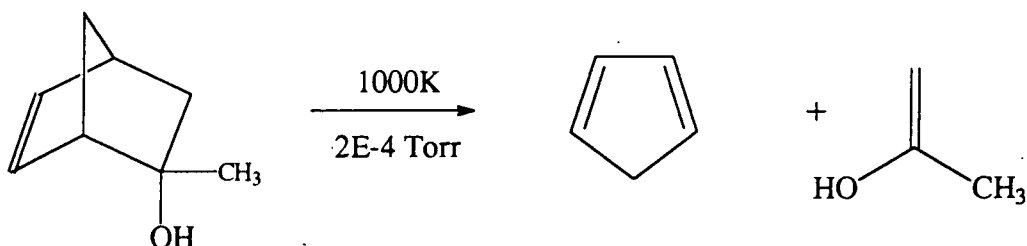


Figure 8

The enols produced are analysed by mass spectrometry and this method has been used to calculate heats of formation of enols²²⁻²⁵. Simple enols have also been generated at low temperatures by the thermolysis of anthracene derivatives²⁸.

See Fig 9.

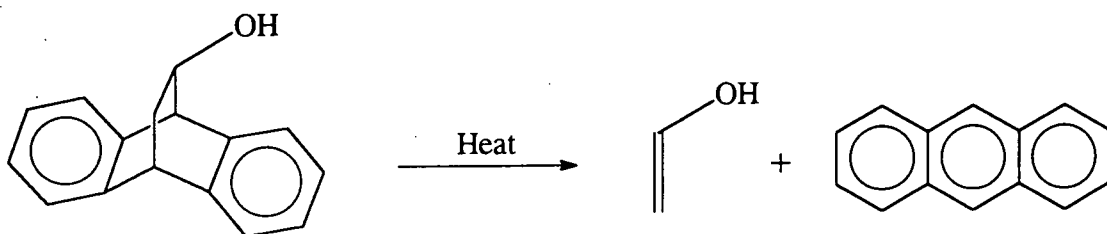
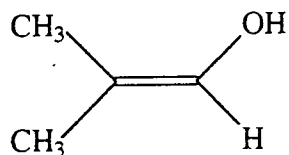


Figure 9

The enols produced are trapped in an inert matrix (CFCl_3 or CD_2Cl_2) at -100°C . The stability of the enols (in hexane) were measured by U.V.-VIS spectrophotometry²⁹. Some of the enols generated show a remarkable stability. See Fig 10.



Half life = 19 hours (276K in Hexane)

Figure 10

As well as thermochemical methods, photochemical methods have been used to generate simple enols. This was first carried out by Mc Millan and co-workers³⁰ who generated propen-2-ol (acetone enol) by the irradiation of 2-pentanone. See Fig 11.

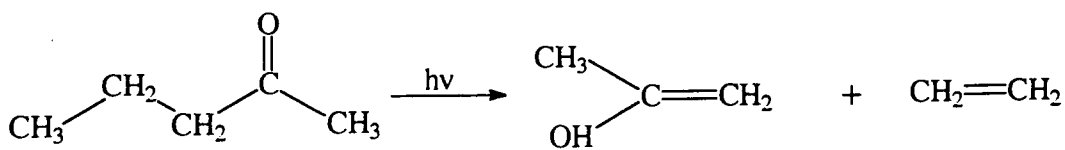


Figure 11

Generation of the enol occurs via a NORRISH Type 2 process. This technique is best suited to aromatic ketones and has been used to generate a series of enols derived from acetophenone derivatives^{31,32}.

Recently enols have been generated by flash photolysis and detected by U.V. spectrophotometry³³.

Kresge and co-workers³⁴⁻³⁷ have used this technique to measure the kinetics of ketonisation of simple enols, and have developed a method for the determination of keto enol equilibrium constants (see section 1.1.3).

The previous methods described for the formation of enols all suffer from a number of drawbacks, primarily that only very low concentrations can be produced and many are only observed fleetingly in mass spectrometers.

Precursors that produce enols faster than they reketonise have been used to produce higher concentrations of enols. Steinberger and Westheimer³⁸ showed that decarboxylation of dimethyloxalacetic acid produces enols. See Fig 12.

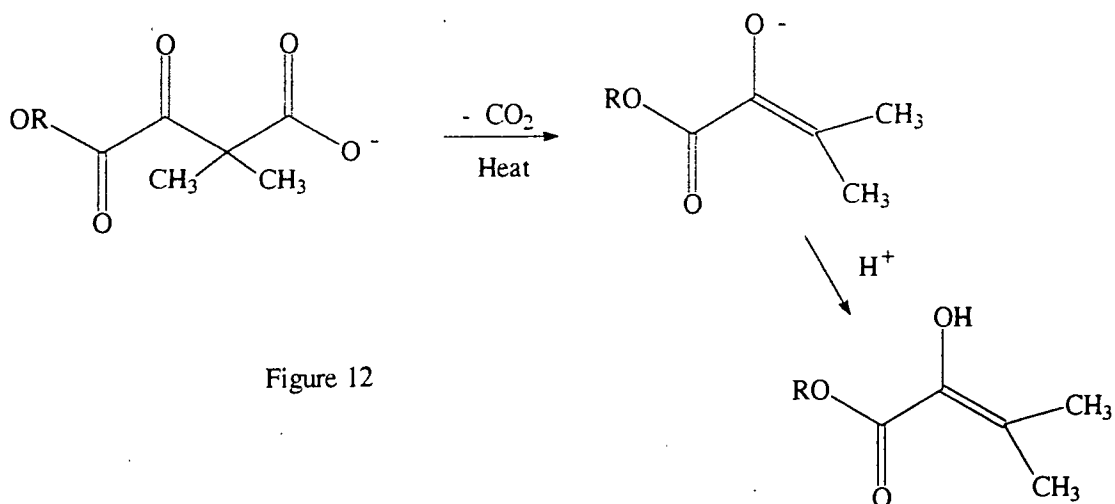


Figure 12

which can be detected by U.V.-VIS Spectrophotometry. Capon et al⁴²⁻⁴⁴ have used a series of substituted and protected enol ethers. Vinyl alcohol is formed from the hydrolysis of methoxyvinylmethyl chloroacetate. See Fig 13.

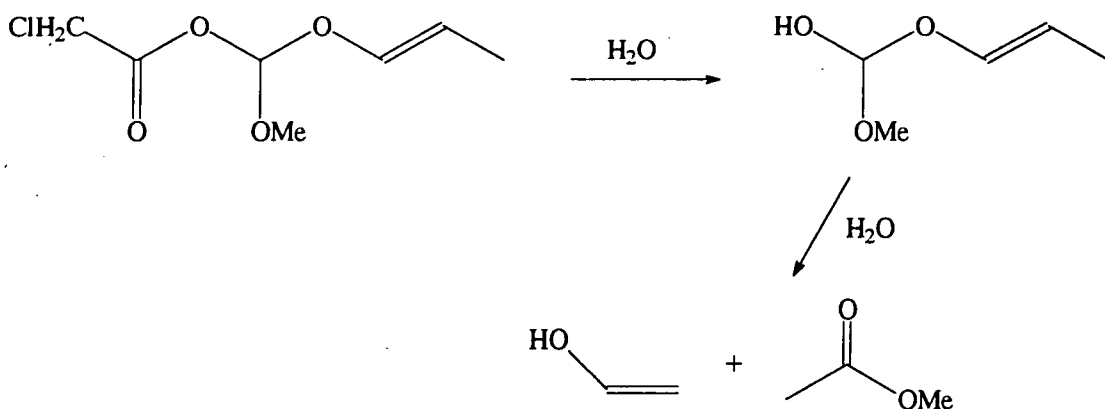


Figure 13

Desilylation of trimethylsilyl ethers using fluoride ion⁴⁰ has been used to generate enols. This methodology has been developed by Hegarty for the formation of carboxylic acid enols (see section 1.5.2).

O-protonation of enolate anions has been used to generate enols,³⁹⁻⁴¹ again this method is only successful if the rate of protonation greatly exceeds that of ketonisation. Usually the enolate anion is generated in an aprotic solvent (CH₃CN, THF) and is added in very small quantities to a buffered acid solution. This technique is limited by the mixing time. The enol of isobutyraldehyde was generated in aqueous buffers by protonation of its enolate anion⁴⁰ (generated in THF). See Fig 14.

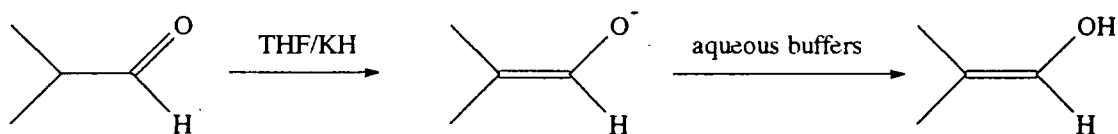


Figure 14

1.1.3 Enol contents of Simple carbonyl compounds

The determination of keto \rightleftharpoons enol equilibrium constant, K_E . (See Fig15) has been



Figure 15

has been at the centre of physical organic chemistry for many years. Measurement of enol contents in the solution phase have centered around the halogen titration method^{45,46} developed by Meyer in 1912. This technique involves reacting the carbonyl compound with a halogen (usually bromine or iodine) and equating the amount of halogen uptake to the amount of enol present. Throughout the 20th century modifications and improvements to this technique have been developed:

- 1) Schwarzenbach^{47,48} used a flow method and potentiometric measurement of Br₂ uptake.
- 2) Gero⁴⁹ used a mixed halogen species (ICl) instead of bromine.
- 3) Walisch and Dubois⁵⁰ used a coulopotentiometric method in which Br₂ is formed from electrolysis of a bromide solution.
- 4) Dubois and Barbier⁵¹ titrated enols by amperometry.

All of the above techniques, which were used up until the seventies suffer from serious experimental problems, these are primarily:

- a) The halogens are very reactive electrophiles and will react with many nucleophilic compounds, consequently it is very important that the compound being studied is present in high purity. Also in the case of simple carbonyl compounds the changes in halogen concentration are very small (due to the small enol contents) and are effected by any small impurity.
- b) The end point of the titration is often not very sharp due to the auto-catalytic nature of the reaction. The hydrogen bromide generated in the reaction acts as a catalyst in the enolisation process thus producing more enol. See Fig16.



Figure 16

- c) If the carbonyl compound has more than one enolisable hydrogen atom then multihalogenation can occur resulting in an over estimation of the enol content. This

can be a common problem because the mono-halogen compounds are usually more reactive than the parent compound.

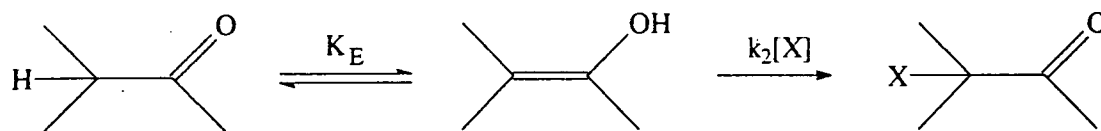
All these problems tend to lead to an over estimation of the enol contents for simple carbonyl compounds. In the seventies it was realised that many attempts to measure enol contents of simple carbonyl compounds had failed and many values reported in the literature were orders of magnitude too high^{52,53}. Accurate K_E values can only be obtained for compounds with relatively large enol contents ($K_E > 1 \times 10^{-4}$) such as β -diketones and β -ketoesters.

Since the seventies three methods have been developed to measure small K_E values, these are:

- 1) Kinetic halogenation method.
- 2) Approximation from rates of hydrolysis of vinyl ethers.
- 3) Determination of individual enolisation and ketonisation rate constants.

1. Kinetic halogenation method.

This technique was developed by Toulllec and co-workers⁵²⁻⁵⁴ in the 1970's. Enols react rapidly with a range of electrophiles (see section 1.4) see Scheme 1.



Scheme 1

X=halogen

Usually the first step (enolisation) in scheme 1 is rate limiting and the reaction is zero order with respect to the halogen. However, using low halogen concentrations and/or high buffer and acid concentrations reaction of the electrophile with the enol can become rate limiting and the reaction shows a first order dependency on the electrophile (halogen). Zucker and Hammett⁵⁵ observed that the rate of iodination of acetophenone becomes dependent on the iodine in 50% H_2SO_4 . When reaction of the enol is rate limiting the following rate equation applies. See equation 1.

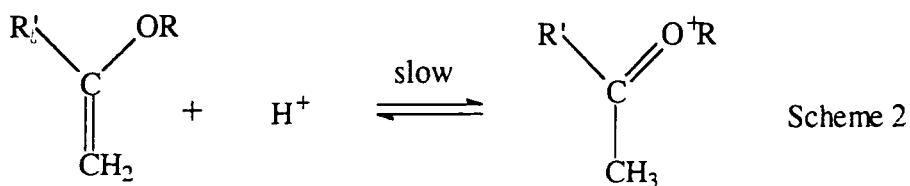
$$\text{Rate} = K_E k_2 [X][\text{Substrate}]$$

Equation 1

Under these conditions the second order rate constant is the product of the keto \rightleftharpoons enol equilibrium constant (K_E) and the micro-molecular rate constant (k_2) for attack of the halogen on the enol. The micro-molecular rate constant for attack of the halogen on the enol has been shown to be very close to the diffusion controlled limit⁵⁶ i.e.) $k_2 = 5 \times 10^9 \text{ l mol}^{-1} \text{ sec}^{-1}$. Knowing the value of k_2 allows an estimation of the K_E value. Table 2 (page 13) shows K_E values determined by this method.

2) Hydrolysis of vinyl ethers.

Hydrolysis of vinyl ethers is known to occur via a similar mechanism to ketonisation of enols. i.e. via slow protonation at the β carbon atom. See Scheme 2.



If the rate constant for hydrolysis of vinyl ethers is taken to be equal to the rate of ketonisation then these can be combined with known rates of enolisation to determine keto \rightleftharpoons enol equilibrium constants⁵⁹ (the keto \rightleftharpoons enol equilibrium constant is simply the ratio of the acid catalysed enolisation and acid catalysed ketonisation rate constants). See equation 2.

$$K_E = \frac{k_e^{\text{H}^+}}{k_{\text{hyd}}^{\text{H}^+}} \quad \text{Equation 2}$$

This method is dependent on the equality of the hydrolysis and ketonisation rate constants. In most cases it has been shown that this is not the case because the OH is better able to stabilise the partial positive charge developed in the transition state than the OR group; consequently rates of enolisation are faster than the corresponding rate

of ether hydrolysis. Some K_E values determined by this method are shown in table 2 (see page 13).

3 Determination of individual enolisation and ketonisation rate constant.

Very recently a new technique has been developed by Kresge and Wirz⁶⁰⁻⁶⁵ for the accurate determination of K_E values that do not rely on any assumptions or approximations. Rates of ketonisation of enols can be measured if the enol can be generated in the absence of the carbonyl tautomer. These rates of ketonisation can be combined with known enolisation rate constants to obtain accurate keto \rightleftharpoons enol equilibrium constants. Kresge *et al* have developed flash photolysis techniques⁶³ for the generation of simple enols under conditions in which the enols are stable and the ketonisation kinetics can be measured. Three basic methods have been used:

- 1) Norrish type 2 reactions (see page 5)
- 2) Photo-oxidation of alcohols⁶⁴. See Fig 17.

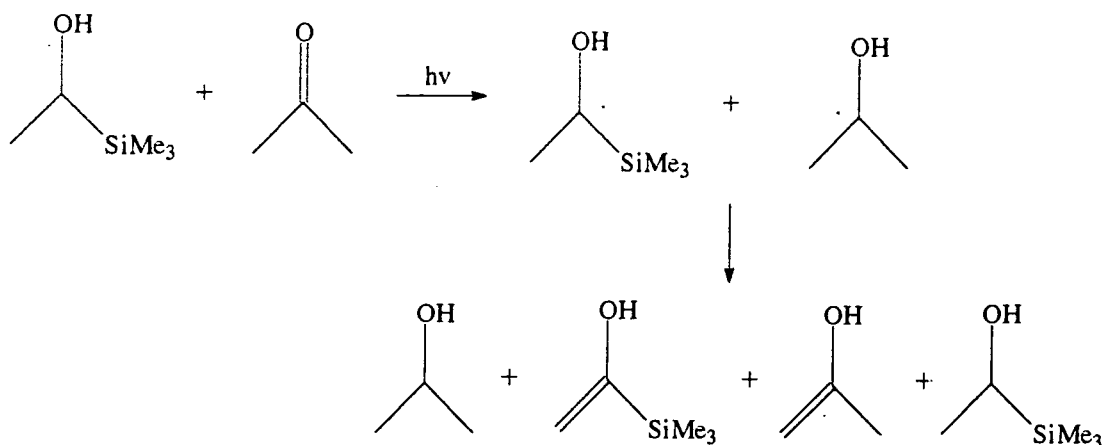


Figure 17

3) Photohydrolysis of vinyl chlorides⁶⁵. See Fig 18.

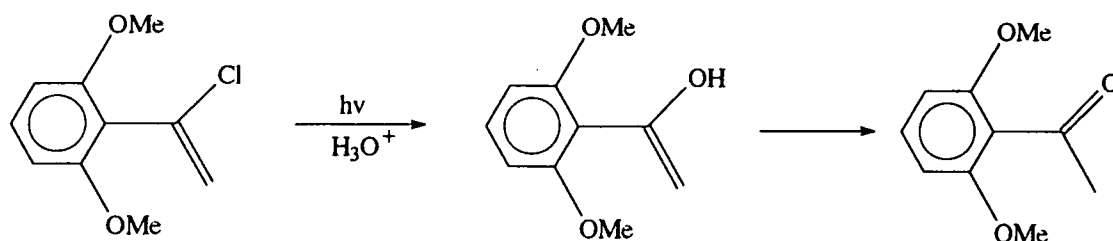


Figure 18

Table 2 shows a comparison between keto \rightleftharpoons enol equilibrium constants determined by the different methods.

Table 2

	pK_E	pK_E	pK_E
Compound	2. comparison with enol ethers	1. kinetic halogenation method	3. direct kinetic determination
ethanal	4.66 (ref 59)		6.23 (ref 37)
acetone	7.02 (ref 59)	8.22 (ref 66)	8.33 (ref 36)
pentan-3-one		7.44 (ref 66)	7.43 (ref 36)

The table shows that there is good agreement between the K_E values determined by the kinetic halogenation method and the direct kinetic method. (methods 1 and 3) This shows that the assumption made in the kinetic halogenation method i.e. that halogenation of the enols occurs at the diffusion controlled limit is valid. The results show that acetone has a smaller enol content than ethanal, approximately 100 times smaller. This has been attributed to the stabilisation of the keto isomer in the case of

acetone by the strong electron donating ability of the methyl group which interacts with the large carbonyl dipole. It is generally observed that the enol contents of aldehydes are larger than those of the corresponding methyl ketone.

The enol content of pentan-3-one is an order of magnitude larger than that of acetone. This increase is due to the hyperconjugative stabilisation by the methyl groups in the enol of pentan-3-one. This is very similar to the hyperconjugation observed in the stability of alkenes^{67,68}.

1.2 Stable and isolable enols

1.2.1 β -Dicarbonyl compounds

β -dicarbonyl compounds⁴⁶ are one of the most widely studied class of compounds in chemistry. In many cases the enol tautomer is the major tautomer and is present in large enough concentrations for it to be determined by conventional spectroscopic methods such as N.M.R., I.R. and U.V.. β -Dicarbonyl enols are stabilised by an intramolecular H-bond which accounts for the exceptionally large enol content, e.g. acetylacetone. See Fig 19.

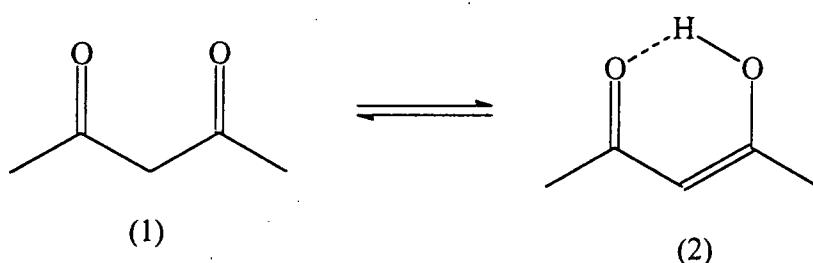


Figure 19

A large number of N.M.R. studies on acetylacetone^{69,70} have shown that the six membered ring structure (2) is the most stable conformation and that the hydrogen bond is not symmetrical but has a double minimum potential⁶⁹. The enol contents^{71,72} of many β -dicarbonyl compounds have been determined in a variety of solvents. Table 3 shows results obtained for acetylacetone and ethylacetoacetate.

Table 3

Acetylacetone		ethylacetoacetate	
Solvent	% enol	solvent	% enol
neat	80 (ref 72)	neat	
H ₂ O	13 (ref 71)	H ₂ O	0.5 (ref 73)
Et ₂ O	92 (ref 71)	Et ₂ O	35 (ref 72)
CCl ₄	95 (ref 71)	CCl ₄	37 (ref 72)
CH ₃ CN	53 (ref 71)	CH ₃ CN	5.8 (ref 74)

These results indicate a general trend for all enols: enol contents are higher in low polarity solvents. This is attributed to the destabilisation of the highly polar carbonyl moiety ($\mu = 3.62D$ for the carbonyl form of acetylacetone⁷⁵). The enol content is also increased in good hydrogen-bond acceptor solvents⁷⁶ eg. DMSO due to strong hydrogen bond stabilisation of the enol moiety. In some cases^{77,78} it is possible for the intramolecular structure to break open and form an intermolecular hydrogen bond. See Fig 20.

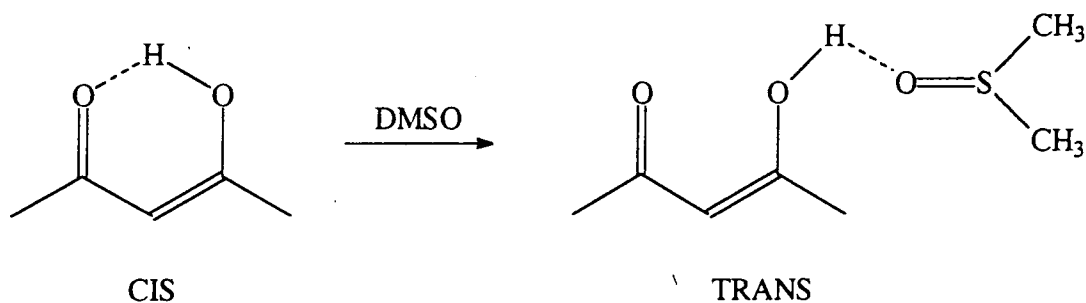


Figure 20

The ability of 1,3-dicarbonyl compounds to form a six membered ring is not a prerequisite for the existence of stable enols. Dimedone (5,5-dimethyl-1,3-cyclohexanedione) and tetronic acid (tetrahydrofuran-2,4-dione) which cannot form a six membered ring have very high enol contents. See Fig 21.

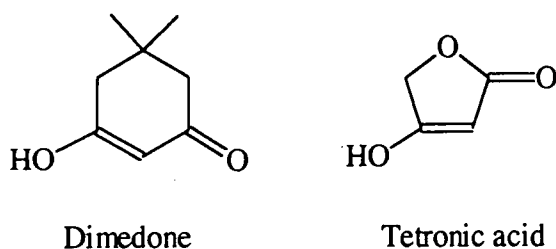


Figure 21

Dimedone exists almost completely in the enol form in aqueous solution (93% enol).¹²⁶

1.2.2 Fuson's Enols

The name Fuson's enol is derived from the work of R.C. Fuson who exploited the fact that bulky aromatic groups, e.g. 2,4,6-trimethylphenyl (mesityl), could be used to stabilise enols. In the 1940's Fuson synthesised and characterised a number of stable aryl substituted enols. The first enol of this type prepared^{79,80} was 1,2-dimesitylpropen-1-ol, which was synthesised from the corresponding enone by a 1,4 addition of hydrogen. See Fig 22.

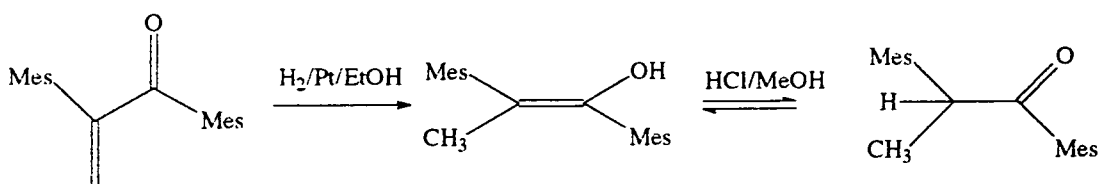
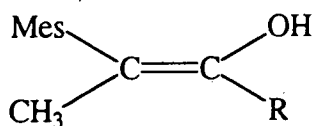


Figure 22

Mes = 2,4,6-trimethylphenyl

The enol formed was characterised by I.R. ($\nu_{OH} = 3623 \text{ cm}^{-1}$). The enol is very stable and can only be converted to the keto form by refluxing with HCl in methanol. Fuson developed this synthetic procedure to prepare a range of alkyl substituted enols^{81,82}. See Fig 23.



R =Dur (2,3,4,6-tetramethylphenyl)
 R =IDur (2,3,5,6-tetramethylphenyl)

Figure 23

Aryl substituted enols have also been prepared by a variety of methods:

a) Acid catalysed rearrangement of 1,2-diols^{83,84}.

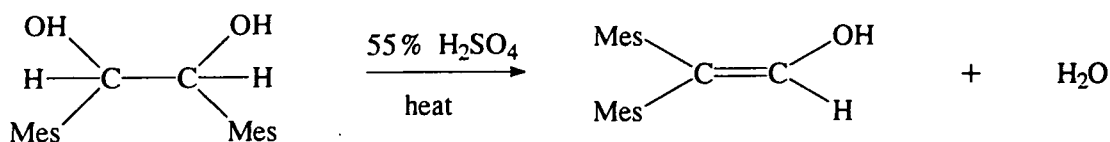


Figure 24

b) Ozonolysis Of 1,1-diarylethene⁸⁵.

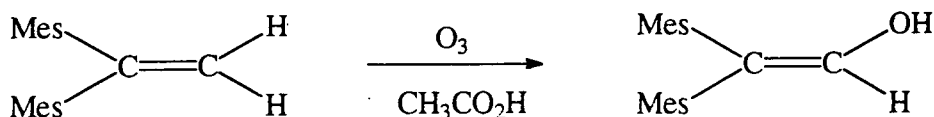


Figure 25

c) Grignard addition to ketenes⁸⁶.

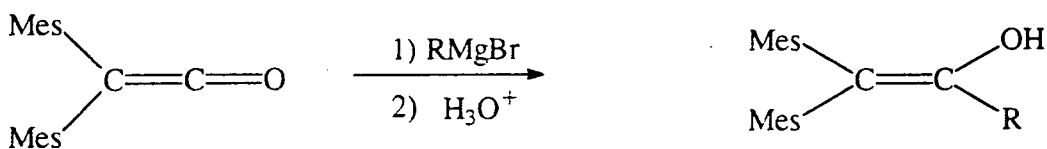


Figure 26

Recently, Rappoport⁸⁷ has extended the work of Fuson and has developed new synthetic routes to stable enols and has measured keto \rightleftharpoons enol equilibrium constants for many compounds as well as investigating the structures of these interesting compounds. In the case of aryl substituted enols the enol contents are sufficiently high for direct measurement of the two isomers by conventional spectroscopic methods. Often, the more highly conjugated enol is coloured and the reaction can easily be monitored by U.V./VIS spectrophotometry eg) 2-triisopropyl-1-acenaphthynol where the enol is an orange colour (in DMSO). See Fig 27.

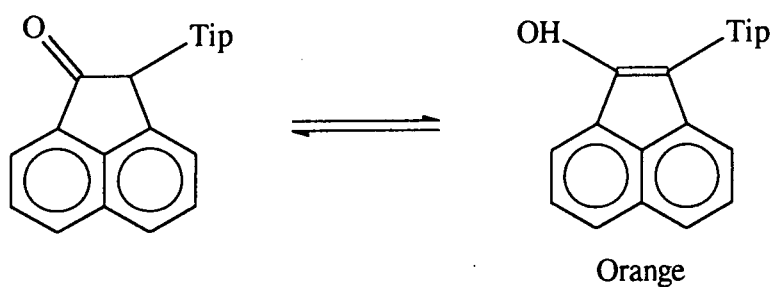


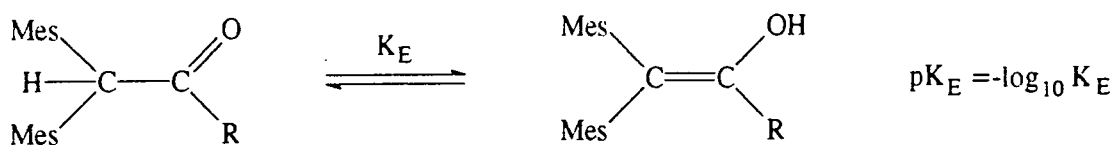
Figure 27

Tip = 2,4,6-tri-isopropylphenyl

The keto \rightleftharpoons enol equilibrium constant for the above compound has been determined in a number of solvents⁸⁸. As expected the enol content increases with the hydrogen bond accepting ability of the solvent. Enol contents (K_E values) are shown in brackets.

DMSO (2.6) > DMF (1.0) > EtOH (0.25) > HOAc (0.17) > n-Hexane (0.004)

This trend is due to the strong hydrogen bonding in these systems. Enol contents for a series of alkyl substituted dimesityl compounds⁸⁹ have been determined by N.M.R. spectroscopy. See Scheme 3.



$$pK_E = -\log_{10} K_E$$

Scheme 3

Table 4 shows the results obtained.

Table 4

R	pK_E	K_E
H	-1.30	20.0
Me	0.20	0.63
Et	0.50	0.32
iPr	0.55	0.28
tBu	2.22	0.006

The results show that the enol content decreases with increasing steric bulk. This effect is due to the interaction of the alkyl groups with the ortho-methyl groups of the mesityl group. With increasing bulk of the alkyl group the mesityl groups are forced out of the plane of the double bond resulting in decreased resonance stability in the enol form. The importance of co-planarity of the aromatic groups has been demonstrated by the high enol content ($K_E = 17$)⁹² for 9-hydroxymethylenefluorene enol which has enforced co-planarity of the phenyl rings. See Fig 28.

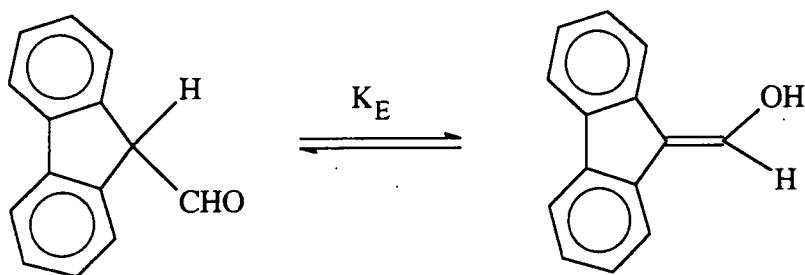


Figure 28

The crystal structures of Fuson's enols have been investigated by Rappoport and Co-workers. They have reported ¹³C and ¹⁷O N.M.R. data⁹⁵ and X-ray crystallographic data. All the results show that the lowest energy conformation is that of a molecular propellor with the two β -aryl groups twisted out of the plane of the double bond. Torsional angles of 55.7° and 57.5° (for 2,2-dimesityl-1-methylethene-1-ol) have been reported⁹⁰ for the orientation of the two mesityl rings relative to the double bond.

An additional effect is that commonly observed for simple enols, that stabilisation of the carbonyl group by 1-alkyl substituents lowers the enol content.

The effect of substituents in the aromatic ring has been investigated by Albrecht⁹¹ *et al.* See Fig 29.

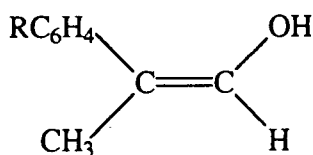


Figure 29

A good correlation of pK_E with σ^- is observed which suggests a significant contribution from a charge separated canonical form. See Fig 30.

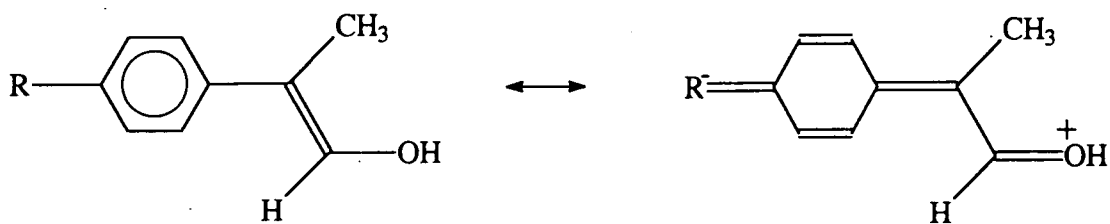


Figure 30

1.2.3 Fluorine stabilised enols

The presence of fluorine atoms in a molecule can have an enormous effect on stability. As stated earlier the enol of acetone is very unstable and can only be prepared under special conditions, conversely the enol of pentafluoroacetone⁹⁶ is a stable distillable liquid (bp=54°C) which can be stored at room temperature. The enol is only converted to its keto isomer when heated to 180°C . Pentafluoroacetone can easily be prepared by the acid catalysed hydrolysis of the corresponding enol phosphate. See Fig 31.

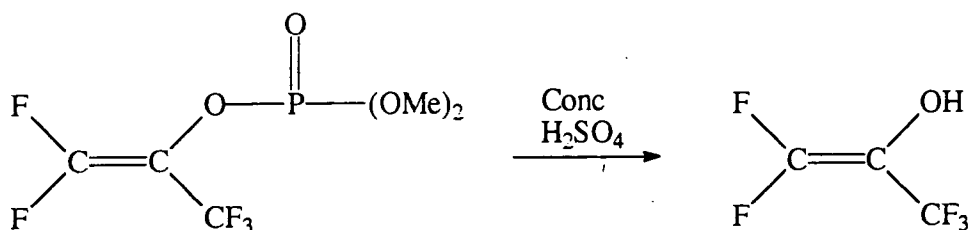


Figure 31

The stability of the enol of pentafluoroacetone has been attributed to stabilisation of the enol¹³ although no explanation is advanced. It may be expected that the trifluoromethyl group will destabilise the carbonyl compound by unfavourable interactions with the polar carbonyl group thus increasing the stability of the enol.

Other stable perfluorinated enols are known; pefluorocyclobutenol and perfluorocyclohexene-1-ol can easily be prepared from the corresponding benzyl ether by hydrolysis. See Fig 32.

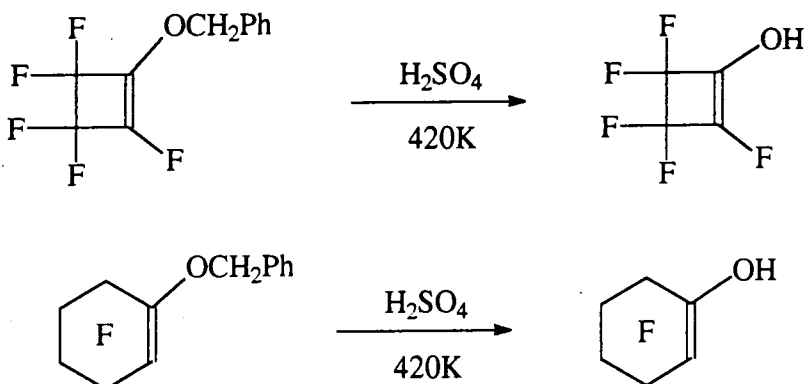


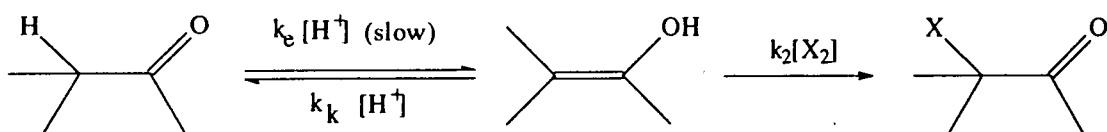
Figure 32

Both these enols are stable, distillable compounds that are stable in acid solutions. No direct measurements of K_E values have been reported for these enols so an indication of the thermodynamic stability of these perfluoro enols is not known. The fact that the enols are converted very slowly to their corresponding carbonyl compounds confirms their kinetic stability. The kinetic stability is due to the deactivation of the double bond by the strongly electron withdrawing fluorine atoms which prevent protonation of the enol. Ketonisation of the enol could also take place via the enolate anion but again the anion formed is very unstable due to the unfavourable interactions with the lone pairs on the fluorine atoms.

1.3 Enolisation and Ketonisation mechanisms.

1.3.1 Acid Catalysis.

Rate constants for acid catalysed enolisation have traditionally been determined by halogenation reactions where the rate limiting step is the enolisation of the carbonyl compound. See Scheme 4.



Scheme 4

A simple steady state treatment (with the enol as the reactive intermediate) on scheme 4 gives the following rate equation.

$$\text{Rate} = \frac{k_2 k_e [\text{H}^+] [\text{X}_2] [\text{Substrate}]}{k_k [\text{H}^+] + k_2 [\text{X}_2]}$$

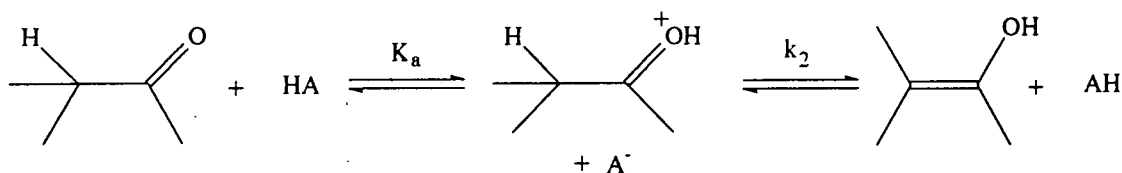
Under conditions in which the rate of halogenation of the enol ($k_2[\text{X}_2]$) is much faster than the rate of ketonisation of the enol ($k_k[\text{H}^+]$) the rate law simplifies to the following.

$$\text{Rate} = k_e [\text{H}^+] [\text{Substrate}]$$

The rate determining step is now the enolisation of the carbonyl compound.

This technique has been used to establish the important mechanistic features for enolisation of carbonyl compounds.

The generally accepted mechanism for acid catalysed enolisation (see Scheme 5) was first proposed by Pederson⁹⁷ after a series of experiments by Dawson⁹⁸ and co-workers had shown that the enolisation of acetone was catalysed by general acids. See Scheme 5.



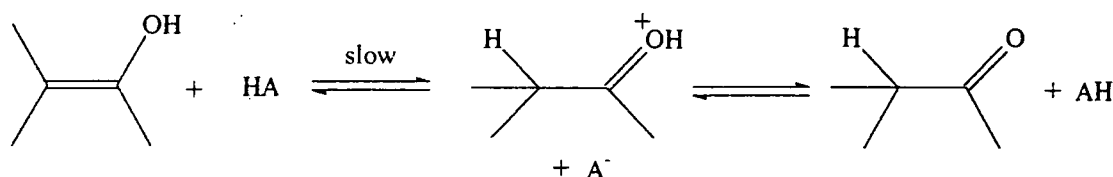
Scheme 5

Evidence for this mechanism comes from a number of sources:

Substrate isotope effects⁹⁹ observed for acetone and deuterioacetone give ($k_H/k_D = 8$) indicating that C-H bond fission is occurring in the rate determining step and that the second step in scheme 5 is rate limiting.

Inverse solvent isotope effects¹⁰⁰ are also consistent with a pre-equilibrium mechanism ($k_{H_2O}/k_{D_2O} = 0.54$ for acetone enolisation).

The principle of microscopic reversibility requires that ketonisation occurs via the same mechanism (via the same T.S.) as enolisation. Thus acid catalysed ketonisation must occur by the inverse of enolisation i.e.) rate limiting proton addition to the α -carbon atom. (See Scheme 6).



Scheme 6

Recent studies^{101,102} on the ketonisation of simple enols has shown that ketonisation does occur via rate limiting protonation of the α -carbon atom. This mechanism has also been supported by studies on the hydrolysis of vinyl ethers which occurs via a similar mechanism to that of ketonisation.

Rate constants for enolisation can easily be obtained by halogenation reactions where the rate determining step is the enolisation of the carbonyl compound. See scheme 4.

Rate constant have been determined for a variety of aliphatic and alicyclic enols.

Table 5 shows a sample of the results.

Table 5:

Compound	$k_{\text{H}^+}^{\text{enol}} / \text{l mol}^{-1} \text{sec}^{-1}$	
Acetone	2.85×10^{-5}	ref 107
acetaldehyde	1.94×10^{-5}	ref 107
acetophenone	1.63×10^{-5}	ref 107
cyclopentanone	6.06×10^{-5}	ref 107
cyclohexanone	23.4×10^{-5}	ref 107

The results show very little variation in rate constant with varying substrates. This small variation supports the two step mechanism. See scheme 5. In the two step mechanism the rate constants $k_{\text{H}^+}^{\text{enol}}$ is the product of K_a (The equilibrium constant for protonation of the carbonyl group) and k_2 (rate constant for carbon-hydrogen bond fission). Usually substituents have opposing effects on these two constants; Electron withdrawing groups increase the carbon acidity of the carbonyl compound thus increasing k_2 , but they also lower the basicity of the carbonyl oxygen, hence reducing K_a consequently the overall affect on $k_{\text{H}^+}^{\text{enol}}$ is small. Electron donating groups have the opposite effects, decreasing k_2 and increasing K_a .

General acid catalysis has been observed in many systems. Recently¹⁰⁴ an extensive study of the general acid catalysis of acetone has measured the catalytic coefficients for over fifty acidic species. For non-bulky mono carboxylic acid species an excellent linear Bronsted relationship is observed and a value of $\alpha=0.46$ is reported. This gives a value of $\beta=0.56$ for the slow proton transfer from the oxonium ion. This beta value suggests that proton transfer is approximately half complete in the transition state. See Fig 33.

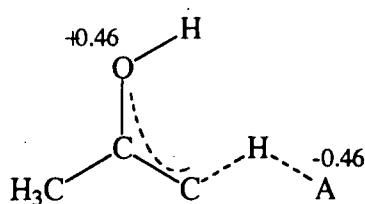
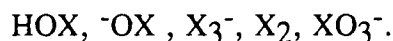


Figure 33

1.3.2 Base catalysis.

Most measurements of base catalysed enolisations are carried out in a similar way to acid catalysis, ie using halogenation reactions. However there are numerous problems associated with halogenation reactions under basic conditions.

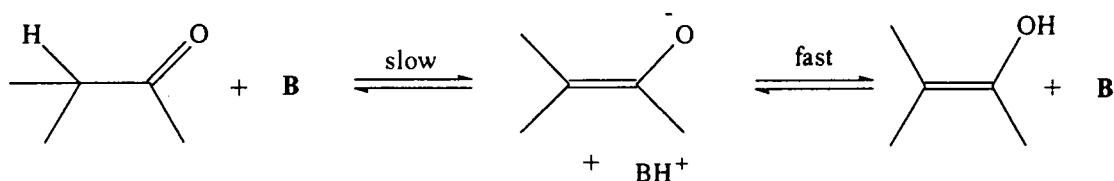
In basic solutions the halogens exist in many different forms;



The proportion in each form depends on the pH and the appropriate acidity constants.

An alternative method is to monitor the deuterium exchange or racemisation of the carbonyl compound. Deuterium exchange has been used to measure the rate of enolisation in 2-methylpropanal¹⁰⁶.

Base catalysed enolisation occurs via rate limiting proton abstraction from the α -carbon atom of the carbonyl compound, followed by rapid protonation on the oxygen of the enolate anion. See Scheme 7.

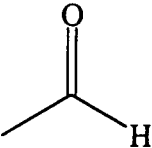
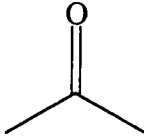
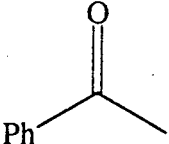


Scheme 7

Evidence for this mechanism comes from substrate isotope effects^{103,104} which show that C-H bond fission is occurring in the rate determining step. ($k_{\text{H}}/k_{\text{D}}=7$ for acetone enolisation catalysed by hydroxide.). The most commonly studied base is the hydroxide

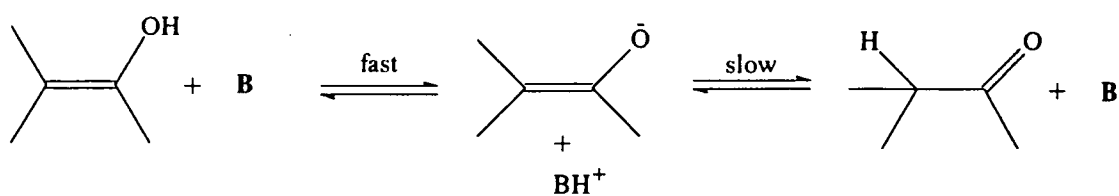
ion. Table 6 shows some results for the hydroxide catalysed enolisation of some simple carbonyl compounds.

Table 6.

Compound	$k_{\text{OH}^-} / \text{l mol}^{-1} \text{sec}^{-1}$
	1.17 (ref 36)
	0.22 (ref 35)
	0.25 (ref 35)

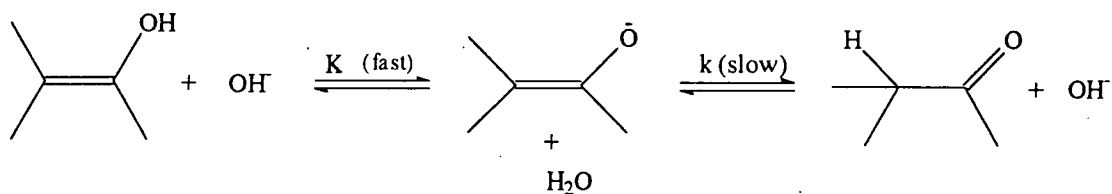
Recently Stewart *et al*¹⁰⁴ have carried out an extensive study of the base catalysed enolisation of acetone and have measured Bronsted coefficients for catalysis by a series of arylphosphate dianions. A value of $\beta=0.72$ is reported. Early work carried out on the base catalysis of acetone with carboxylate anions¹⁰⁵ gave a higher Bronsted coefficient of $\beta=0.89$. Both these values are consistent with a mechanism involving rate limiting deprotonation of the carbonyl group where the proton is about three quarters transferred in the transition state. This result is entirely expected given the very low acidity of acetone, $\text{pK}_a=20$.

In the last few years measurements³⁶ of base catalysed ketonisation of enols have shown that this reaction occurs via rate limiting protonation on the carbon of the enolate anion. See Scheme 8.



Scheme 8

Using hydroxide as the base it has been shown that C-protonation of the enolate anion is the rate determining step. See Scheme 9.



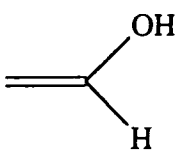
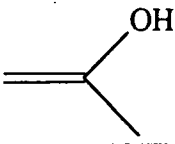
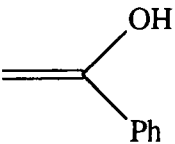
Scheme 9

The rate law for Scheme 9 is as follows.

$$\text{Rate} = \frac{Kk[\text{OH}^-][\text{ENOL}]_T}{1 + K[\text{OH}^-]}$$

This rate law predicts that at high hydroxide ion concentration the reaction will become independent of hydroxide i.e.) when all the enol is present as the enolate anion the rate determining step is simply protonation of the enolate anion by water. At low hydroxide concentration the reaction becomes first order in hydroxide and the product **Kk** can be calculated. See Table 7.

Table 7

Compound	$k_k / 1 \text{ mol}^{-1} \text{ sec}^{-1}$
	1.7×10^6 (ref 36)
	3.6×10^7 (ref 33)
	2.1×10^7 (ref 35)

If the first step in scheme 9 (deprotonation of the enol) was rate determining, a linear relationship on hydroxide would be observed for all hydroxide concentrations. The recent developments concerning the mechanism of ketonisation have shown that the early ideas concerning general acid / general base catalysis in enolisation are correct.

1.3.3 Concerted Catalysis

The concerted mechanism for enolisation was first reported in 1930 by Dawson *et al*¹²⁵ . Evidence for a concerted mechanism comes from studies on the enolisation of acetone in acetic acid buffers where the reaction is found to have a third order kinetic term.

$$\text{Rate} = k[\text{acetone}][\text{HAc}][\text{Ac}^-]$$

This third order kinetic term is interpreted as concerted catalysis by the undissociated acetic acid and the acetate anion. The transition state for the reaction includes both the acetic acid and acetate anion. See Fig 34.

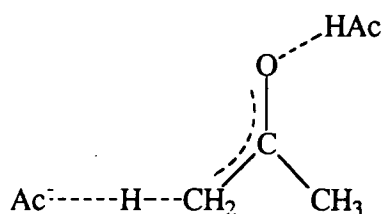
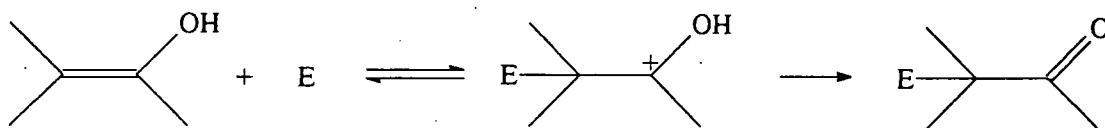


Figure 34

In the transition state, proton abstraction from carbon and proton addition to the carbonyl group are occurring at the same time but not necessarily to the same degree. Similar third order kinetic terms have been found in other carboxylic acid systems as well as trimethylamine N-oxide buffers¹²⁶.

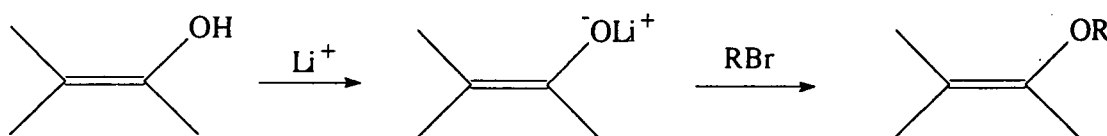
1.4 Reactions of Enols

The most important reaction of enols and enolate anions is electrophilic addition at the α -carbon atom. See Scheme 10.



Scheme 10

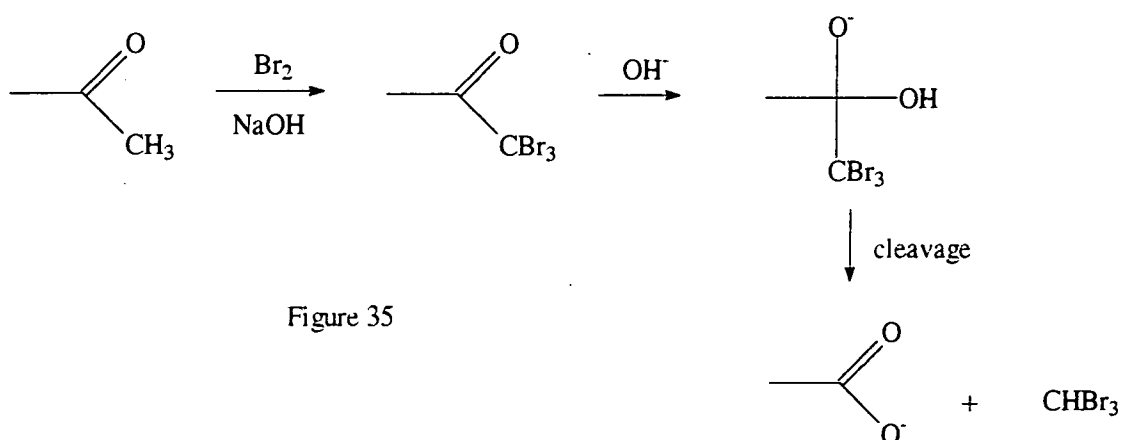
A wide range of carbon, nitrogen and halogen electrophiles are reactive towards enols and enolates. Reaction at the oxygen of the enol can also occur and the formation of vinyl ethers and vinyl esters occurs readily through the enolate. See Scheme 11.



Scheme 11

1.4.1 Halogenation.

Electrophilic addition of halogens to carbonyl compounds occurs via the enol or enolate anion. A wide variety of reagents are available for the synthesis of α - halo ketones. The use of molecular halogens is not widely used because the regioselectivity and stereochemistry are hard to control. Copper (II) halide salts in a variety of solvents are commonly used synthetic reagents¹⁰⁸. The reactions are usually carried out in acidic solutions due to the problems associated with halogenations in basic media. In basic media cleavage of the carbonyl compound can occur leading to the formation of the carboxylic acid. (See Figure 35). Historically the reaction of bromine with methyl ketones has served as a test for the presence of methyl ketones (Haloform Test).

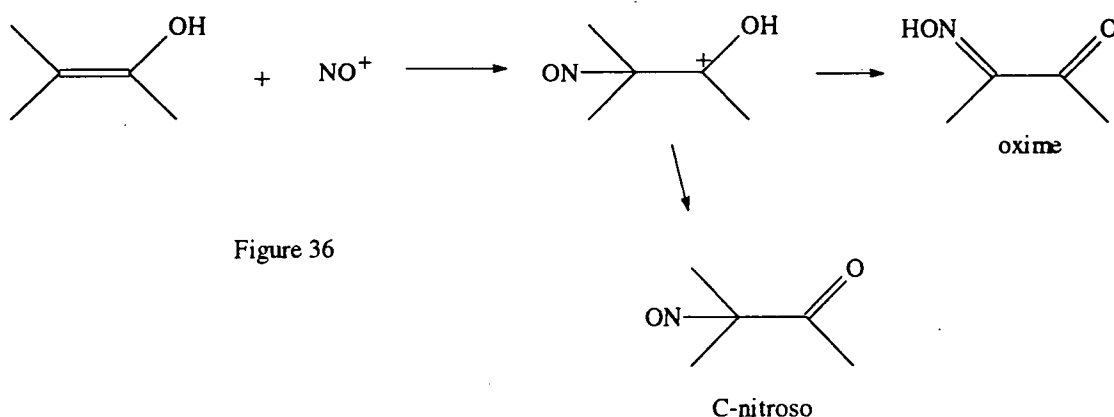


The reaction of molecular halogens with enols is known to be a very fast reaction, at or close to the diffusion limit⁵⁸. Consequently direct measurement of rates of halogenation of enols is difficult unless the enol content is small.

Compounds that exist predominantly in the enol form such as 5,5-dimethyl-1.3-cyclohexanedione (dimedone) and tetrahydrofuran-2,4-dione (tetronic acid) see (page 15) react with halogens at the same rate, but at a rate that is lower than that expected for a diffusion controlled reaction⁵⁸, $k=2 \times 10^6 \text{ l mol}^{-1} \text{ sec}^{-1}$.

1.4.2 Nitrosation.

The most commonly studied electrophilic nitrogen reaction is nitrosation. Nitrosation of carbonyl compounds occurs via the enol or enolate and produces the corresponding oxime or C-nitroso compound¹¹⁰. See Fig 36.



Nitrosation is usually carried out with acidified sodium nitrite solutions or with alkyl nitrites (RONO) in non-aqueous solvents. A wide range of nitrosating reagents are available in aqueous solution; these are H_2NO_2^+ , Nitrosyl halides (XNO), N_2O_3 . The reactivity of these electrophiles towards simple enols has been measured. Table 8 shows the reactivity of nitrosyl bromide with three enols.

Table 8.

Compound	$k_{\text{BrNO}} / \text{l mol}^{-1} \text{sec}^{-1}$
	7.0×10^7 (ref 109)
	3.8×10^9 (ref 109)
	1.4×10^7 (ref 109)

Again, this shows the high reactivity of enols towards electrophiles, with rate constants close to the diffusion controlled limit for some nitrosating reagents.

The reactivity of enols is primarily controlled by substituents attached to the double bond, particularly groups that are in direct resonance with the double bond. The effect of adding an acetyl group is shown by a 5000 fold decrease in reactivity between the enol of acetone and the enol of acetylacetone¹⁰⁹.

1.5 Enols of carboxylic acid derivatives

The simplest carboxylic acid enol (1,1-ethenediol) is 1,1-ethenediol, the enol form of acetic acid. 1,1-ethenediol has never been observed directly. See Fig 37.



Figure 37

Calculations of the energy difference between acetic acid and 1,1-ethenediol⁸ show that the keto isomer is favoured by approximately 150 kJ mol⁻¹. A recent determination of the pK_E of acetic acid¹¹² using thermodynamic cycles gives a value of pK_E=21±2. As is the case with simple carbonyl compounds 1,1-enediols have been proposed as reactive intermediates in electrophilic substitution reactions. Halogenation and nitrosation reactions of Malonic acid¹¹³ have shown that the enolisation of the malonic acid is rate limiting, giving a value of k = 3 ± 1 x10⁻³ sec⁻¹. The enolisation of malonic acid has also been studied by deuterium exchange¹¹⁴, (k = 1.7 ± 1 x10⁻³ sec⁻¹) the two sets of results are in very good agreement. The effect of α-substitution on the enolisation of malonic acid has shown that alkyl groups reduce the rate of enolisation. This is due to the lower acidity of the C-H system caused by an inductive effect. Phenyl substitution causes an increase in the enolisation rate constant, this is caused by resonance stabilisation of the partial double bond formed in the transition state.

An estimate of the enol content (K_E)¹¹³ for malonic acid has been calculated from nitrosation kinetics by assuming that reaction of the enol with nitrosyl chloride (NOCl) occurs at the diffusion limit. A value of $K_E = 1 \times 10^{-8}$ is reported.

A similar investigation has been carried out on the enol formed from malonamide¹¹⁵. Conditions where the enolisation of malonamide is rate limiting give a value of $k = 3.3 \times 10^{-3} \text{ l mol}^{-1} \text{ sec}^{-1}$ for the acid catalysed enolisation process. See Fig 38.

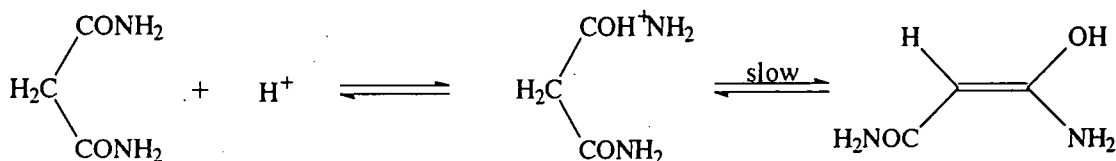


Figure 38

An estimate of the enol content for malonamide ($K_E = 4 \pm 2 \times 10^{-10}$)¹¹⁵ is calculated from the halogenation and nitrosation reactions where the reaction of the enol with the electrophile is rate limiting. Enol contents for esters have been determined in a similar way. Table 9 shows K_E values of carboxylic acid derivatives determined by the indirect kinetic method.

Table 9

Compound	K_E
$\begin{array}{c} \text{CO}_2\text{H} \\ \\ \text{H}_2\text{C} \\ \\ \text{CO}_2\text{H} \end{array}$	1×10^{-8} (ref 113)
$\begin{array}{c} \text{CONH}_2 \\ \\ \text{H}_2\text{C} \\ \\ \text{CONH}_2 \end{array}$	4×10^{-10} (ref 115)
$\begin{array}{c} \text{CO}_2\text{Et} \\ \\ \text{H}_2\text{C} \\ \\ \text{CO}_2\text{Et} \end{array}$	2×10^{-11} (ref 116)

The very low enol contents of carboxylic acids means that special techniques are needed to prepare 1,1-enediols. The use of very bulky groups (see section 1.2.1) to stabilise enols can be applied to enediols as well. Hegarty and co-workers have synthesised carboxylic acid enols by a variety of methods; See Fig 39.

a) protonation of the dianion¹¹⁷ (A)

b) desilylation of (B) using tetrabutylammonium fluoride (TBAF)¹¹⁸.

c) hydration of the corresponding ketene (C)^{117,118}

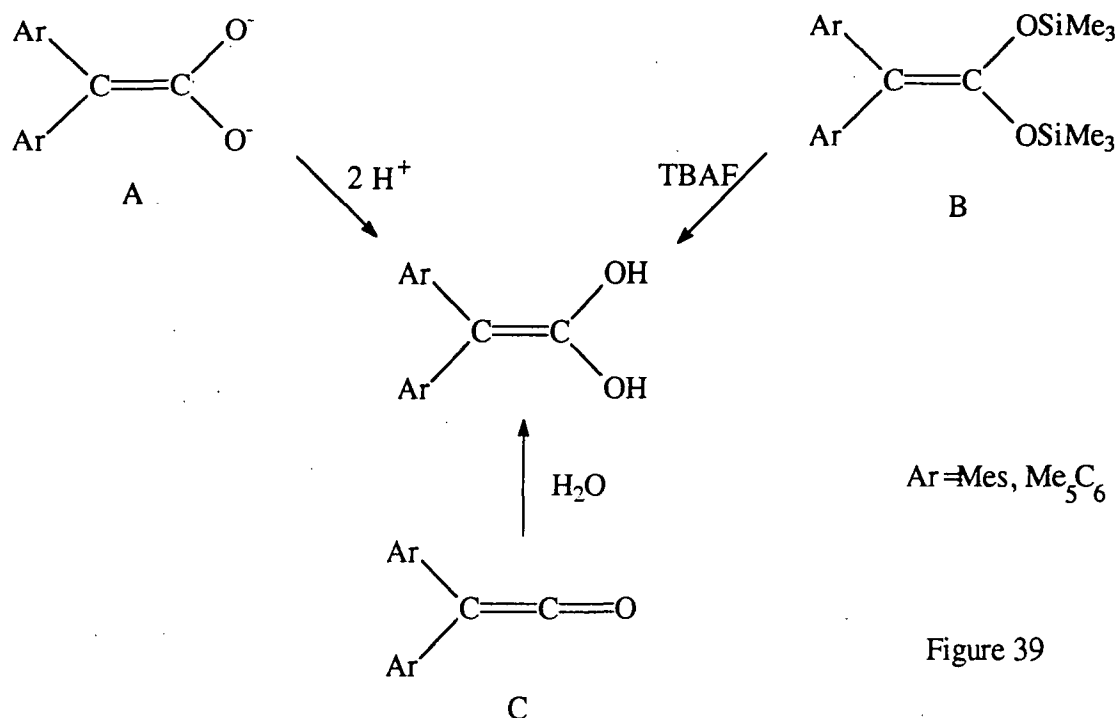


Figure 39

The 1,1-enediols formed are kinetically stable due to the slow rate of ketonisation of the enol. The 2,2-bis (pentamethylphenyl)ethene-1,1- diol¹¹⁸ is very stable, In 50:50 (v/v) acetonitrile/water the enol has a half life of 11mins at pH=3. In neutral solutions the enol has a half life of several hours and can be characterised by conventional spectroscopic methods. The enol has, an infra red band at 1615cm⁻¹ (which is characteristic of a double bond stretch) and a $\lambda_{\text{max}} = 270\text{nm}$ in the U.V. region.

Recently 2,2-bis (2,4,6 triisopropylphenyl)ethene-1,1-diol¹¹⁹ has been prepared by the hydration of the corresponding ketene. The enol is very stable, conversion to the carboxylic acid being almost undetectable at 0°C in 10:1 (v/v) THF/H₂O mixture.

Very little is known about the chemistry of these compounds except that they are readily oxidised to stable free radicals. See fig 40.

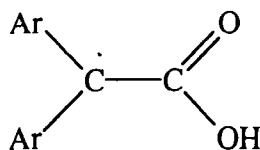


Figure 40

Preparation of 1,1-enediols not stabilised by bulky groups has only been carried out recently using advanced laser flash photolysis experiments¹²⁰. 1,1-enediols have been observed as reactive intermediates in the photolysis of diazonaphthoquinones. See Fig 41.

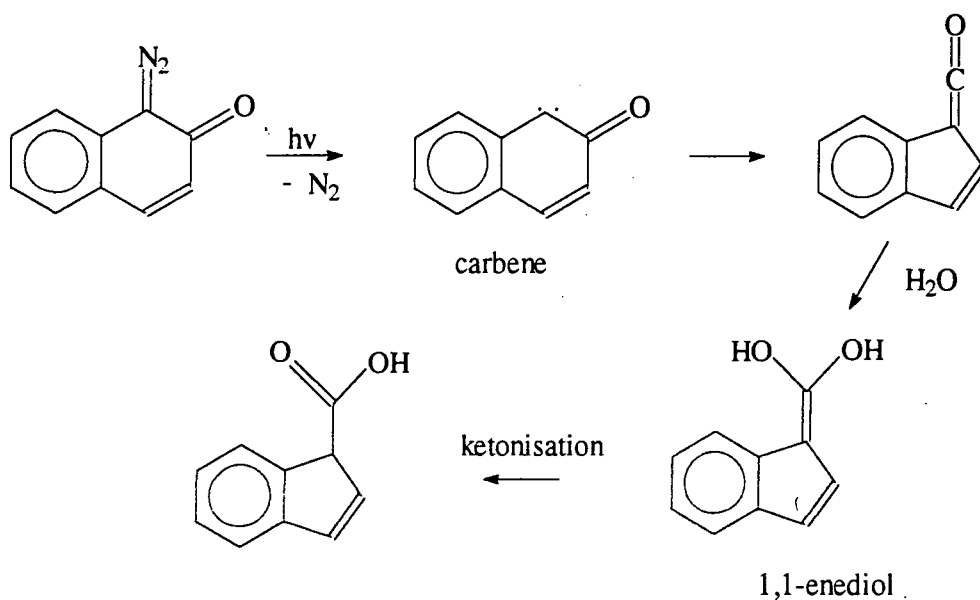


Figure 41

Using this technique to generate 1,1-enediols it is possible to estimate the enol contents of carboxylic acids^{121,122}. The enol contents for indene-1-carboxylic acid and cyclopentadienyl-1-carboxylic acid are shown in Fig 42.

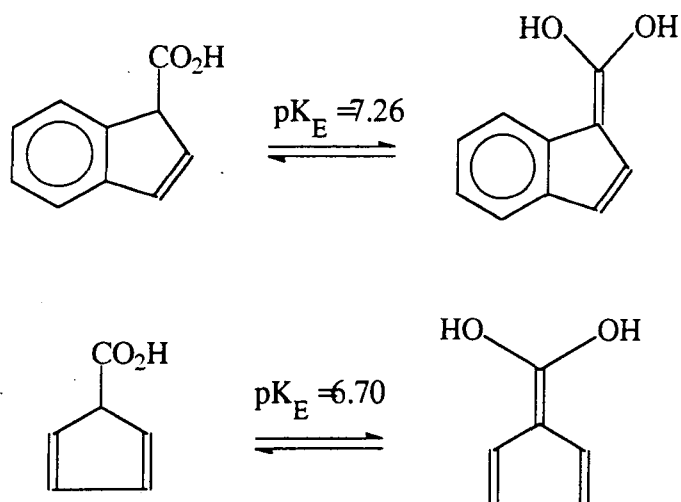


Figure 42

Kinetic studies regarding the ketonisation of 1,1-enediols have shown that the reaction is base catalysed and that the reaction occurs via rate limiting protonation of the enolate anion (See section 1.3.2) even in concentrated acid solutions.

The enol of mandelic acid (α -hydroxyphenylacetic acid) has been generated by a Norrish type 2 reaction. See Fig 43. The kinetic and thermodynamic properties of the enol have been recorded¹²³.

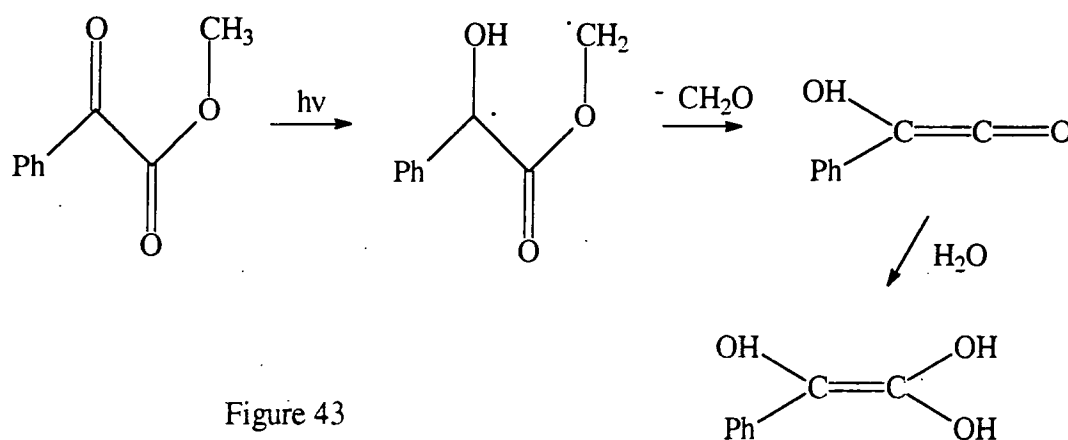


Figure 43

The enol content (K_E) of mandelic acid was determined from the ratio of enolisation and ketonisation rate constants. Combination of the pK_E and carbon acidity constant gives an estimate of the acid strength of 1,1-enediols. See Fig 44.

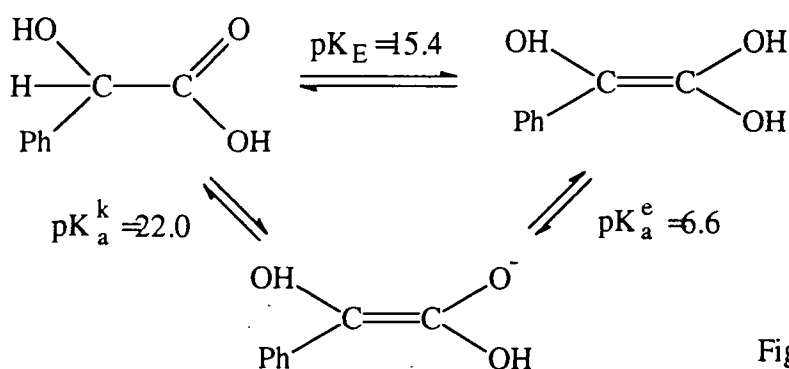


Figure 44

A similar photolysis reaction¹²⁴ has been used to identify the enol formed from the methyl ester of mandelic acid.

References

1. E.Erlenmeyer, *Chem. Ber.*, 1881, **14**, 320.
2. E.Erlenmeyer, *Chem. Ber.*, 1875, **8**, 309.
3. B.Blank and H.Fisher, *Helv. Chim. Acta.*, 1973, **56**, 506.
4. S.Saito, *Chem.Phys.Lett.*, 1976, **42**, 399.
5. N.Heinrich, W. Koch, G.Frenking and H. Schwarz, *J. Am. Chem. Soc.*, 1986, **108**, 593.
6. O.N.Ventura, A. Lledos, R. Bonaccorsi, J. Bertram and J. Tomasi, *Theor. Chim. Acta.*, 1987, **72**, 175.
7. M.T.Nguyen, A.F. Hegarty, T.K. Ha and G.R. DeMare, *J. Chem. Soc., Perkin Trans. 2*, 1986, 147.
8. P.V.R. Schleyer, *Pure. Appl. Chem.*, 1987, **59**, 1647.
9. A.Greenberg and T.A. Stevenson, *J. Am. Chem. Soc.*, 1985, **107**, 3488.
10. Y. Apeloig, D.Arad and Z.Rappoport, *J. Am. Chem. Soc.*, 1990, **112**, 9131.
11. M. Rodler and A. Bauder, *J. Am. Chem. Soc.*, 1984, **106**, 4025.
12. S.Saito, *Pure. Appl. Chim.*, 1978, **50**, 1239.
13. W.J. Hehre and W.A Lathan, *J. Chem. Soc., Chem. Commun.*, 1972, 771.
14. P. Bowers and L. Schafer, *J. Mol. Struc.*, 1980, **69**, 233.
15. W.J. Bouma, D. Poppinger and L. Radom, *J. Am. Chem. Soc.*, 1977, **99**, 6443.
16. W.J. Bouma, M.A. Vincent and L. Radom, *Int. J. Quan. Chem.*, 1978, **14**, 767.
17. W.R. Rodwell, W.J. Bouma and L. Radom, *Int. J. Quan. Chem.*, 1980, **18**, 107.
18. J.L. Holmes and F.P.Lossing, *J. Am. Chem. Soc.*, 1982, **104**, 2648.
19. B.Albrecht, M. Allan, E. Haselbach and L. Neuhaus, *Helv. Chem. Acta*, 1984, **67**, 216.
20. F. Turecek, Z. Havlas, F. Maquin, N. Hill and T. Gaumann, *J. Org. Chem.*, 1986, **51**, 4061.

21. F. Turecek and Z. Havlas, *J. Chem. Soc., Perkin Trans. 2*, 1986, 1011.
22. F. Turecek, I. Brabec and J. Korvala, *J. Am. Chem. Soc.*, 1988, **110**, 7984.
23. F. Turecek, *Tet. Lett.*, 1986, **27**, 4219.
24. F. Turecek, *Tet. Lett.*, 1984, **25**, 5133.
25. F. Turecek, *J. Chem. Soc., Chem. Commun.*, 1984, 1374.
26. F. Turecek, *Org. Mass Spectros.*, 1992, **27**, 1087.
27. F. Turecek, *Org. Mass Spectros.*, 1995, **30**, 144.
28. M.C. Lasne and J. L. Ripoll, *Tet. Lett.*, 1982, **23**, 1587.
29. J. L. Ripoll, *Nouv. J. Chim.*, 1979, **3**, 195.
30. G.R. Mc Millan, J.G. Calvert and N. J. Pitts, *J. Am. Chem. Soc.*, 1964, **86**, 3602.
31. P. Häspra, A. Sutter and J. Wirz, *Angew. Chem., Intl. Ed. Engl.*, 1979, **18**, 617.
32. R. Hochstrasser, A.J. Kresge, N.P. Schepp and J. Wirz, *J. Am. Chem. Soc.*, 1988, **110**, 7875.
33. Y. Chiang, A.J. Kresge, Y.S. Tang and J. Wirz, *J. Am. Chem. Soc.*, 1984, **106**, 460.
34. Y. Chiang, A.J. Kresge, J.A. Santabella and J. Wirz, *J. Am. Chem. Soc.*, 1988, **110**, 5506.
35. Y. Chiang, A.J. Kresge and J. Wirz, *J. Am. Chem. Soc.*, 1984, **106**, 6392.
36. Y. Chiang, M. Hojiatti, J.R. Keefe, A.J. Kresge, N.P. Schepp and J. Wirz, *J. Am. Chem. Soc.*, 1987, **109**, 4000.
37. J.R. Keefe, A.J. Kresge and N.P. Schepp, *J. Am. Chem. Soc.*, 1988, **110**, 1993.
38. R. Steinberger and F.H. Westheimer, *J. Am. Chem. Soc.*, 1951, **73**, 429.
39. Y. Chiang, A.J. Kresge and P.A. Walsh, *J. Am. Chem. Soc.*, 1982, **104**, 6122.
40. Y. Chiang, A.J. Kresge and P.A. Walsh, *J. Am. Chem. Soc.*, 1986, **108**, 6314.

41. Y. Chiang, A.J. Kresge and E.T. Krogh, *J. Am. Chem. Soc.*, 1988, **110**, 2600.
42. B. Capon, D.S. Rycroft and T.W. Walton, *J. Chem. Soc., Chem. Commun.*, 1979, 724.
43. B. Capon, D.S. Rycroft, T.W. Walton and C. Zueco, *J. Am. Chem. Soc.*, 1981, **103**, 1761.
44. B. Capon, B.Z. Guo, F.C Kwok, A.K. Siddhanta and C. Zucco, *Acc. Chem. Res.*, 1988, **21**, 135.
45. K.H. Meyer, *Chem. Ber.*, 1912, **45**, 2843.
46. S. Forsen and M. Nilson, "The Chemistry of the Carbonyl group" (J.Zabicky.ed), Vol.2, Wiley Interscience, London and New York, P157.
47. G. Schwarzenbach and C. Wittwer, *Helv. Chim. Acta.*, 1947, **30**, 656.
48. G. Schwarzenbach and E. Felder, *Helv. Chim. Acta.*, 1944, **27**, 1044.
49. A. Gero, *J. Org. Chem.*, 1954, **19**, 469.
50. W. Walish and J.E. Dubois, *Chem. Ber.*, 1959, **92**, 1028.
51. J.E. Dubois and G. Barbier, *Bull. Soc. Chim. Fr.*, 1965, 682.
52. J. Toullec, *Adv. Phys. Org. Chem.*, 1982, **18**, 1.
53. J. Toullec and J.E. Dubois, *Tetrahedron*, 1973, **29**, 2859.
54. J. Toullec, J.E. Dubois and M. El. Alaoui, *J. Am. Chem. Soc.*, 1981, **103**, 5393.
55. L. Zucker and L.P. Hammett, *J. Am. Chem. Soc.*, 1939, **61**, 2791.
56. A.J. Kresge, N.P. Schepp, J. Wirz, R. Hochstrasser, *J. Am. Chem. Soc.*, 1988, **110**, 7875.
57. J. Toullec and J.E. Dubois, *J. Am. Chem. Soc.*, 1974, **96**, 3524.
58. J.H.Ridd, *Adv. Phys. Org. Chem.*, 1978, **16**, 1.
59. J. P. Guthrie, *Can. J. Chem.*, 1979, **57**, 797.
60. Y. Chiang, A.J. Kresge, M. Capponi and J. Wirz, *Helv. Chim. Acta.*, 1986, **69**, 1331.
61. J.R. Keefe, A.J. Kresge and Y. Yin, *J. Am. Chem. Soc.*, 1988, **111**, 8201.

62. Y. Chiang, A.J. Kresge, P.A. Walsh and Y. Yin, *J. Chem. Soc., Chem. Commun.*, 1989, 869.
63. A.J. Kresge, *Acc. Chem. Res.*, 1990, **23**, 43.
64. A.J. Kresge and J.B. Tobin, *J. Org. Chem.*, 1993, **58**, 2652.
65. A.J. Kresge, J. Jones, R. Eliasson and Y. Chiang, *Can. J. Chem.*, 1993, **71**, 1964.
66. J. Toullec, *Tet. Lett.*, 1984, **25**, 4401.
67. J. Hine, "Structural Effects on Equilibria in Organic Chemistry", Wiley, New York, 1974, p257.
68. J. Hine and N.W. Flachskam, *J. Am. Chem. Soc.*, 1973, **95**, 1179.
69. J. Emsley, *Structure and Bonding*, 1984, **57**, 148.
70. P. Alcais and R. Brouillard, *J. Chem. Soc., Perkin Trans.2*, 1972, 1214.
71. J. Emsley and N.J. Freeman, *J. Mol. Struct.*, 1987, **161**, 193.
72. M. Moriyasu, A. Kato and Y. Hashimoto, *Chem. Lett.*, 1984, 1181; *J. Chem. Soc., Perkin Trans.2*, 1986, 515.
73. A.S.N. Murthy, C.N.R. Rao and T.R. Kastrum, *Can. J. Chem.*, 1962, **40**, 2267.
74. H. Mauser and B. Nickel, *Chem. Ber.*, 1964, **97**, 1745.
75. M.M. Naoum, M.G. Botros, *Indian. J. Chem., Part A*, 1986, **25A**, 639.
76. R.S. Noy, V.A. Gundin, B.A. Ershov, A.I. Koltsov and V.A. Zubkov, *Org. Magn. Reson.*, 1975, **7**, 109.
77. A.A. Bothner-By and R.K. Harris, *J. Org. Chem.*, 1965, **30**, 254.
78. W.O. George and V.G. Mansell, *J. Chem. Soc. (B)*, 1968, 132.
79. R.C. Fuson, J. Corse and C.H. McKeever, *J. Am. Chem. Soc.*, 1940, **62**, 3250.
80. R.C. Fuson, D.J. Byers and N. Rabjohn, *J. Am. Chem. Soc.*, 1941, **63**, 2639.
81. H. Hart, *Chem. Rev.*, 1979, **79**, 515.
82. R.C. Fuson and C.A. Sperati, *J. Am. Chem. Soc.*, 1941, **63**, 2643.
83. R.C. Fuson and S.P. Rowland, *J. Am. Chem. Soc.*, 1943, **65**, 992.

84. R.C. Fuson P.L.Southwick and S.P.Rowland, *J. Am. Chem. Soc.*, 1944, **66**, 1109.
85. R.C. Fuson, M.O. Armstrong, W.E. Wallace and J.W. Kneisley, *J. Am. Chem. Soc.*, 1944, **66**, 274.
86. R.C. Fuson, L.J. Armstrong, J.W. Kneisley and W.J. Shenk. Jr., *J. Am. Chem. Soc.*, 1944, **66**, 1464.
87. Z. Rappoport and S.E. Biali, *Acc. Chem. Res.*, 1988, **21**, 442.
88. A.R. Miller, *J. Org. Chem.*, 1976, **41**, 3599.
89. D.A. Nugiel and Z. Rappoport, *J. Am. Chem. Soc.*, 1985, **107**, 3669.
90. M. Kaftory, D.A. Nugiel, S.E. Biali and Z. Rappoport, *J. Am. Chem. Soc.*, 1989, **111**, 8181.
91. H. Albrecht, W. Fink and M. T. Reiner, *Tetrahedron*, 1976, **32**, 479.
92. M. P. Harcourt and R.A. More O' Ferrall, *J. Chem. Soc., Chem Commun.*, 1987, 822.
93. E. Rochlin and Z. Rappoport, *J. Am. Chem. Soc.*, 1992, **114**, 230.
94. A.Y. Meyer and Z. Rappoport, *J. Org. Chem.*, 1991, **56**, 3948.
95. J. Frey, I. Eventova, Z. Rappoport, T. Mitter, Y. Tubai and M. Sawada, *J. Chem. Soc., Perkin Trans.2.*, 1995, 621.
96. R.A. Bekker, G.G. Melikyan, B.L. Dyatkin and I.L. Knunyants, *Zh. Org. Khim.*, 1975, **11**, 1370.
97. K.J. Pederson, *J. Phys. Chem.*, 1934, **38**, 581.
98. H.M. Dawson, C.R. Hoskins and J.E. Smith, *J. Chem. Soc.*, 1929, 1884.
99. O. Reitz, *Z. Phys. Chem A*, 1937, **119**, 179.
100. W.J. Albery and J.S. Gelles, *J. Chem. Soc., Faraday Trans. 1*, 1982, **78**, 1569.
101. A.J. Kresge, J. Andros, P. Obroztsov. *J. Phys. Org. Chem.*, 1992, **5**, 322.
102. A.J. Kresge and J.B. Tobin, *J. Org. Chem.*, 1993, **58**, 2652.
103. Y. Chiang, A.J. Kresge, H. Morimoto and P.G. Williams, *J. Am. Chem. Soc.*, 1992, **114**, 3981.
104. K.P. Shelley, K. Nagarozan and R. Stewart, *Can. J. Chem.*, 1989, **67**, 1274.

105. R.P. Bell, "Acid and Base Catalysis", Oxford University Press, London, 1941, p54.
106. J. Hine, J.G. Houston, J.H. Henson and J. Mulders, *J. Am. Chem. Soc.*, 1965, **87**, 5050.
107. J.R. Keefe, A.J. Kresge and N.P. Schepp, *J. Am. Chem. Soc.*, 1990, **112**, 4862.
108. K.D. King, D.M. Gidden and S.W. Benson, *J. Am. Chem. Soc.*, 1970, **92**, 5541.
109. P.H. Beloso, P. Roy and D.L.H. Williams, *J. Chem. Soc., Perkin Trans. 2*, 1991, 17.
110. O. Touster, "In Organic Reactions" , Ed. R. Adams, Wiley, New York, Vol 7, 1953, p327.
111. J.R. Leis, M.E. Pena and D.L.H. Williams, *J. Chem. Soc., Perkin Trans. 2*, 1988, 157.
112. J.P Guthrie, *Can. J. Chem.*, 1993, **71**, 2123.
113. A. Graham and D.L.H. Williams, *Tetrahedron*, 1992, **48**, 7973.
114. E.W. Hansen and P. Ruoff, *J. Phys. Chem.*, 1988, **92**, 2641.
115. L. Xia and D.L.H. Williams, *J. Chem. Soc. Perkin Trans. 2*. 1993, 1429.
116. A. Graham and D.L.H. Williams, *J. Chem. Soc. Perkin Trans.2*. 1992, 747.
117. A.F. Hegarty, B.M. Allen, P. O'Neill and M.T. Nyguyen. *J. Chem. Soc. Perkin Trans.2*. 1992, 927.
118. A.F. Hegarty and P. O'Neill, *J. Chem. Soc., Chem Commun.*, 1987, 744.
119. J. Frey and Z. Rappoport, *J. Am. Chem. Soc.*, 1995, **117**, 1161.
120. Y. Chiang, J. Andros, A.J. Kresge, C.G. Huang and J.C. Scaiano. *J. Am. Chem. Soc.*, 1993, **115**, 10605.
121. J. Andros, A.J. Kresge and V.V. Popik, *J. Am. Chem. Soc.*, 1994, **116**, 961.
122. B. Urwyler and J. Wirz, *J. Angew. Chem. Int. Ed. Engl.*, 1990, **29**, 790.
123. A.J. Kresge, Y. Chiang, N.P. Schepp, J. Wirz and P. Pruszyński, *J. Angew. Chem. Int. Ed. Engl.*, 1990, **29**, 792.

124. A.J. Kresge, Y. Chiang, N.P. Schepp, J. Wirz and P. Pruszynski, *J. Angew. Chem. Int. Ed. Engl.*, 1991, **30**, 1356.
125. H.M. Dawson and E. Spivey, *J. Chem. Soc.*, 1930, 2180.
126. A.F. Heagarty and W.P. Jencks, *J. Am. Chem. Soc.*, 1975, **97**, 7188.
127. R.P. Bell and G.G. Davies, *J. C. Soc.*, 1965, 353.

Chapter 2

Halogenation of Malonic acid

2.1 Introduction

The halogenation of malonic acid (MAL) has been studied for many years.^{1,2} In 1912 Meyer first proposed the idea that the reaction proceeds via the enol form of malonic acid and that the rate limiting step is the formation of the enol. This is the first mention in the literature of the enol form of a carboxylic acid. Synthetically, the halogenation of malonic acid can be carried out in a number of ways;

Bromine in chloroform produces mono and di-brominated malonic acid compounds³.

Sulfuryl chloride (SOCl_2) reacts with malonic acid to produce mono-chlorinated malonic acid⁴.

Bromination of malonic acid is one of many steps involved in oscillating chemical reactions. The Belousov-Zhabotinsky oscillating reaction⁸ involves the simultaneous bromination and oxidation of malonic acid in the presence of metal ions eg. Ce^{4+} . The enolisation of malonic acid is an important parameter in understanding oscillating chemical reactions. Kinetic investigations^{5,6,7} into the halogenation of malonic acid have shown that the reaction is usually zero order in the halogen (indicating rate limiting formation of the enol) and the enolisation step is not acid catalysed. A recent investigation⁶ (using deuterium exchange, measured by proton N.M.R.) has proposed an acid catalysed mechanism but this work is complicated by the use of strongly acidic solutions. The lack of acid catalysis in the enolisation of malonic acid has been attributed to an intramolecular acid catalysed process. See Fig 2.1.1.

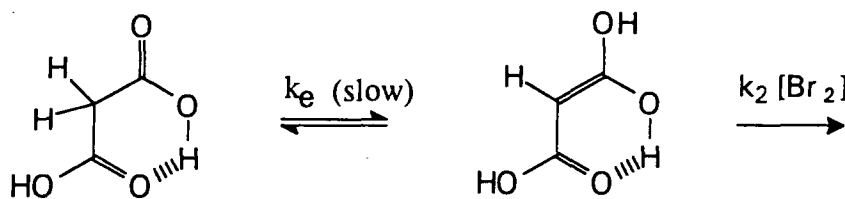
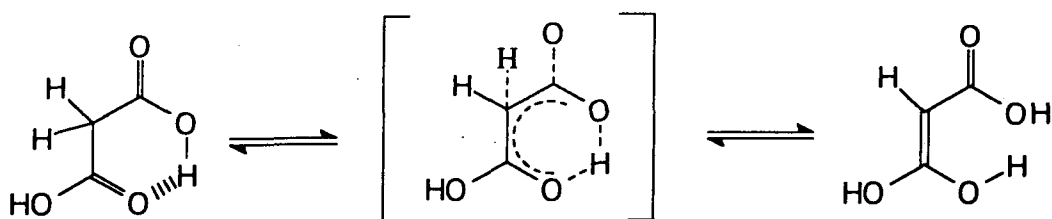


Figure 2.1.1

The mechanism involves a six membered transition state which enables the transfer of the proton and catalysis of the enolisation step.



It has been noted by Bhale⁹ that there is a second order dependence on malonic acid which becomes evident at higher pH values. This suggests that an alternative mechanism exists but no explanation has been given for this. It is expected to involve malonate ion catalysis. The present work aims to investigate this mechanism and to investigate the effects of base catalysis by carboxylate anions on the enolisation of malonic acid.

2.2 Zero order halogenation

The bromination of malonic acid was carried out in aqueous solution at 298K. The kinetics were measured by monitoring the decrease in the bromine absorbance at 395nm using a stopped flow spectrophotometer and the reaction was studied in the pH range 2-5. Bromination reactions using molecular bromine can only be carried out in acidic solutions due to the formation of other species such as bromate, bromite and hypobromous acid.

The pH of the reaction was maintained at a constant value by using the malonic acid/malonate as the buffer ($pK_a=2.85$ and 5.70). Each pH value was achieved by adding the appropriate quantity of sodium hydroxide and hydrochloric acid to a solution of malonic acid. The pH change during the reaction was negligible due to the very small concentration of bromine relative to the concentration of malonic acid.

Bromine solutions were made up and used on the same day. The concentration of bromine was determined from its known extinction coefficient at 395nm ($\epsilon=128.4 \text{ l mol}^{-1} \text{ cm}^{-1}$).

Every kinetic run was carried out with the malonic acid concentration in at least 25 fold excess over the bromine.

To obtain good zero order kinetics the use of relatively concentrated bromine solutions is required ca $3 \times 10^{-3} \text{ mol l}^{-1}$. The use of concentrated bromine solutions can bring about problems; the most common being a downward curvature in the absorbance vs time plots. Figure 2.2.1 shows one such plot. This problem may be due to multi-halogenation, which becomes more significant at higher bromine concentrations. Consequently a compromise is needed to obtain good kinetics. Figure 2.2.2 shows a good zero plot. All the results recorded showed good zero order dependence for approximately 80% of the reaction.

Figure 2.2.1

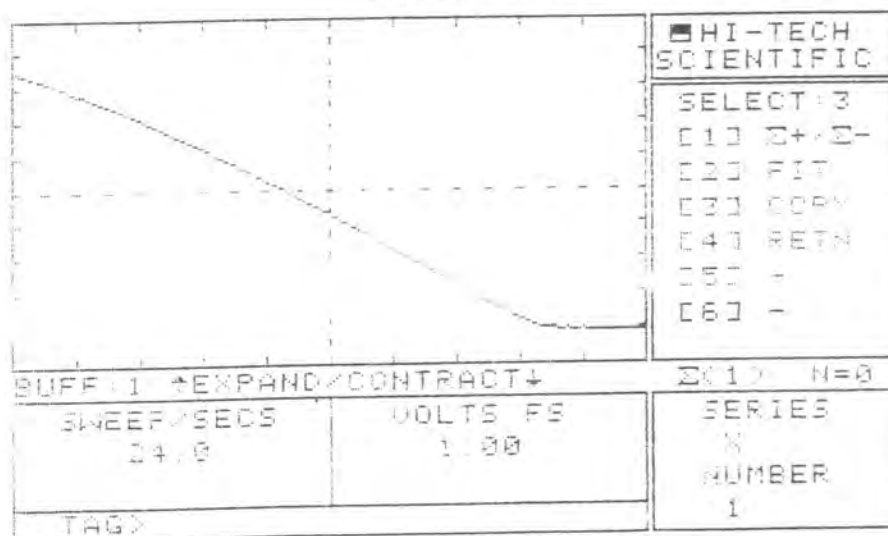
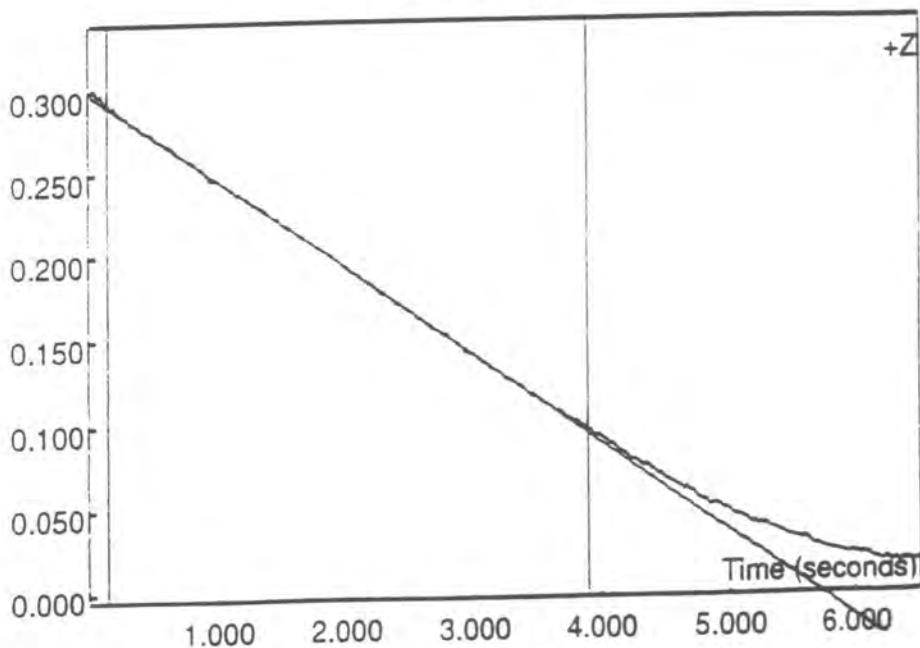


Figure 2.2.2



The variation of the observed zero order rate constant with pH and substrate concentration was determined. The results are shown in tables 2.2.1-2.2.4.

Table 2.2.1

$$[\text{Br}_2] = 2.3 \times 10^{-3} \text{ mol l}^{-1} \quad \text{pH} = 2.75$$

$[\text{MAL}]_T/\text{M}$	$10^4 k_{\text{obs}}/\text{mol l}^{-1} \text{ sec}^{-1}$	$10^3 k_{\text{obs}}/[\text{MAL}]_T \text{ sec}^{-1}$
0.05	2.19	4.38
0.10	5.50	5.50
0.15	11.00	7.33
0.20	18.24	9.12
0.25	24.00	9.60

Table 2.2.2

$$[\text{Br}_2] = 2.47 \times 10^{-3} \text{ mol l}^{-1} \quad \text{pH} = 3.30$$

$[\text{MAL}]_T/\text{mol l}^{-1}$	$10^4 k_{\text{obs}} / \text{mol l}^{-1} \text{ sec}^{-1}$	$10^3 k_{\text{obs}} / [\text{MAL}]_T \text{ sec}^{-1}$
0.1	4.04	4.04
0.15	8.12	5.40
0.175	10.29	5.88
0.20	13.18	6.59

Table 2.2.3

$$[\text{Br}_2] = 2.43 \times 10^{-3} \text{ mol l}^{-1} \quad \text{pH} = 3.80$$

$[\text{MAL}]_{\text{T}}/\text{mol l}^{-1}$	$10^4 k_{\text{obs}} / \text{mol l}^{-1} \text{ sec}^{-1}$	$10^3 k_{\text{obs}} / [\text{MAL}]_{\text{T}} \text{ sec}^{-1}$
0.10	1.97	1.97
0.15	4.10	2.72
0.175	7.37	3.68
0.20	10.99	4.40

Table 2.2.4

$$[\text{Br}_2] = 2.45 \times 10^{-3} \text{ mol l}^{-1} \quad \text{pH} = 4.30$$

$[\text{MAL}]_{\text{T}}/\text{mol l}^{-1}$	$10^4 k_{\text{obs}} / \text{mol l}^{-1} \text{ sec}^{-1}$	$10^3 k_{\text{obs}} / [\text{MAL}]_{\text{T}} \text{ sec}^{-1}$
0.10	1.06	1.06
0.15	2.10	1.40
0.20	3.75	1.88
0.25	5.84	2.34

Up to pH 5 the reaction is found to be zero order with respect to bromine, thus enolisation is the rate limiting step in the reaction. The reaction is no longer independent of the pH as is found when $\text{pH} < 1.5$. These results are consistent with a mechanism involving base (MAL^-) catalysed enolisation.

If it is assumed that two parallel mechanisms (See Fig 2.2.3) are in operation then the following rate equation can be derived.

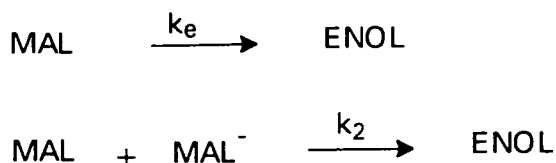


Figure 2.2.3

The rate of bromine depletion is given by the following equation (eqn 2.2.1).

$$\text{rate} = k_{\text{obs}} = k_e[\text{MAL}]_e + k_2[\text{MAL}]_e[\text{MAL}^-]_e \quad \text{equation 2.2.1}$$

The free concentrations of malonic acid $[\text{MAL}]_e$ and malonate anion $[\text{MAL}^-]_e$ can be expressed in terms of the total malonic acid concentration $[\text{MAL}]_T$ using the known acid dissociation constant (K_a) of malonic acid and the mass balance equation for the total concentration of malonic acid $[\text{MAL}]_T$ used in the reaction.

$$K_a = \frac{[\text{MAL}^-]_e [\text{H}^+]}{[\text{MAL}]_e} \quad \text{equation 2.2.2}$$

$$[\text{MAL}]_T = [\text{MAL}]_e + [\text{MAL}^-]_e \quad \text{equation 2.2.3}$$

Combination of equations 2.2.2 and 2.2.3 leads to the following equation for $[\text{MAL}]_e$ and $[\text{MAL}^-]_e$.

$$[\text{MAL}]_e = \frac{[\text{MAL}]_T [\text{H}^+]}{(K_a + [\text{H}^+])} \quad \text{equation 2.2.4}$$

$$[\text{MAL}^-]_e = \frac{[\text{MAL}]_T K_a}{([\text{H}^+] + K_a)} \quad \text{equation 2.2.5}$$

Substitution of equations 2.2.4 and 2.2.5 into equation 2.2.1 leads to the following expression for the overall rate of the reaction (equation 2.2.6).

$$\text{rate} = k_{\text{obs}} = \frac{k_e [\text{H}^+] [\text{MAL}]_T}{([\text{H}^+] + K_a)} + \frac{k_2 K_a [\text{H}^+] [\text{MAL}]_T^2}{([\text{H}^+] + K_a)^2} \quad \text{equation 2.2.6}$$

Equation 2.2.6 can be divided by $[\text{MAL}]_T$ to produce the following equation:

$$\frac{k_{\text{obs}}}{[\text{MAL}]_T} = \frac{k_e [\text{H}^+]}{([\text{H}^+] + K_a)} + \frac{k_2 K_a [\text{MAL}]_T [\text{H}^+]}{([\text{H}^+] + K_a)^2} \quad \text{equation 2.2.7}$$

This equation shows that a plot of $k_{\text{obs}}/[\text{MAL}]_T$ against $[\text{MAL}]_T$ should be linear and the slope and intercept should show a characteristic dependence on pH. Figure 2.2.4 shows the appropriate plots at four different pH values, the gradients and intercepts are recorded in table 2.2.5 (along with results recorded by L.Xia¹⁰).

Figure 2.2.4

Plot of $k_{\text{obs}} / [\text{MAL}]_{\text{T}}$ vs $[\text{MAL}]_{\text{T}}$ at four different pH values

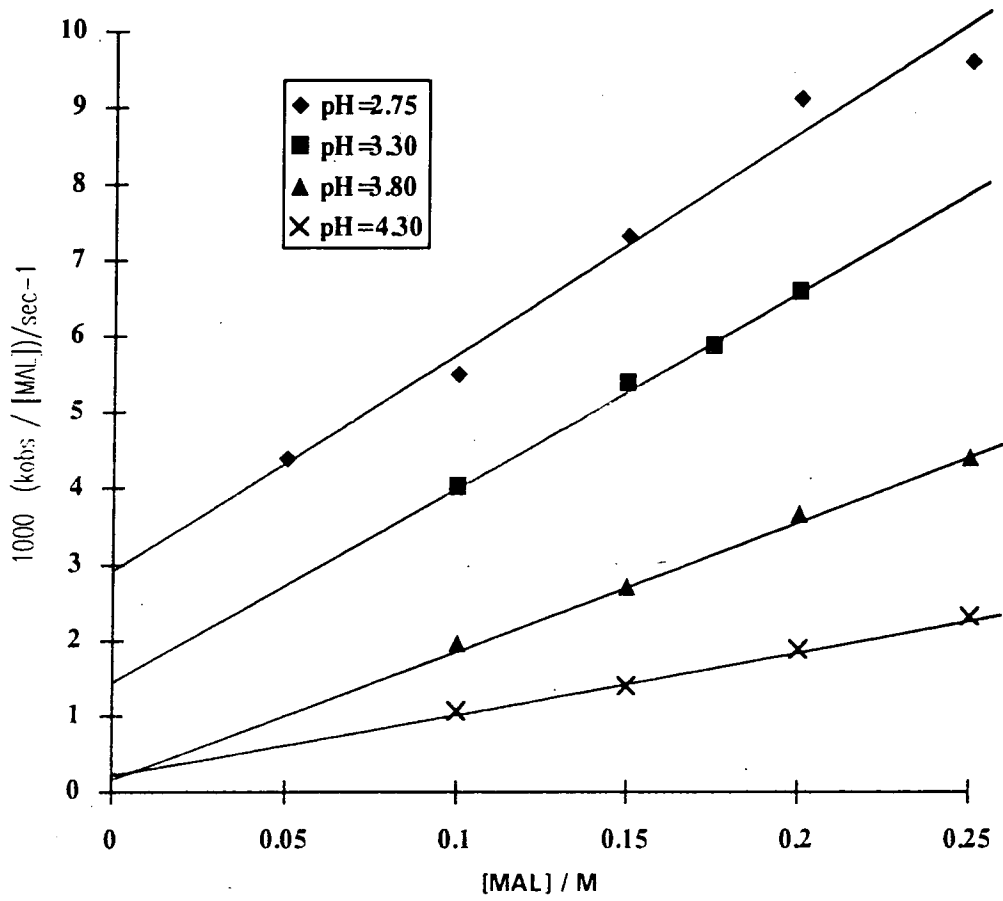


Table 2.2.5

pH	10^3 intercept/ sec^{-1}	10^3 slope / $\text{mol l}^{-1} \text{sec}^{-1}$
1.00	3.90	0
1.40	4.02	2.56
1.85	4.04	10.80
2.75	2.57	32.10
3.30	1.54	25.20
3.80	0.31	16.50
4.30	0.16	8.61

Equation 2.2.7 shows the intercept can be used to calculate a value for k_e (the rate constant for the intramolecular catalysed reaction). Table 2.2.6 shows the values calculated.

Table 2.2.6

pH	$10^3 k_e / \text{sec}^{-1}$
1.85	4.45
2.75	4.61
3.30	5.87
3.80	3.07
4.30	4.66

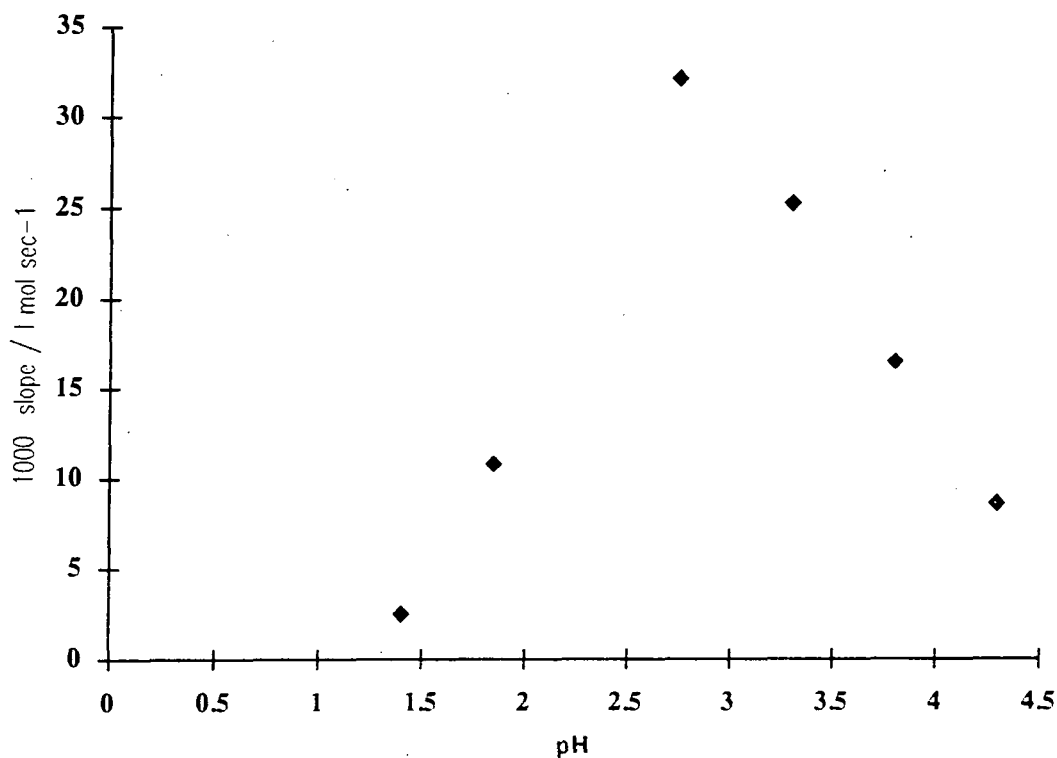
From table 2.2.6 an average value of;

$$k_e = 4.53 \pm 1.0 \times 10^{-3} \text{ sec}^{-1}$$

is calculated.

The value of k_2 can be evaluated from the slopes of figure 2.2.4. A plot of pH against slope is shown in figure 2.2.5, this shows a characteristic parabolic dependence of the slope on pH.

Figure 2.2.5
Plot of slope against pH



The maximum value of the slope can be calculated by differentiating the second part of equation 2.2.7, this leads to the following expression.

$$\frac{d(\text{slope})}{d([\text{H}^+]} = \frac{K_a k_2 ([\text{H}^+]^2 - K_a^2)}{([\text{H}^+] + K_a)^4}$$

Thus the maximum value of the slope occurs when $[\text{H}^+] = K_a$, ($\text{pH} = \text{p}K_a$) and the value of the slope should be $k_2/4$.

Thus from Fig 2.2.5

$$k_2 = 0.13 \text{ l mol}^{-1} \text{ sec}^{-1}$$

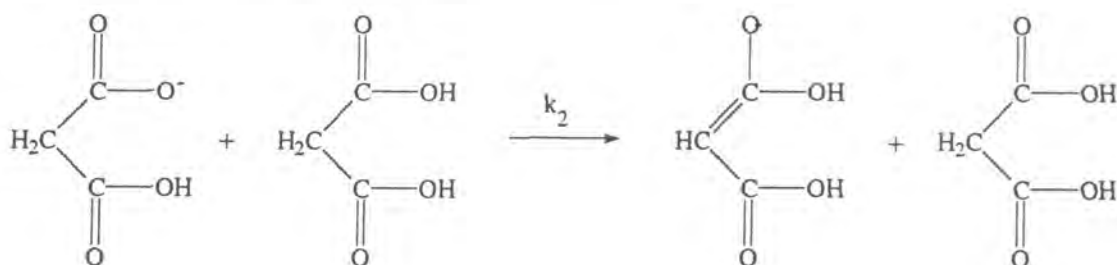
An alternative procedure involves calculating k_2 at each individual pH. The calculated values are shown in table 2.2.7.

Table 2.2.7

pH	$k_2 / \text{l mol}^{-1} \text{ sec}^{-1}$
1.85	0.13
2.75	0.13
3.30	0.13
3.80	0.18
4.30	0.25

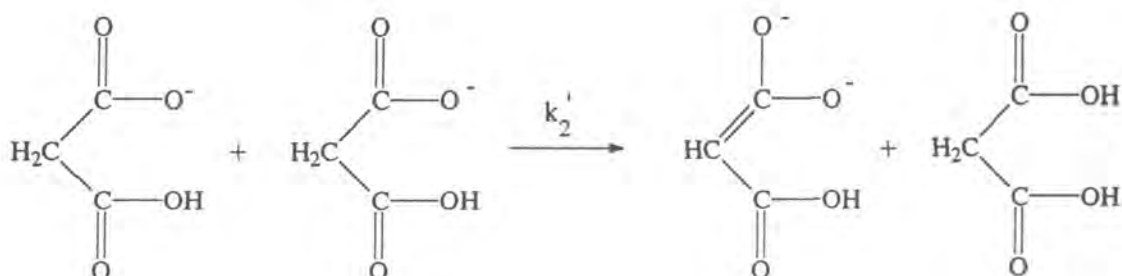
The calculated values are in excellent agreement at pH values up to 3.3 but as the pH rises the value increases significantly. This could be due to an extra kinetic term in the enolisation mechanism (See below).

The calculated value of $k_e = 4.53 \times 10^{-3} \text{ sec}^{-1}$ is in very good agreement with those previously determined by this method⁷. The pH dependency of the reaction is entirely consistent with an enolisation mechanism involving attack by the malonate ion (acting as a base) on malonic acid (scheme 2.2.1), and a value for the second order rate constant (k_2) of $0.13 \text{ mol}^{-1} \text{ l s}^{-1}$ is calculated.



Scheme 2.2.1

As stated above there is an increase in the calculated value of k_2 when the pH is greater than 3.3. At this pH the concentration of undissociated malonic acid is very small and it is possible that a third reaction mechanism is involved with attack of malonate ion on malonate ion (scheme 2.22).



If this extra kinetic term is incorporated into the analysis then equation 2.2.6 contains an extra term and becomes. equation 2.2.8.

$$\frac{k_{obs}}{[MAL]_T} = \frac{k_e[H^+]}{([H^+] + K_a)} + \frac{k_2 K_a [MAL]_T [H^+]}{([H^+] + K_a)^2} + \frac{k'_2 K_a^2 [MAL]_T}{([H^+] + K_a)^2} \quad \text{equation 2.2.8}$$

this can be rearranged to the following: equation 2.2.9

$$\frac{k_{obs}}{[MAL]_T} = \frac{k_e[H^+]}{[H^+] + K_a} + \left[\frac{k_2 K_a [H^+] + k'_2 K_a^2}{([H^+] + K_a)^2} \right] [MAL]_T \quad \text{equation 2.2.9}$$

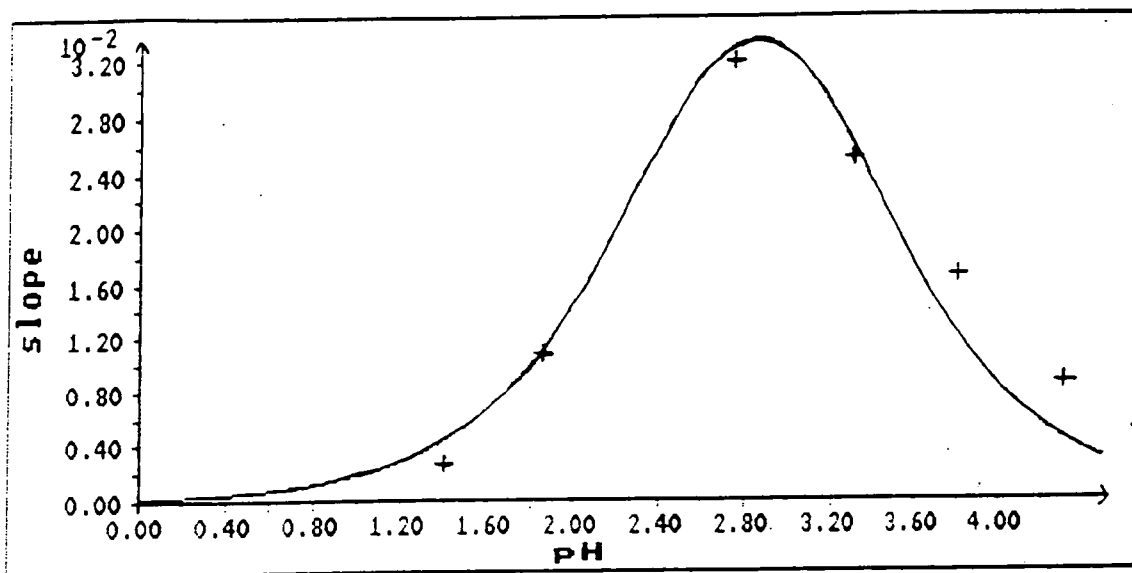
Equation 2.2.9 shows that the slope from a plot of $k_{obs}/[MAL]_T$ versus $[MAL]_T$ is given by the following. equation 2.2.10.

$$\text{slope} = \frac{k_2 K_a [H^+] + k'_2 K_a^2}{([H^+] + K_a)^2} \quad \text{equation 2.2.10}$$

Using a non-linear computer fitting program we can fit the above equation to the parabolic shaped curve (See Figure2.2.5). Fig 2.2.6. shows the fit using equation

2.2.6. (without adding on the extra kinetic term). This shows a reasonable fit (giving $k_2=0.12\pm 0.04 \text{ l mol}^{-1} \text{ sec}^{-1}$ but the fit is poorer at the higher pH values.

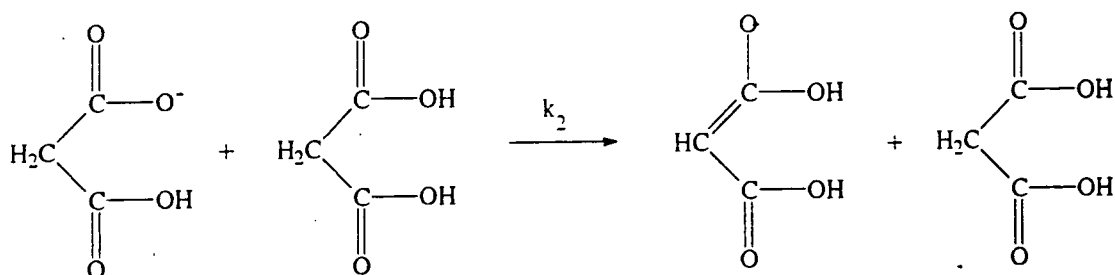
Figure 2.2.6
Graph showing the variation in slope with pH



the curve shown is the best fit to the following equation.

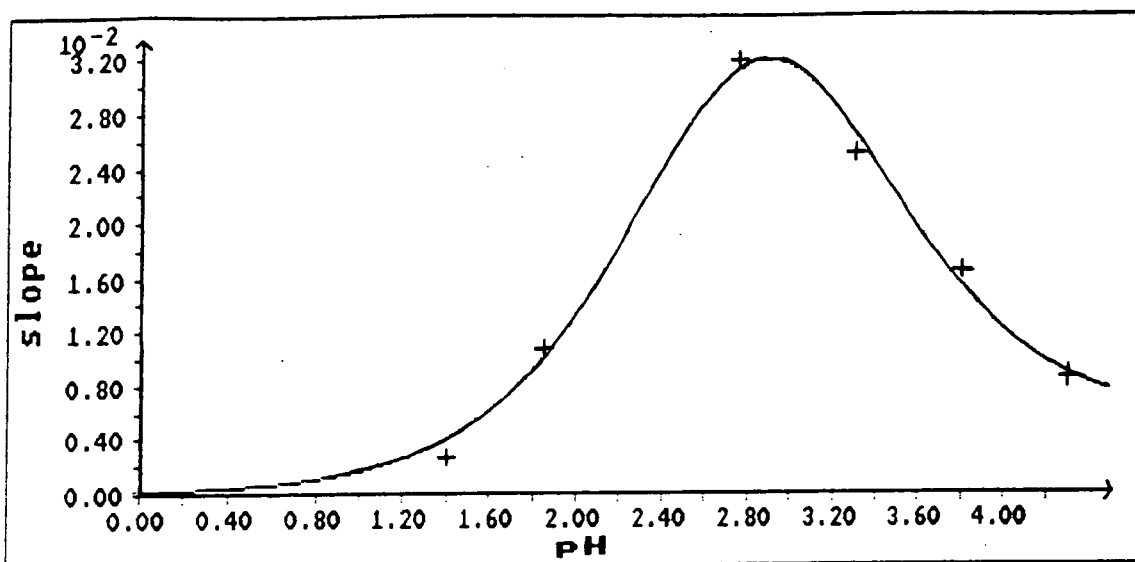
$$\text{slope} = \frac{k_2 K_a [\text{H}^+]}{([\text{H}^+] + K_a)^2}$$

A value of $k_2=0.12\pm 0.04 \text{ l mol}^{-1} \text{ sec}^{-1}$ is calculated.



Scheme 2.2.3

Figure 2.2.7
Graph of slope against pH

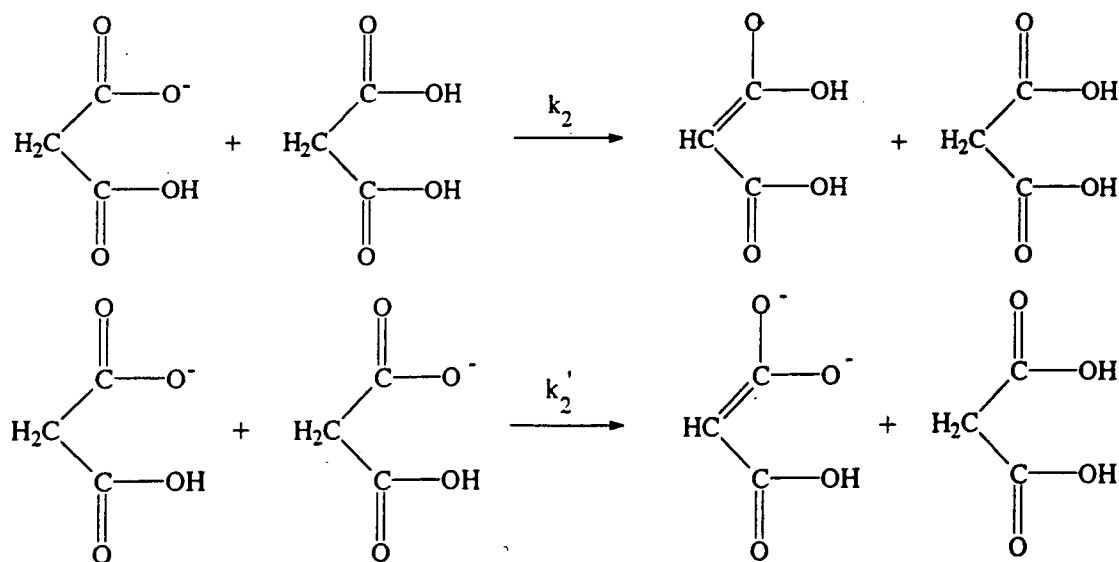


The curve shown is the best fit to the following equation.

$$\text{slope} = \frac{k_2 K_a [H^+] + k'_2 K_a^2}{([H^+] + K_a)^2}$$

This gives $k_2 = 0.12 \pm 0.041 \text{ mol}^{-1} \text{ sec}^{-1}$ and,

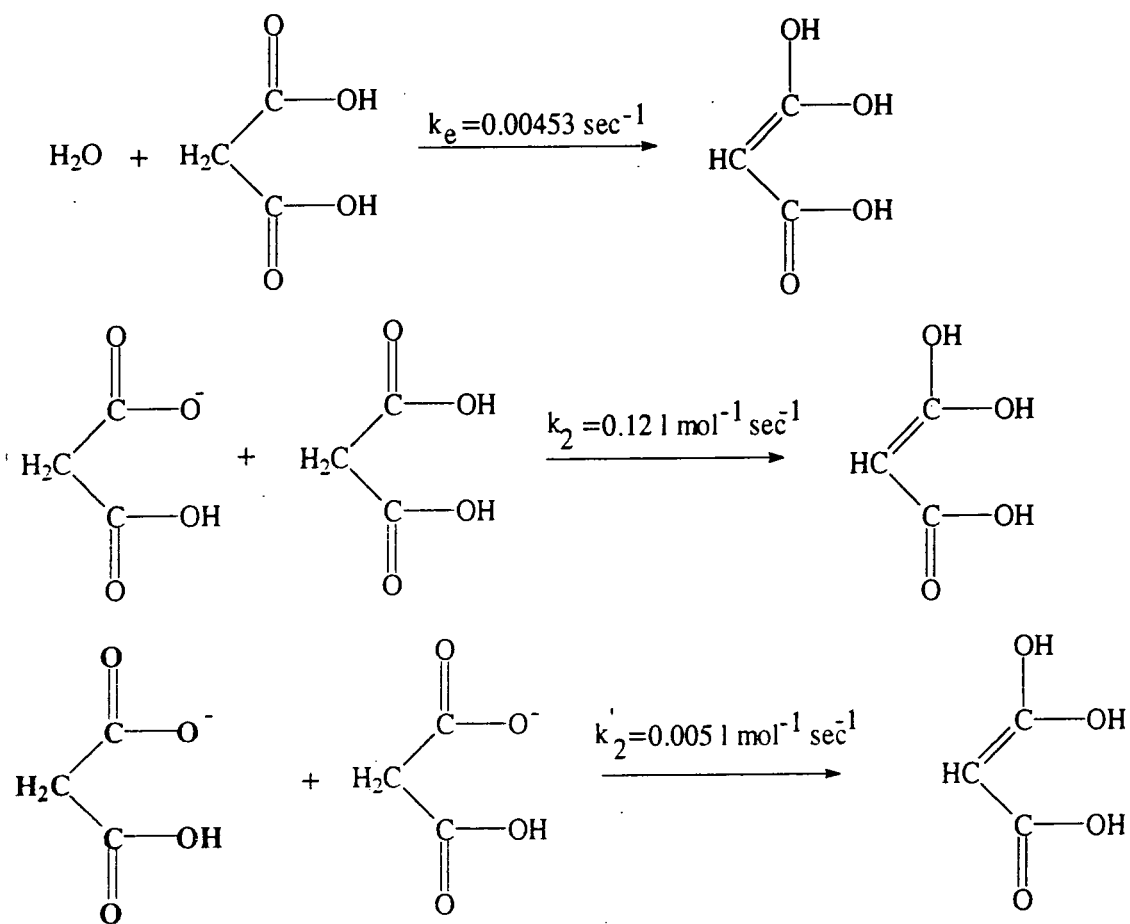
$k'_2 = 5.2 \pm 1.1 \times 10^{-3} \text{ l mol}^{-1} \text{ sec}^{-1}$



Scheme 2.2.4

Figure 2.2.7 shows the fit when the extra kinetic term is included in the analysis. This gives a much better fit at higher pH values and gives an estimate of k'_2 .

The results show excellent agreement with the theory. The following scheme summarizes the individual mechanisms and rate constants.



Scheme 2.2.5

The analysis shows that the enolisation of malonic acid occurs via three parallel reactions with base catalysis by water and malonate anion the dominant mechanisms up to $\text{pH}=3.5$. At higher pH values a slower reaction involving two molecules of malonate anion becomes significant. The results show the expected trend in the catalytic coefficients of the two bases. If the rate constant for water is divided by 55.6 to give a second order rate constant then comparison with malonate anion gives the following ratio.

$$\frac{k_{\text{MAL}^-}}{k_{\text{H}_2\text{O}}} = 1500$$

Malonate anion is approximately 39000 times more basic than water . Consequently malonate anion is expected to have a much larger catalytic coefficient. The rate constant for attack of malonate anion on malonate anion is 25 times smaller than that for attack of malonate anion on undissociated malonic acid. This reflects the unfavourable electrostatic interactions between the two charged species.

The enolisation of malonic acid is not an acid catalysed process. This could be due to two factors:

1. The formation of a stable six membered ring transition state.
2. The greater carbon acidity caused by the presence of two strong electron withdrawing groups.

Kresge *et al*^{11,12} have shown that enolisation of carboxylic acids with strong electron withdrawing groups (in the α position) but which are unable to form a six membered transition state are not acid catalysed. Hence the presence of strong electron withdrawing groups favours the base catalysed mechanism by stabilisation of the carbanion intermediate. This effect is also observed in the enolisation of ketones. The enolisation of 1,3 -dichloroacetone¹³ is not acid catalysed, again this is attributed to the increased carbon acidity (relative to acetone). The enolisation of ethylacetoacetate has been investigated by Swain¹⁴ who observed base catalysis and calculated the following catalytic coefficients;

$$k_{\text{H}_2\text{O}} = 0.019 \text{ l mol}^{-1} \text{ sec}^{-1}$$
$$k_{\text{OAc}^-} = 8.2 \text{ l mol}^{-1} \text{ sec}^{-1}$$

The value calculated for water is *ca* 2 larger than the value for malonic acid, this probably reflects the greater electron withdrawing capacity of the acetyl group over the carboxy group.

2.3 Base Catalysis

Bromination of malonic acid was carried out in chloroacetic acid buffers to investigate the extent of buffer catalysis in the reaction. Chloroacetic acid was chosen because it has the same pK_a as malonic acid and consequently a similar reactivity. The reaction was followed in the normal way with malonic acid in excess over the bromine. The effect of mono-chloroacetic acid was investigated by varying the buffer concentration at a series of pH values (from 2.0-3.5). The pH of the reaction was recorded before and after the reaction and in no case was there a significant change in the pH. The bromine shows a very slow reaction with mono-chloroacetic acid buffers but not at a rate comparable to the reaction with malonic acid. The reaction showed good zero order kinetics. Tables 2.3.1-2.3.4 show the variation in the observed zero order rate constant with the concentration of the buffer anion. The concentration of mono-chloroacetate was calculated from the Henderson - Hasselbach equation using $pK_a = 2.85$.

$$pH = pK_a + \log_{10} \frac{[A^-]}{[AH]} \quad \text{equation 2.3.1}$$

No catalysis by undissociated monochloroacetic acid is expected since the reaction is not catalysed by the hydronium ion.

Tables 2.3.1 - 2.3.4 show the variation of the observed rate constant with the concentration of mono-chloroacetate. Figure 2.3.1 shows the plots at the four different pH values.

Table 2.3.1

$$[\text{Br}_2] = 2.43 \times 10^{-3} \text{ mol l}^{-1}, [\text{MAL}]_{\text{T}} = 0.05 \text{ mol l}^{-1}$$

$$\text{pH} = 2.05$$

$[\text{ClCH}_2\text{CO}_2^-]/\text{M}$	$10^4 k_{\text{obs}}/ \text{M sec}^{-1}$
0.0434	4.34
0.0326	3.90
0.0217	3.35
0.0163	3.10
0.0109	2.81

Table 2.3.2

$$[\text{Br}_2] = 1.8 \times 10^{-3} \text{ mol l}^{-1}, [\text{MAL}]_{\text{T}} = 0.05 \text{ mol l}^{-1}$$

$$\text{pH} = 2.25$$

$[\text{ClCH}_2\text{CO}_2^-]/\text{M}$	$10^4 k_{\text{obs}}/ \text{M sec}^{-1}$
0.080	4.63
0.060	4.09
0.040	3.67
0.020	3.22
0.013	2.80

Table 2.3.3

$$[\text{Br}_2] = 2.6 \times 10^{-3} \text{ mol l}^{-1}, [\text{MAL}]_{\text{T}} = 0.05 \text{ mol l}^{-1}$$

$$\text{pH} = 2.74$$

$[\text{ClCH}_2\text{CO}_2^-]/\text{M}$	$10^4 k_{\text{obs}}/ \text{M sec}^{-1}$
0.175	5.90
0.131	5.09
0.087	4.43
0.044	3.40
0.0218	2.98

Table 2.3.4

$$[\text{Br}_2] = 2.44 \times 10^{-3} \text{ mol l}^{-1}, [\text{MAL}]_{\text{T}} = 0.05 \text{ mol l}^{-1}$$

$$\text{pH} = 3.52$$

$[\text{ClCH}_2\text{CO}_2^-]/\text{M}$	$10^4 k_{\text{obs}}/ \text{M sec}^{-1}$
0.319	2.06
0.247	1.91
0.165	1.65
0.082	1.30
0.041	1.18

Figure 2.3.1

Plot of k_{obs} vs $[\text{ClCH}_2\text{CO}_2^-]$ at pH= 2.05 and 2.25

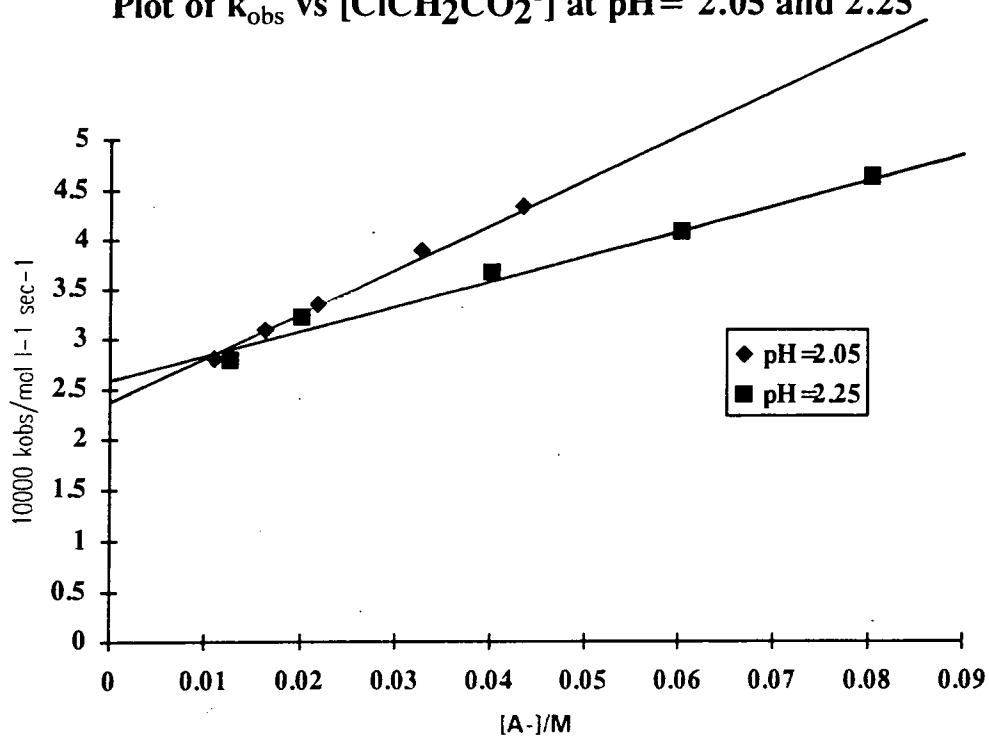
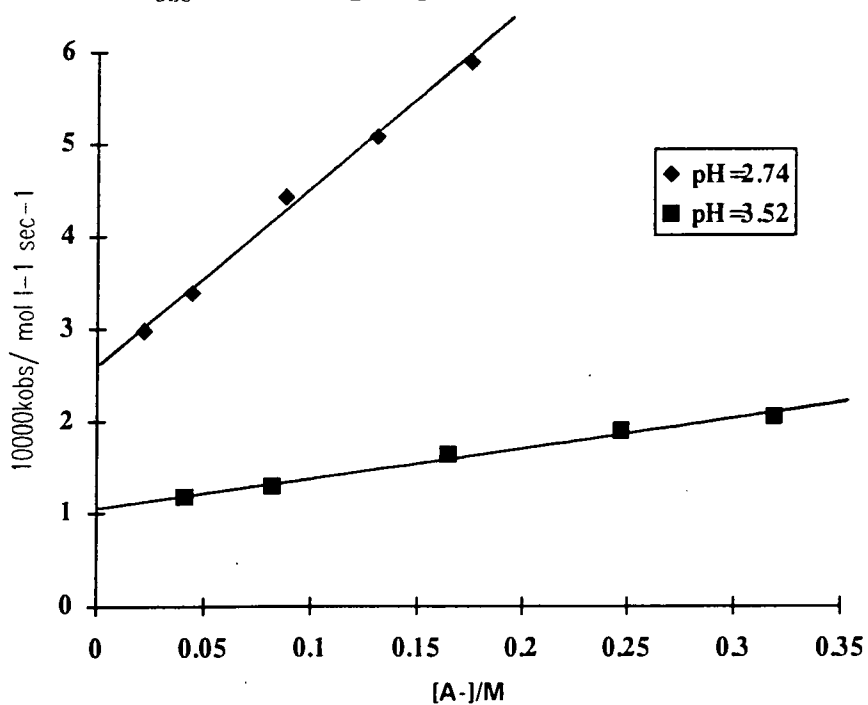


Figure 2.3.2

Plot of k_{obs} vs $[\text{ClCH}_2\text{CO}_2^-]$ at pH=2.74 and pH=3.52



Base catalysis in buffered solutions is expected to occur via two mechanisms;
See Figure 2.3.3.

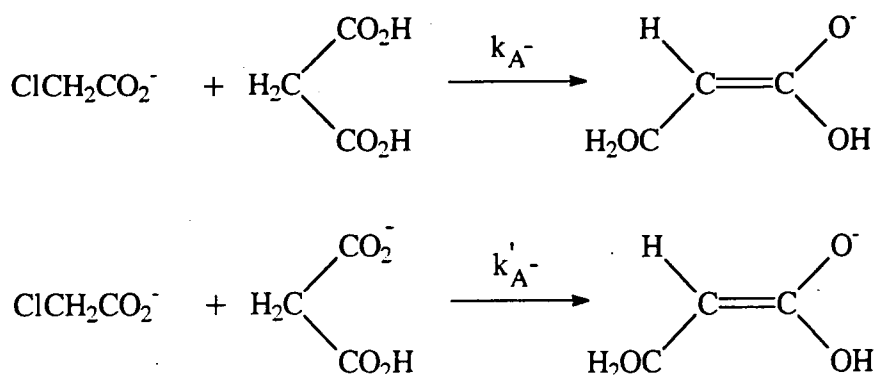


Figure 2.3.3

The concentrations of the dissociated and undissociated malonic acid and monochloroacetic acid (MCAA) are given by the following equations.

$$[\text{MAL}]_e = \frac{[\text{MAL}]_T [\text{H}^+]}{(K_a + [\text{H}^+])}$$

$$[\text{MAL}^-]_e = \frac{[\text{MAL}]_T K_a}{([\text{H}^+] + K_a)}$$

$$[\text{MCAA}]_e = \frac{[\text{MCAA}]_T [\text{H}^+]}{(K'_a + [\text{H}^+])}$$

$$[\text{MCAA}^-]_e = \frac{[\text{MCAA}]_T K'_a}{([\text{H}^+] + K'_a)}$$

Substitution of the above equations in to figure 2.3.3 gives the following kinetic expression.

$$k_{\text{obs}} = k_{\text{MAL}} + \left(\frac{k_{\text{A}} [\text{H}^+] [\text{MAL}]_T}{[\text{H}^+] + K_a} + \frac{k'_{\text{A}} K'_a [\text{MAL}]_T}{[\text{H}^+] + K'_a} \right) [\text{MCAA}^-] \quad \text{equation 2.3.2}$$

k_{MAL} includes all the kinetic terms independent of the MCAA^- . The above equation shows that the slopes obtained from figures 2.3.1 and 2.3.2 should have a characteristic dependence on pH. See Table 2.3.5.

Table 2.3.5

pH	[H ⁺]/ Mol l ⁻¹	slope/ mol l ⁻¹ sec ⁻¹
2.05	8.91 x 10 ⁻³	4.07 x 10 ⁻³
2.25	5.62 x 10 ⁻³	2.55 x 10 ⁻³
2.74	1.82 x 10 ⁻³	1.91 x 10 ⁻³
3.52	3.02 x 10 ⁻⁴	0.317 x 10 ⁻⁴

The slope is given by the following expression.

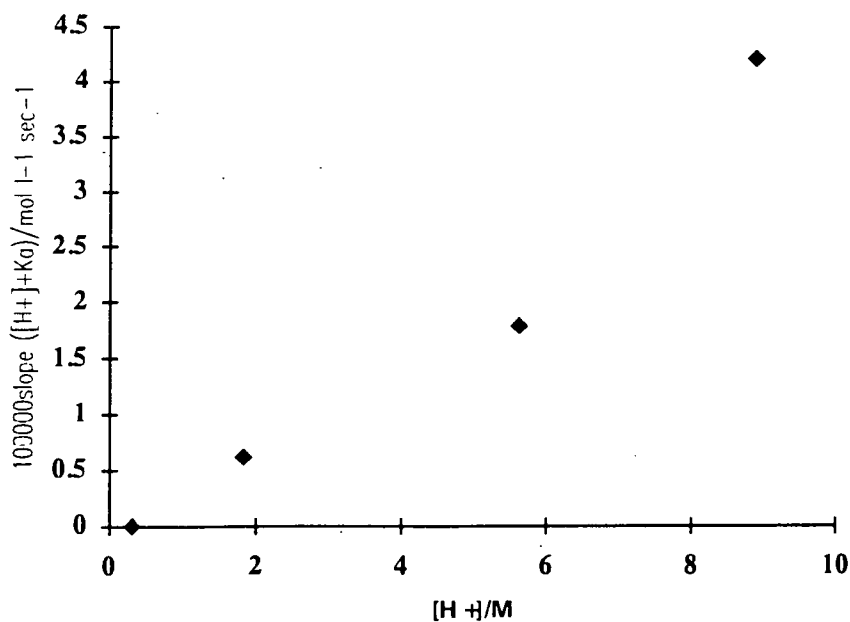
$$\text{Slope} = \frac{k_{A-}[\text{H}^+][\text{MAL}]_T + k'_A - K'_a[\text{MAL}]_T}{[\text{H}^+] + K'_a} \quad \text{equation 2.3.3}$$

Rearranging equation 2.3.3 gives the following expression.

$$\text{Slope}([\text{H}^+] + K'_a) = k_{A-}[\text{H}^+][\text{MAL}]_T + k'_A - K'_a[\text{MAL}]_T \quad \text{equation 2.3.4}$$

Hence a plot of $\text{Slope}([\text{H}^+] + K'_a)$ vs $[\text{H}^+]$ should be linear and from the slope and intercept k_{A-} and k'_A can be calculated. Figure 2.3.4 shows the corresponding plot.

Figure 2.3.4



The graph shows a reasonable straight line considering the large errors involved in taking the slopes of linear plots. The best fit line gives a value for the slope of $4.6 \pm 0.7 \times 10^{-3} \text{ mol l}^{-1} \text{ sec}^{-1}$. which gives a value of;

$$k_{A^-} = 0.09 \pm 0.01 \text{ l mol}^{-1} \text{ sec}^{-1}.$$

The plot has a negative intercept, but the error on the intercept is greater than the value itself. Consequently a value of k'_{A^-} cannot be determined. The value of the catalytic coefficient for mono-chloroacetate is very similar (the same within experimental error) to that for malonate anion. This is entirely expected given that the two anions have the same base strength.

The enolisation of malonic acid was also studied in dichloroacetic acid buffers but no catalysis was observed. Dichloroacetic acid has a pK_a of 1.45 which makes its conjugate base a very weak base. It appears that it is too weak a base to be an effective catalyst and that solvent attack is the dominant reaction.

The effect of metal ions on the enolisation of malonic acid was also investigated. Table 2.3.6 shows the observed zero order rate constant recorded for one metal ion concentration.

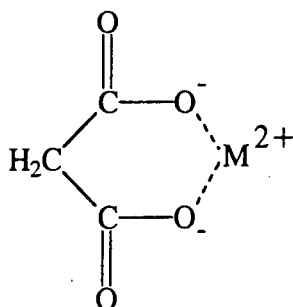
Table 2.3.6

$$[\text{Br}_2] = 2.0 \times 10^{-3} \text{M}, [\text{MAL}]_T = 0.125 \text{M}, [\text{H}^+] = 0.1 \text{M}$$

Metal	Concentration	$10^4 k_{\text{obs}} / \text{mol l}^{-1} \text{ sec}^{-1}$
Copper(II)	0.0046M	6.50
Zinc(II)	0.0010M	6.40
Nickel(II)	0.00982M	6.95
Cobalt(II)	0.0135M	6.56

The observed rate constants show little variation with the metal ion added and are consistent with the rate constants expected when no metal ions are added.

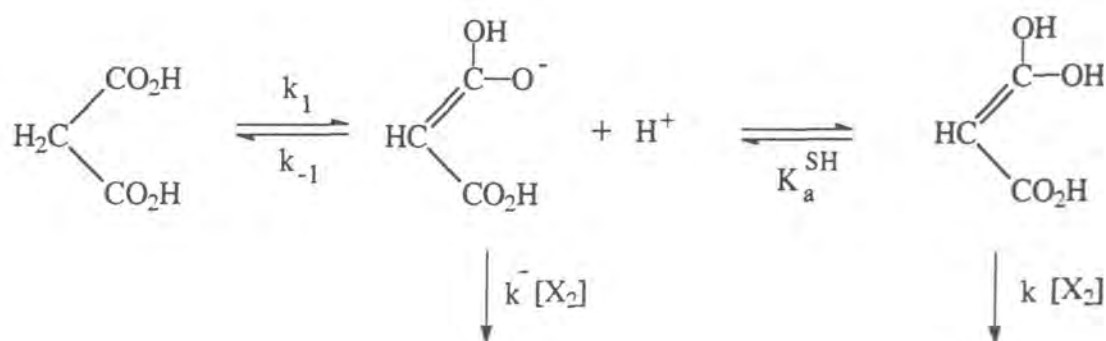
Thus, no metal ion catalysis was observed in 0.1M H^+ . Metal ion catalysis was perhaps expected based on the known co-ordination of ions by the dianion of malonic acid.



In 0.1M H^+ malonic acid will be present in the undissociated form, it appears that this form is not able to complex the metal ions to the same extent as the dianion, consequently metal ions have no effect on the rate of enolisation.

2.4 First order Halogenation of Malonic acid.

Under most experimental conditions the halogenation of malonic acid occurs via rate limiting enolisation. However, under certain conditions it is possible to change the rate determining step of the reaction to that of attack of the halogen on the enol. Under these conditions the reaction is first order in the halogen and first order in malonic acid. See Scheme 2.4.1.



Scheme 2.4.1

A steady state treatment on scheme 2.4.1 gives the following equation 2.4.1.

$$\text{Rate} = \frac{k_1[\text{MAL}] \left(k^- [\text{X}_2] + \frac{k[\text{H}^+][\text{X}_2]}{K_a^{\text{SH}}} \right)}{k_{-1}[\text{H}^+] + \left(k^- [\text{X}_2] + \frac{k[\text{H}^+][\text{X}_2]}{K_a^{\text{SH}}} \right)} \quad \text{equation 2.4.1}$$

Equation 2.4.1 shows that when $k_{-1}[\text{H}^+] \gg k^- [\text{X}_2] + \frac{k[\text{H}^+][\text{X}_2]}{K_a^{\text{SH}}}$ then the kinetics simplify to give the following equation, equation 2.4.2.

$$\text{Rate} = \frac{k_1[\text{MAL}] \left(k^- [\text{X}_2] + \frac{k[\text{H}^+][\text{X}_2]}{K_a^{\text{SH}}} \right)}{k_{-1}[\text{H}^+]} \quad \text{equation 2.4.2}$$

The reaction now shows a first order dependency on the halogen (this is most likely to occur at low $[\text{Br}_2]$ and higher $[\text{H}^+]$) with the following k_{obs} . See equation 2.4.3.

$$k_{\text{obs}} = \frac{k_1[\text{MAL}] \left(k^- + \frac{k[\text{H}^+]}{K_a^{\text{SH}}} \right)}{k_{-1}[\text{H}^+]} \quad \text{equation 2.4.3}$$

The bromination and iodination kinetics were measured using very low halogen concentrations, *ca* 5×10^{-5} M for bromine and 3×10^{-5} for iodine. Using these low concentrations the absorbance changes observed are very small, *ca* 0.01 for bromine and 0.02 for iodine. As a result it was necessary to obtain an average (using a computer averaging program) of approximately 10 runs in order to remove the noise from the kinetic traces. The variation of the first order rate constant with substrate concentration and pH was investigated. Tables 2.4.1 and 2.4.2 shows the results.

Table 2.4.1

$[\text{I}_2] = 2 \times 10^{-5}\text{M}$, ionic strength (I) = 0.16M

$[\text{MAL}]_T/\text{M}$	$[\text{H}^+]/\text{M}$	$k_{\text{obs}}/\text{sec}^{-1}$
0.00625	0.16	0.18
0.0125	0.16	0.43
0.025	0.16	0.82
0.0375	0.16	1.12
0.05	0.16	1.53
0.05	0.12	1.26
0.05	0.08	1.56
0.05	0.04	1.57
0.05	0.02	1.65

Table 2.4.2 $[\text{Br}_2]=5 \times 10^{-5}$, $I=0.16\text{M}$

$[\text{MAL}]_T/\text{M}$	$[\text{H}^+]/\text{M}$	$k_{\text{obs}}/\text{sec}^{-1}$
0.0125	0.16	0.41
0.025	0.16	0.85
0.0375	0.16	1.20
0.05	0.16	1.69
0.05	0.12	1.65
0.05	0.08	1.72
0.05	0.04	1.78
0.10	0.08	3.54
0.15	0.08	5.67

Figures 2.4.1 and 2.4.2 show the linear dependency of the rate constant on malonic acid for the bromination and iodination reactions

Figure 2.4.1

Plot of k_{obs} vs $[\text{MAL}]_{\text{T}}$ for bromination of Malonic acid.

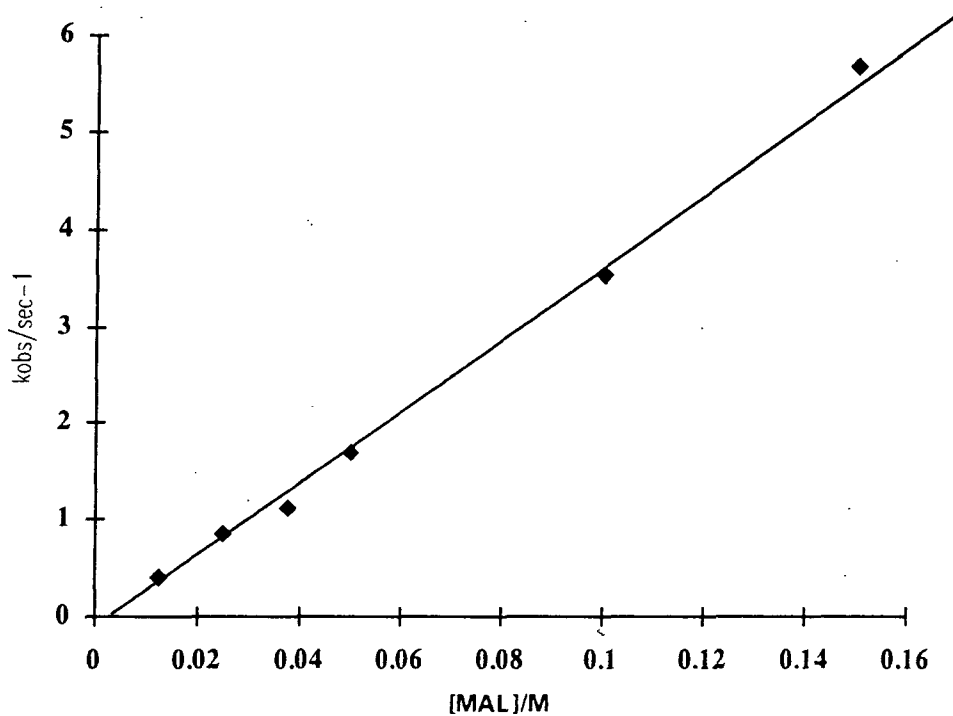
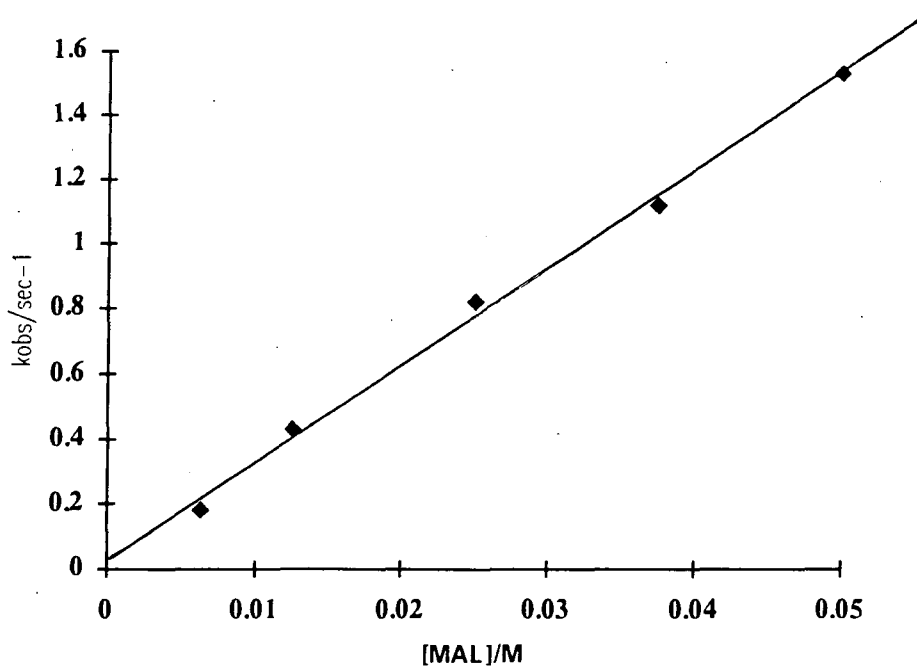


Figure 2.4.2

Plot of k_{obs} vs $[\text{MAL}]_{\text{T}}$ for the Iodination of Malonic acid.



The Tables 2.4.1 and 2.4.2 show that the reaction is independent of acidity and that the reaction is first order in Malonic acid. The reaction is expected to be independent of acidity in strongly acidic solutions because the reaction proceeds exclusively through the enol due to the pK_a of the enol¹² which is estimated to be *ca* 3. Hence equation 2.4.3 simplifies to the following. Equation 2.4.4.

$$k_{\text{obs}} = \frac{k_1 k [\text{MAL}]}{k_{-1} K_a^{\text{SH}}} \quad \text{equation 2.4.4}$$

The ratio k_1/k_{-1} is equivalent to the ionisation of malonic acid as a carbon acid. ie.

$\frac{k_1}{k_{-1}} = K_a^{\text{HS}}$. Thus equation 2.4.4 becomes.

$$k_{\text{obs}} = \frac{K_a^{\text{HS}} k [\text{MAL}]}{K_a^{\text{SH}}} \quad \text{equation 2.4.5}$$

The ratio of the two acidity constant (ionisation of malonic acid as a carbon acid and ionisation of the enol) is equal to the enol content of Malonic acid (K_E).

$$K_E = \frac{K_a^{\text{HS}}}{K_a^{\text{SH}}} \quad \text{equation 2.4.6}$$

Thus k_{obs} is given by the following simple equation.

$$k_{\text{obs}} = K_E k [\text{MAL}] \quad \text{equation 2.4.7}$$

Thus from a plot of k_{obs} vs $[\text{MAL}]$ we can calculate a value of kK_E . The values of kK_E calculated from this work and those calculated from nitrosation reactions are shown in Table 2.4.3

Table 2.4.3

Electrophile	$k K_E / \text{l mol}^{-1} \text{sec}^{-1}$
Bromine	35
Iodine	30
Nitrosyl chloride	46 (ref 7)

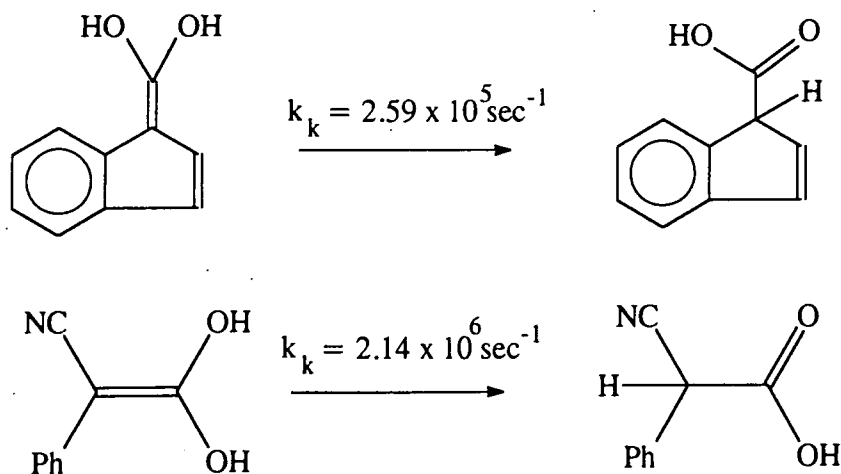
The similarity in the values kK_E for all three electrophiles, suggests that the value of k differs only slightly on changing the electrophile. This is most easily rationalised if the reaction between the enol and the electrophile is at the diffusion controlled limit. Making this assumption a value of $5 \times 10^9 \text{ l mol}^{-1} \text{sec}^{-1}$ can be assigned to k . This allows the calculation of K_E , this gives an average value of

$$K_E = 7.4 \pm 0.9 \times 10^{-9}$$

If the rate of enolisation and the keto \rightleftharpoons Enol equilibrium (K_E) constant is known then it is possible to calculate the rate of ketonisation. Using the average value of K_E gives the following value for the rate of ketonisation of the malonic acid enol.

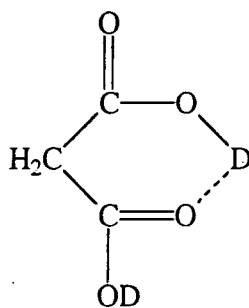
$$k_k = 6.1 \pm 2.4 \times 10^5 \text{ sec}^{-1}$$

Recently Kresge *et al*^{11,12} have measured the rates of ketonisation of carboxylic acid enols by direct measurement of the enol (generated by flash photolysis). The rates of ketonisation of indene-1-carboxylic acid and α -cyanophenylacetic acid are shown.



The rate constant for ketonisation of α -cyanophenylacetic acid is larger than those for malonic acid and indene-1-carboxylic acid. This is due to the presence of two electron withdrawing groups present on the α -carbon, which make the enol of α -cyanophenylacetic acid a very strong acid. ($pK_a=0.99$).

The six membered transition state model⁵ proposed for the enolisation of malonic acid is a very convenient way of explaining the absence of acid catalysis but there is no *direct* evidence to support this. It has been shown (see chapter 3) that the enolisation of compounds without carboxylic acid groups eg. α -cyanoethylacetate also exhibit no acid catalysis, this shows that the ability of a compound to form a six membered ring is not essential for the lack of acid catalysis. Direct evidence for the six membered transition state may come from deuterium isotope effect experiments on the di-deuterated carboxylic acid, see below.



Experiments on the di-deuterated carboxylic acid would have to be carried out in D_2O (or rapid exchange would occur) so there would be an underlying solvent isotope effect which would make it very difficult to interpret the results. Evidence for and against the six membered transition mechanism comes from a comparison with other compounds (see chapters 3 and 5).

Chapter 2 References

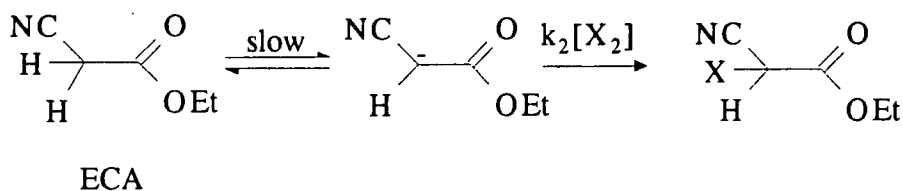
1. K.H. Meyer, *Chem. Ber.*, 1912, **45**, 2864.
2. R.W. West, *J. Chem. Soc.*, 1924, **125**, 1280.
3. W.Petrieff, *Ber.*, **7**, 401.
4. M.Conrad and H.Reinbach, *Ber.*, **35**, 1814.
5. K.R. Leopold and A. Haim, *Int.J.Chem. Kinetic*, 1974, **9**, 83.
6. E.W. Hansen and P.J. Ruoff, *Phys.Chem.*, 1988, **92**, 2641.
7. A. Graham and D.L.H. Williams, *Tetrahedron*, 1992, **37**, 7973.
8. R.J. Field, In "Oscillations and travelling waves in chemical systems"., Wiley, New York, 1985.
9. V.M. Bhale, S.L. Bafna and W.V.Z. Bhagwart, *J. Phys.Chem.*, 1957, **12**, 298.
10. L. Xia, M.Sc. Thesis, 1992, University of Durham.
11. J.Andros, A.J.Kresge, V.V. Popik, *J. Am.Chem. Soc.*, 1994, **116**, 961.
12. J.Andros, Y.Chiang, A.J.Kresge, N.P.Schepp, J.Wirz, *J. Am.Chem. Soc.*, 1994, **116**, 73.
13. J.R. Leis, M.E, Pena, D.L.H. Williams, *J. Chem. Soc. Perkin Trans.2*. 1988, 157.
14. C.G.Swain, *J.Am.Chem.Soc.*, 1950, **72**, 4578.

Chapter 3

Halogenation and deuterium exchange studies of α -cyanoethylacetate.

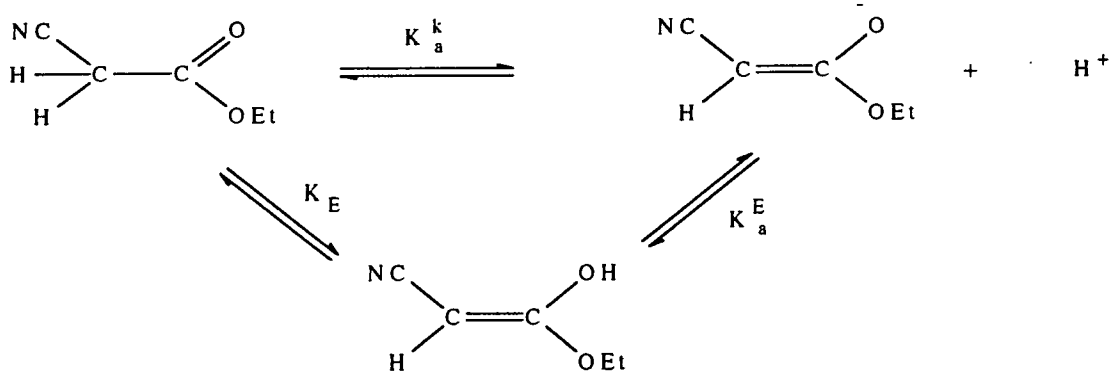
3.1 Introduction

The halogenation of α -cyanoethylacetate (ECA) has been studied by Pearson¹ in 1953. The results were interpreted in terms of a mechanism involving rate limiting ionisation of ECA as a carbon acid, followed by rapid reaction of the carbanion with the halogen (Scheme 3.1.1).



Scheme 3.1.1

Pearson reported no contribution from the enol in the reaction (this is not unexpected since the reactions were carried in neutral solutions). Recent studies on the nitrosation² of ECA have shown that the electrophilic nitrosation in acid solutions can occur via the enol as well as the enolate anion. From these studies an estimated value of the enol content ($\text{p}K_E=11$) has been determined. All the results for nitrosation are consistent with a mechanism involving rate limiting attack of the nitrosating species (NOX , where $\text{X}=\text{Cl}$, Br and SCN) on the enol/enolate anion. So far no rate limiting enolisation process has been observed for ECA in acidic solutions. A value of $\text{p}K_a=11.75$ for the ionisation of α -cyanoethylacetate as a carbon acid has been determined³ from a kinetic study; consequently if a value for the keto \rightleftharpoons enol equilibrium constant can be calculated then information regarding the acidity of the enol can be obtained. See Scheme 3.1.2.



Scheme 3.1.2

The present work attempts to obtain values for the keto \rightleftharpoons enol equilibrium constant and obtain information regarding the enolisation mechanism in acidic solutions.

3.2 Halogenation of α -cyanoethylacetate.

The halogenation of ECA could not be carried out in water because of the insolubility of the compound, thus all experiments were carried out in a 30% dioxan/water mixture (percentage by volume). It was necessary to use the ECA solutions immediately after preparation to avoid hydrolysis of the ester. All the measurements were carried out on a Hi-tech stopped flow spectrophotometer. The previous experiments on the nitrosation² of ECA were also carried out in a 30% dioxan/water mixture so a direct comparison was possible. The reactions were monitored by following the decrease in absorbance due to the the halogen ($\lambda_{\max} = 390\text{nm}$ for bromine and $\lambda_{\max} = 460\text{nm}$ for iodine and $\lambda_{\max} = 323\text{nm}$ for chlorine).

The iodination of ECA was complicated by the interaction of dioxan with iodine. Iodine dissolves in dioxan/water mixtures (up to a concentration of approximately $1 \times 10^{-3}\text{M}$) but only very slowly. This can be speeded up by the use of a sonic bath, however there are problems associated with this as the final dissolved solution always contains a high proportion of tri-iodide. It is known^{4,5} that iodine can form charge transfer complexes with dioxan (See Figure 3.2.1) which can increase the concentration of tri-iodide.

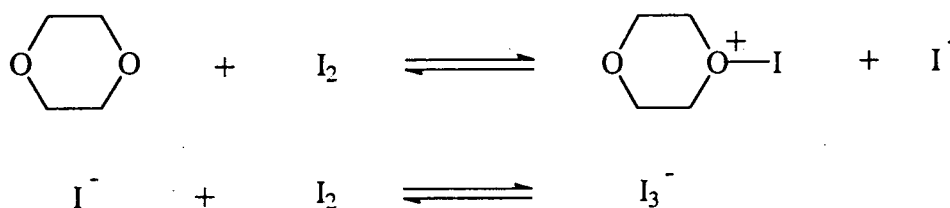
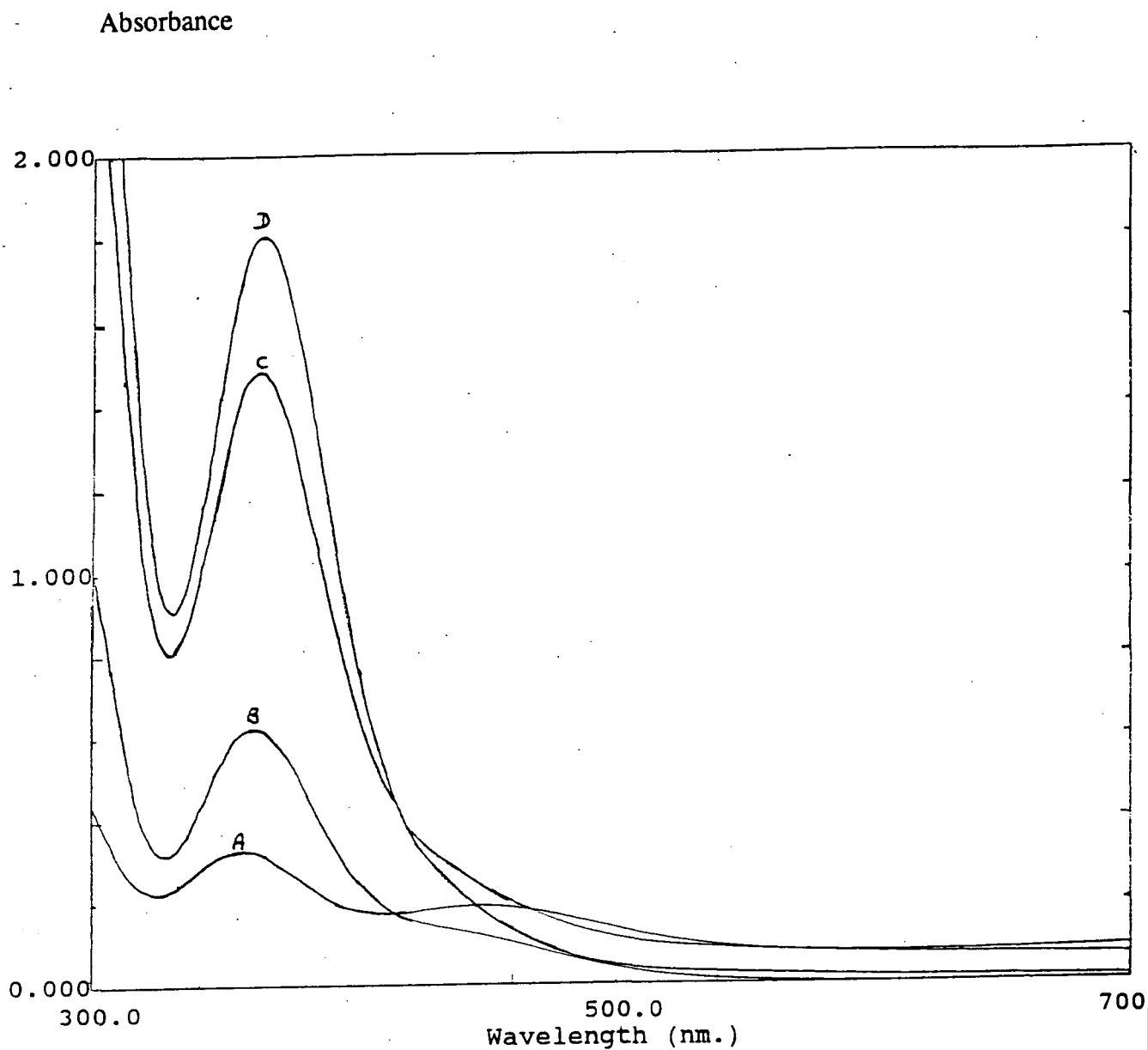


Figure 3.2.1.

Figure 3.2.2. shows how the u.v. spectrum of iodine is affected by the addition of dioxan to an aqueous solution of iodine. Iodine solutions were prepared by mixing an

accurate volume of standardised aqueous iodine solution to the appropriate amount of dioxan rather than dissolving solid iodine in a 30% dioxan/water mixture.

FIGURE 3.2.2



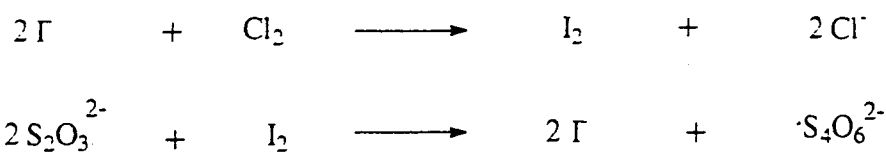
A = 80% water 20% dioxane
B = 60% water 40% dioxane
C = 40 % water 60% dioxane
D = 20% water 80% dioxane

Any aqueous solution of iodine has a small amount of tri-iodide present (the peak at 353nm is due to the presence of tri-iodide ion) but as the percentage of dioxan increases there is a gradual conversion of iodine to tri-iodide.

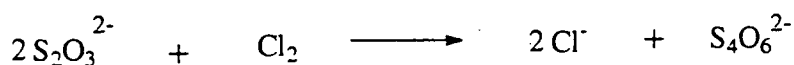
There is also a change in the absorbance maxima for the iodine and tri-iodide species. The maxima for tri-iodide is increased from 353nm in water to 363nm in 80% dioxane/water mixture.

From the known extinction coefficients for iodine ($\epsilon=697 \text{ l mol}^{-1} \text{ cm}^{-1}$ at $\lambda=459\text{nm}$) and tri-iodide ($\epsilon=2.6 \times 10^4 \text{ l mol}^{-1} \text{ cm}^{-1}$ at $\lambda=353\text{nm}$) it is possible to work out the percentage of total iodine which is present as tri-iodide.

Chlorine solutions were prepared by bubbling chlorine gas into a 1M perchloric acid solution. The chlorine was bubbled through for about 30 mins to produce a "saturated" solution. Any excess chlorine was trapped in a flask containing 5% sodium hydroxide. After bubbling for 30 minutes the chlorine solution was transferred to a glass stoppered flask with the minimum of air space to prevent loss of chlorine gas. The saturated solutions of chlorine were diluted ten fold and the resulting solutions were standardised by titrating with iodide followed by titration with sodium thiosulphate ($\text{Na}_2\text{S}_2\text{O}_3$). See scheme 3.2.2.



Overall equation



Scheme 3.2.2

The standardisation of chlorine solutions using iodometry is an inherently inaccurate method due to the problems of loss of chlorine and iodine during the titration. The loss of iodine can be overcome by adding an excess of iodide, which converts the

iodine to the much less volatile tri-iodide. Using the standardised chlorine solutions a value for the extinction coefficient at $\lambda_{\text{max}}=323\text{nm}$ was determined as $\epsilon=53\pm 2 \text{ l mol}^{-1} \text{ cm}^{-1}$ in 0.5M perchloric acid. This value of the extinction coefficient was subsequently used to determine the concentration of the chlorine solutions used in the kinetic studies. The chlorine solutions prepared were used immediately because of the volatility of the chlorine.

Bromine solutions were prepared in the usual manner, by dissolving neat bromine in a solution of dioxan/water. The u.v.-vis spectrum of bromine was not affected by the presence of dioxan and the reaction was studied in the usual manner by monitoring the decrease in bromine absorbance at $\lambda_{\text{max}} = 395\text{nm}$.

The iodination of ECA was studied in the pH range 1-6 using the following buffer solutions:

pH 1.5 - 3.5 chloroacetic acid buffer ($\text{pK}_a=2.75$).

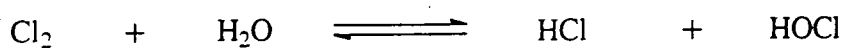
pH 3.5 - 5.5 phthalate buffer ($\text{pK}_a=5.41$).

and in strongly acidic solutions.

The reaction was found to be first order in iodine under all conditions, this indicates that the rate limiting step is attack of the iodine on the enol or enolate anion intermediate. The variation in the first order rate constant with pH and substrate concentration was investigated. No zero order rate constants could be determined, even at high iodine concentration and high pH. The inability to 'force' the reaction into the case where enolisation/ionisation of the ECA is rate limiting may be due to the presence of tri-iodide in the solution which is known⁶ to be less reactive than iodine. The bromination of ECA was studied in acidic solutions up to $\text{pH}=1$. With the bromination reactions it was not possible to obtain good first order data at pH values higher than 1 (cf iodine above). The absorbance versus time plots obtained were characteristic of dibromination reactions. Bell⁷ has reported that the second step in bromination reactions is significantly faster than the first and that the rate increases with pH. The difference between bromine and iodine may be due to a steric effect in which the larger iodine atom reduces the rate of di-iodination. The reactions showed

good first order dependency on bromine and the effect of pH and substrate concentration on the rate was investigated. Again, no zero order kinetics could be obtained for the bromination reactions.

The chlorination of ECA was carried in acidic solutions. The reaction was not studied over a higher pH range because the molecular chlorine is hydrolysed to hypochlorous acid at higher pH values. See scheme 3.2.3.



Scheme 3.2.3

Good first order kinetics were obtained and the variation in the first order rate constant with acidity and substrate concentration was investigated.

The results for all three halogens are shown in tables 3.2.1 - 3.2.6.

Table 3.2.1

$$[\text{Br}_2] = 5 \times 10^{-4} \text{ M} \quad [\text{ECA}] = 0.05 \text{ M}$$

$[\text{H}^+] / \text{M}$	$10^2 k_{\text{obs}} / \text{sec}^{-1}$
0.10	7.12
0.20	6.82
0.30	6.61
0.40	6.92
0.50	7.03
0.70	6.88
1.00	6.76

Table 3.2.2

$$[\text{Br}_2] = 5 \times 10^{-4} \text{ M} \quad [\text{H}^+] = 0.10 \text{ M}$$

[ECA]/M	$10^2 \times k_{\text{obs}} / \text{sec}^{-1}$
0.05	9.30
0.075	14.60
0.10	18.40
0.15	28.80
0.20	37.40

Table 3.2.3

$$[\text{I}_2] = 6.0 \times 10^{-4} \text{ M} \quad [\text{H}^+] = 0.1 \text{ M}$$

[ECA]/M	$10^2 k_{\text{obs}} / \text{sec}^{-1}$
0.05	5.62
0.075	7.63
0.10	9.20
0.15	11.50
0.20	13.40

Table 3.2.4 $[I_2] = 6.0 \times 10^{-4} \text{ M}$ $[ECA] = 0.05 \text{ M}$

pH	$[H^+] / \text{M}$	$k_{\text{obs}} / \text{sec}^{-1}$
0.40	0.398	0.0787
0.52	0.302	0.0730
0.70	0.200	0.0663
0.82	0.151	0.0558
1.00	0.10	0.0499
1.53	0.0295	0.0730
1.69	0.0204	0.0640
2.97	0.00107	0.0931
3.32	0.000479	0.185
3.57	0.000269	0.371
4.50	0.0000316	1.31
5.24	0.00000575	14.84

Table 3.2.5 $[Cl_2] = 1 \times 10^{-3} \text{ M}$ $[H^+] = 0.525 \text{ M}$

$[ECA] / \text{mol l}^{-1}$	$k_{\text{obs}} / \text{sec}^{-1}$
0.025	0.0459
0.050	0.0735
0.100	0.1145
0.150	0.1798
0.200	0.2415

Table 3.2.6

$[\text{Cl}_2] = 1.5 \times 10^{-3} \text{ M}$

$[\text{ECA}] = 0.05 \text{ M}$

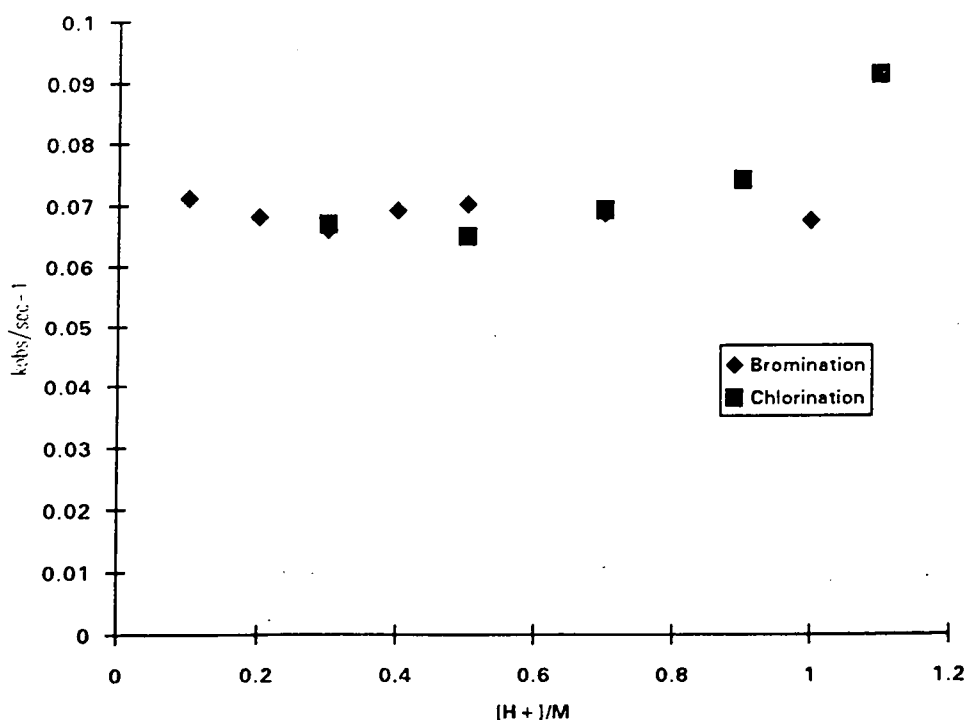
$[\text{H}^+]/\text{mol l}^{-1}$	$k_{\text{obs}}/\text{sec}^{-1}$
0.3	0.0670
0.5	0.0651
0.7	0.0693
0.9	0.0742
1.1	0.0915

Tables 3.2.1, 3.2.4 and 3.2.6 show that the halogenation of ECA is independent of acid concentration at low pH.

Figure 3.2.3 shows the variation in the k_{obs} with acidity for the bromination and chlorination.

Figure 3.2.3

Plot of k_{obs} versus $[\text{H}^+]/\text{M}$ for the bromination and chlorination of ECA



This kinetic saturation at low pH is characteristic of reactions involving enol intermediates with rate limiting attack of the halogen on the enol.

The acid dependency for the iodination reaction is shown in figure 3.2.4

Figure 3.2.4
Plot of k_{obs} versus pH for the iodination of ECA

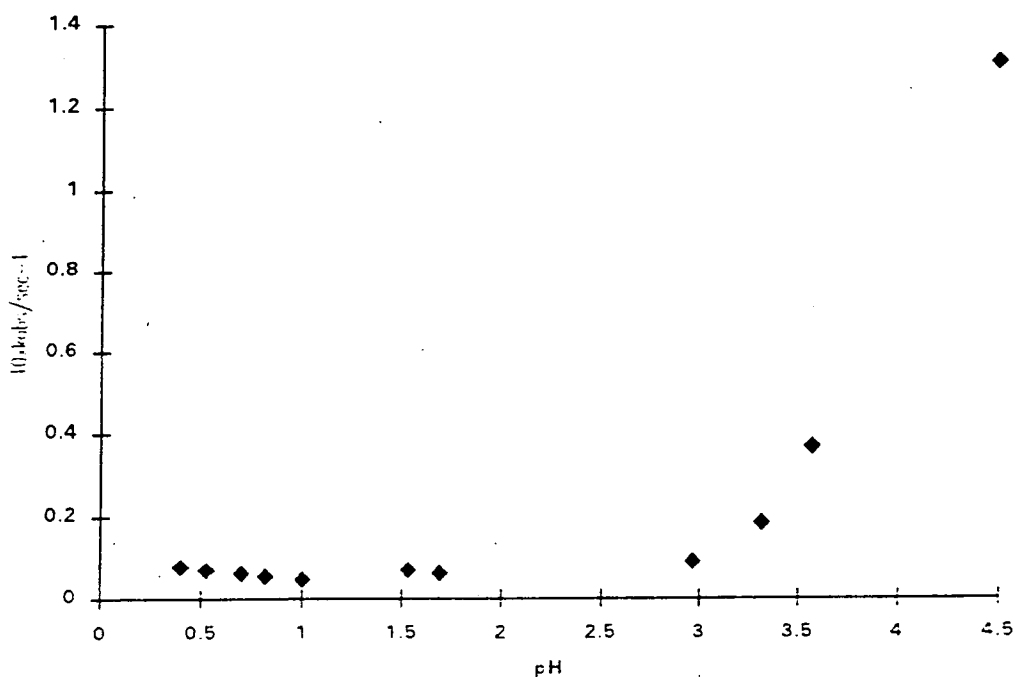
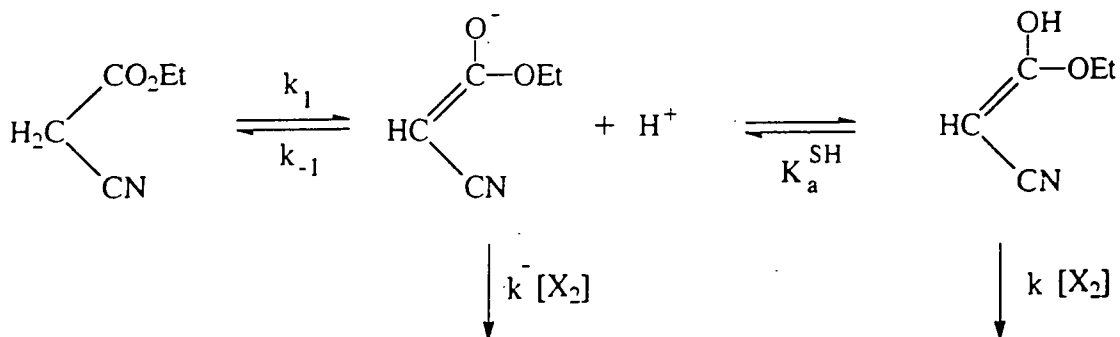


Figure 3.2.4 shows that the iodination of ECA is independent of acidity at low pH but increases rapidly as the pH increases. These results can be interpreted in terms of the following mechanistic scheme. (scheme 3.2.4).



Scheme 3.2.4

A steady state treatment on scheme 3.2.4 gives the following kinetic expression

$$\text{Rate} = \frac{k_1[\text{ECA}] \left(k^- [\text{X}_2] + \frac{k[\text{H}^+][\text{X}_2]}{K_a^{\text{SH}}} \right)}{k_{-1}[\text{H}^+] + \left(k^- [\text{X}_2] + \frac{k[\text{H}^+][\text{X}_2]}{K_a^{\text{SH}}} \right)} \quad \text{Equation 3.2.1}$$

Equation 3.2.1 show that when the rate of re-protonation of the enolate anion ($k_{-1}[\text{H}^+]$) is much faster than the reaction of the enol and enolate anion with the halogen then equation 3.2.1 simplifies to the following. See equation 3.2.2

$$\text{Rate} = \frac{k_1[\text{ECA}] \left(k^- [\text{X}_2] + \frac{k[\text{H}^+][\text{X}_2]}{K_a^{\text{SH}}} \right)}{k_{-1}[\text{H}^+]} \quad \text{Equation 3.2.2}$$

Equation 3.2.2 shows that there should be a first order dependency on the halogen (as is determined experimentally) and that k_{obs} is given by the following expression.

$$k_{\text{obs}} = \frac{k_1[\text{ECA}] \left(k^- + \frac{k[\text{H}^+]}{K_a^{\text{SH}}} \right)}{k_{-1}[\text{H}^+]} \quad \text{Equation 3.2.3}$$

Equation 3.2.3 shows that when $[\text{H}^+]$ is high then the reaction proceeds through the enol only and equation 3.2.3 gives the following expression for k_{obs} . See equation 3.2.4.

$$k_{\text{obs}} = \frac{k_1 k [\text{ECA}]}{k_{-1} K_a^{\text{SH}}} \quad \text{Equation 3.2.4}$$

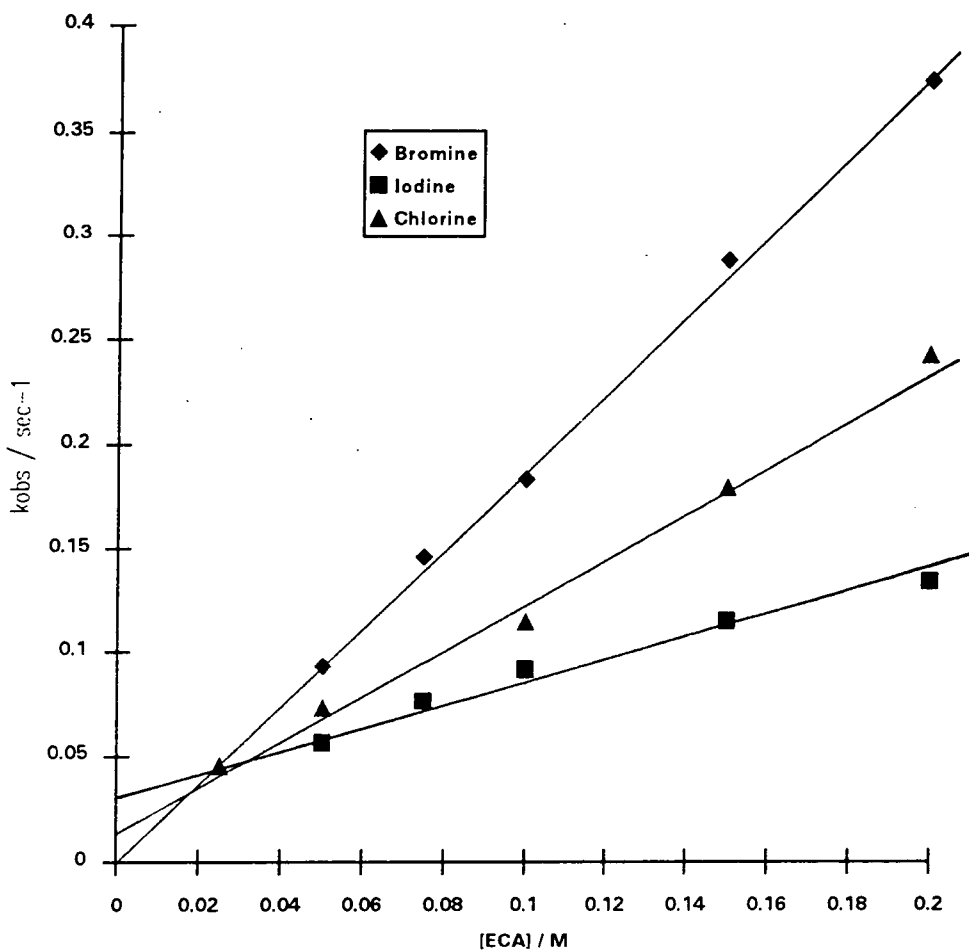
Equation 3.2.4 can be simplified to the following, Where, K_E is the keto enol equilibrium constant.

$$k_{\text{obs}} = k K_E [\text{ECA}] \quad \text{Equation 3.2.5}$$

Equation 3.2.5 show that k_{obs} should have a linear dependency on the concentration of ECA. Figure 3.2.5 shows the plots obtained for the three different halogens.

Figure 3.2.5

Plot of k_{obs} vs [ECA] concentration for chlorine bromine and iodine



The iodination reaction plot has a considerable intercept on the y-axis which is diagnostic of a reversible reaction. This is not unexpected because of the increased concentration of iodide and the greater nucleophilicity of iodide. Toulecc⁶ has shown that the equilibrium constant in iodination reactions can be approximated by the following equation where K_a is the carbon acidity of the substrate.

$$K_{\text{Iod}} = \frac{3 \times 10^{-4}}{K_a^{0.3}}$$

From the substrate dependency (See figure 3.2.5) and acid dependency (See figures 3.2.3 and 3.2.4) a value of kK_E can be calculated. Table 3.2.7 shows the values of kK_E determined.

Table 3.2.7

HALOGEN	$kK_E / \text{l mol}^{-1} \text{ sec}^{-1}$		
	chlorine	bromine	iodine
ACID dependency	1.47 ± 0.09	1.37 ± 0.07	1.46 ± 0.05
SUBSTRATE dependency	1.11 ± 0.06	1.88 ± 0.05	0.52 ± 0.04

In the case of iodine the reaction can be studied at much higher pH values and under these conditions the reaction proceeds through the enolate anion as well as through the enol. Consequently the reaction is not expected to be independent of pH, but will vary with acidity according to equation 3.2.6.

$$k_{\text{obs}} = \frac{k_1[\text{ECA}] \left(k^- + \frac{k[\text{H}^+]}{K_a^{\text{SH}}} \right)}{k_{-1}[\text{H}^+]} \quad \text{Equation 3.2.6}$$

Equation 3.2.6. can be re-arranged to the following. Equation 3.2.7.

$$k_{\text{obs}}[\text{H}^+] = \frac{(k_1 k^- K_a^{\text{SH}} + k k_1 [\text{H}^+]) [\text{ECA}]}{k_{-1} K_a^{\text{SH}}} \quad \text{Equation 3.2.7}$$

Using expressions for the carbon acidity of ECA: ($K_a^{HS} = \frac{k_1}{k_{-1}}$) and the keto enol

equilibrium constant: ($K_E = \frac{k_1}{k_{-1}K_a^{SH}}$) Equation 3.2.7 simplifies to the following.

Equation 3.2.8.

$$k_{obs}[H^+] = (K_a^{HS}k^- + K_Ek[H^+])[ECA] \quad \text{Equation 3.2.8.}$$

equation 3.2.8. shows that a plot of $k_{obs}[H^+]$ against $[H^+]$ should show a linear relationship. Figure 3.2.8 shows the corresponding plot.

Figure 3.2.8

Plot of $k_{obs}[H^+]$ against $[H^+]$, $[ECA]=0.05M$

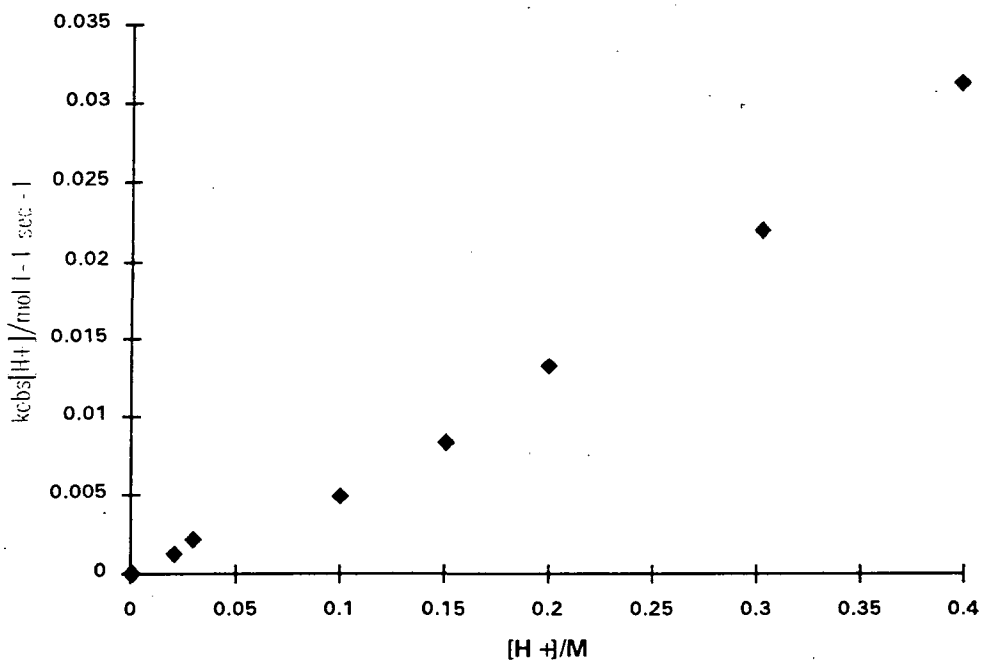


Figure 3.2.8 shows a reasonable linear relationship, the best fit line gives a slope of $0.074 \pm 0.003 \text{ sec}^{-1}$ which gives a value of 1.49 for kK_E (cf. Table 3.2.7). Unfortunately, the intercept gives a small negative value. The intercept is expected to be small, from the known carbon acidity² of ECA and assuming the enolate anion

reacts with the halogen at the diffusion controlled limit ($k^- = 5 \times 10^9 \text{ l mol}^{-1} \text{ sec}^{-1}$) a value of $4.5 \times 10^{-4} \text{ mol l}^{-1} \text{ sec}^{-1}$ for the intercept is expected.

3.3 Discussion

Table 3.2.7 shows the values of kK_E obtained for the three different halogens studied. The values show very little variation with the halogen. This result is interpreted as meaning that the reaction of the enol with the halogen occurs at the diffusion controlled limit. It has been shown by A.J.Kresge⁸ that reaction of simple enols with halogens is almost a diffusion controlled limit but there is a slight variation in k with the structure of the enol. It is expected that the reaction of enols derived from carboxylic acid derivatives with halogens will be a diffusion controlled process given their greater reactivity. The greater reactivity of these enols may be due a significant contribution from a charge separated canonical form whereby a significant amount of negative charge is located on the α -carbon. See figure 3.3.1.

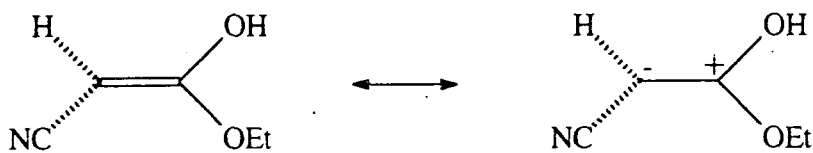


Figure 3.3.1

Consequently, the enol reacts more as a carbanion than a 'conventional' double bonded enol. A significant contribution from a charge separated canonical form has been reported by Ainsworth¹⁰ who studied the N.M.R. spectrum of dimethoxycarbonylsilylacetal ketene. See figure 3.3.2.

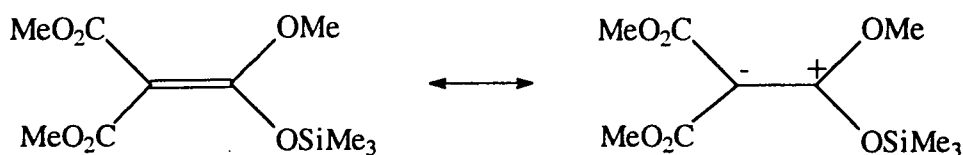


Figure 3.3.2

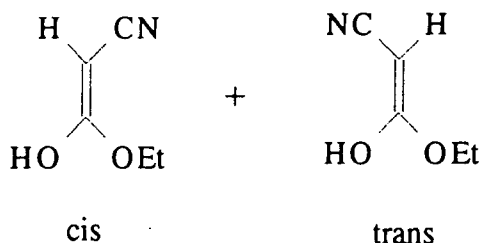
Using proton N.M.R. it can be shown that the methyl groups of the methoxycarbonyl moieties are equivalent. This suggests that there is relatively fast rotation about the double bond which is due to a significant contribution from the charge separated canonical form. It is well known¹¹ that the hydroxyl group is better able to stabilise a positive charge than an alkoxide group ($\sigma^+(\text{OH}) = -0.92, \sigma^+(\text{OMe}) = -0.78$). This is due to the ability of the hydroxyl group to disperse the positive charge onto the neighbouring solvent molecules via hydrogen bonding.

Hence the charge separated form should be more favoured in enol derivatives than in the case of ketene acetals.

Using the assumption that reaction of the enol with the halogens is at the diffusion limit then a value of $k = 5 \times 10^9 \text{ l mol}^{-1} \text{ sec}^{-1}$ can be used. Using this value an average value for the keto \rightleftharpoons enol equilibrium (K_E) can be calculated.

$$K_E = 2.6 \pm 0.4 \times 10^{-10}$$

The enol form of ECA can exist in cis and trans forms. The K_E determined represents the total enol content of ECA (cis and trans forms).



It may be expected that the trans form will be the most stable due to a weak hydrogen bond between the -OH group and the cyano group. This interaction will be fairly

weak because the linear cyano group can't bend round to form a tight six membered ring structure. (cf. malonic acid enol. Chapter 2).

Recent studies² on the nitrosation of ECA gave an estimated minimum value of $K_E = 5 \times 10^{-12}$. This value was calculated on the basis of a diffusion controlled reaction between nitrosyl thiocyanate (NOSCN) and the enol form of ECA. In the light of these results it appears that this reaction is not at the diffusion limit, but has a value of ca. $8 \times 10^7 \text{ l mol}^{-1} \text{ sec}^{-1}$. This is not unexpected since NOSCN is a relatively unreactive electrophile and diffusion controlled reactions involving NOSCN are only observed with very reactive carbanions i.e. the carbanions formed from malononitrile¹⁴ and diethylmalonate². The new value of K_E determined can be used with a value of the carbon acidity of ECA to obtain an estimate of the acidity of the enol. See Figure 3.3.4.

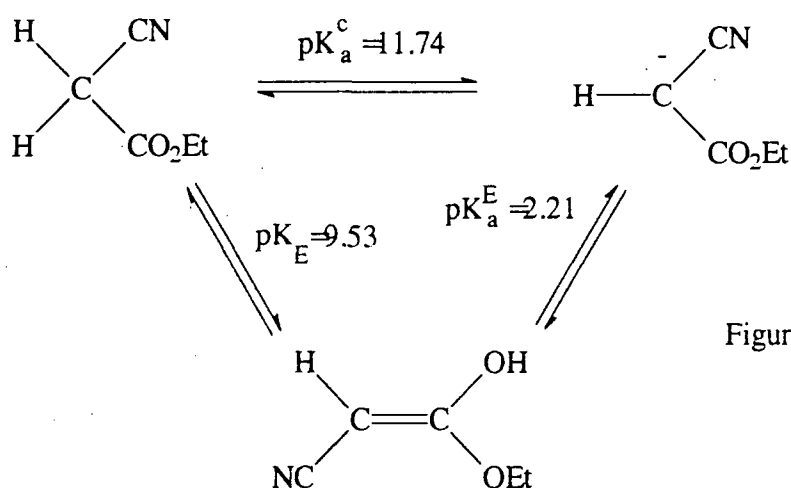


Figure 3.3.4

This gives a value of 2.21 for the pK_a of the enol. Thus the enol formed from ECA is a very strong acid (cf. chloroacetic acid $pK_a = 2.85$). Enols formed from simple carbonyl compounds are much less acid. The pK_a of propen-2-ol¹⁵ (acetone enol) is ca 11. Kresge¹⁶ *et al* have measured the acidity of 2-cyano-2-phenylethen-1,1-diol (enol formed from 2-cyano-2-phenylacetic acid). They have reported the following value. See figure 3.3.5.

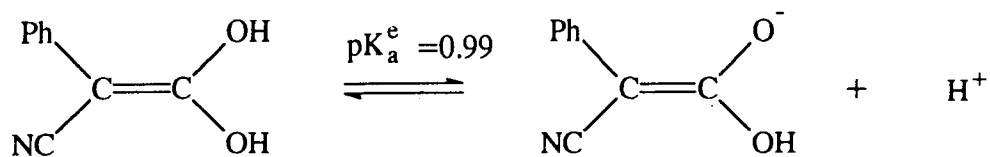


Figure 3.3.5

The greater acidity of 2-cyano-2-phenylethene-1,1-diol is presumably due to the presence of the phenyl group. The large difference in acidity between 1,1-enediols and enols may be due to a large contribution from a charge separated canonical form in the case of 1,1-enediols. See Figure 3.3.6.

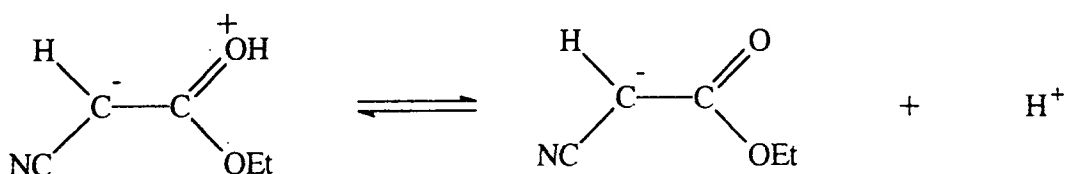


Figure 3.3.6

In all the studies carried out on the electrophilic substitution reactions (nitrosation and halogenation) of ECA it has never been possible to 'force' the reaction into conditions where the rate limiting step is ionisation of ECA. It has been noticed that for carboxylic acid derivatives containing α -cyano groups it is very difficult to obtain conditions where enolisation is rate limiting. For compounds not containing α -cyano groups eg. malonic acid and ethylhydrogenmalonate it is usually possible to obtain rate limiting enolisation of the substrate. In order to obtain rate limiting enolisation of the substrate the rate of reaction of the enol with the halogen must be much greater than the rate of ketonisation of the enol. The presence of the cyano group should have a significant effect on the rate constant for reaction of the halogen with the enol, but if this reaction is at the diffusion limit the effect in this case will be small. Hence the cyano group must be increasing the rate constant for ketonisation, making it more difficult to obtain rate limiting enolisation. The increased rate of ketonisation may be

due to the acid strength of 2-cyano-1,1-enediols. ketonisation occurs via ionisation of the enol and reprotonation of the carbanion. See Figure 3.3.7.

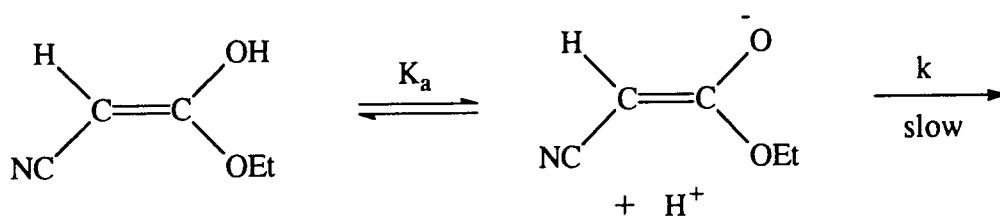


Figure 3.3.7

Under these conditions the rate constant for ketonisation is:

$$k_{\text{keto}} = K_a k$$

Thus the rate of ketonisation depends on the acidity of the enol, and it has been shown in this work and work by Kresge¹⁶ that 1,1-enediols with strong electron withdrawing groups (such as a cyano group) in the 2- position are strong acids.

The difficulty in obtaining rate limiting enolisation kinetics from halogenation and nitrosation kinetics necessitated the use of a different technique. The technique employed was deuterium exchange, monitored by N.M.R. Section 3.4 describes this technique and the results obtained.

3.4 Deuterium exchange in α -cyanoethylacetate

3.4.1 Introduction

As mentioned in section 3.3 the rate of enolisation of ECA cannot be measured by classical halogenation studies. An alternative procedure using P.M.R (proton magnetic resonance) has been used to measure enolisation rates by monitoring the exchange of methylene protons for deuterium. Hansen and Ruoff¹⁷ have used this technique to measure the enolisation of malonic acid. The results are consistent with those obtained from halogenation studies.

When ECA is placed in deuterium oxide (D_2O) exchange of the two methylene protons occurs via the enol of ECA. See Figure 3.4.1.

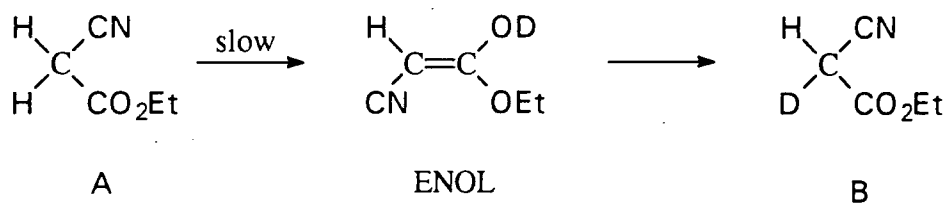


Figure 3.4.1

When the reaction is carried out in pure deuterium oxide the conversion to the enol is effectively irreversible due to the small amount of H_2O present. In figure 3.4.1. the rate of ketonisation of the enol is much faster than the rate of enolisation, consequently the rate of deuterium exchange corresponds to the rate of enolisation. If the reaction is left for long enough complete exchange occurs and both methylene hydrogens are replaced.

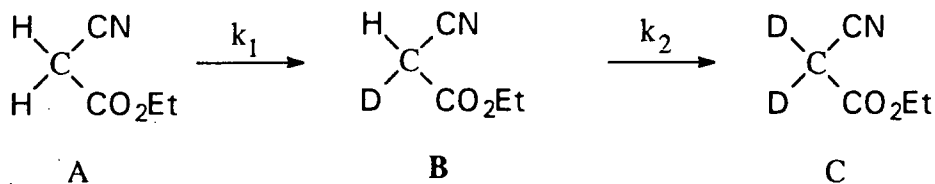


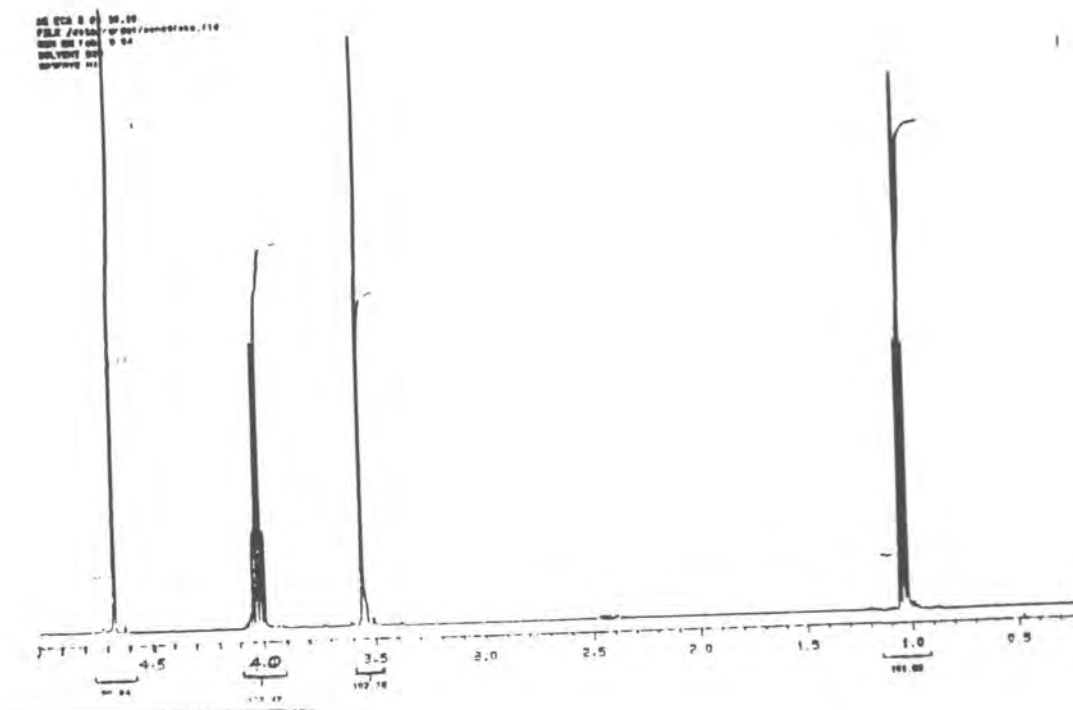
Figure 3.4.2

From the deuterium exchange kinetics k_1 and k_2 can be measured. These provide information regarding the deuterium solvent isotope effect and secondary substrate isotope effect.

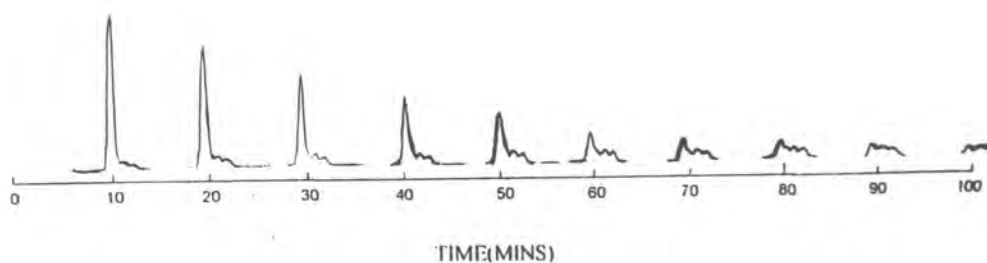
3.4.2 Results

The kinetics of deuterium exchange were measured by monitoring the ^1H N.M.R. spectrum of ECA as a function of time. The N.M.R. samples were prepared by adding a small volume of pure ECA (ca 0.1cm^3) to a standard $\text{D}_2\text{O}/\text{D}_2\text{SO}_4$ solution. Both solutions were maintained at 25°C prior to mixing. No temperature control was available once the N.M.R. tube was in the machine. The reactions were too rapid to allow the N.M.R. tube to be removed between taking spectra and thermostatted at 25°C . Figure 3.4.3 show a typical experiment and shows how the spectrum of ECA changes with time.

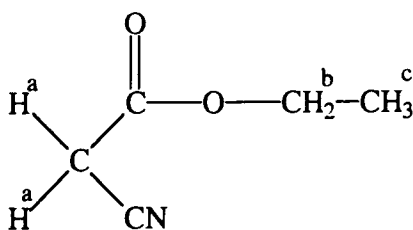
Figure 3.4.3
Initial spectrum of ECA in D₂O



Variation in peak at 3.34ppm with time

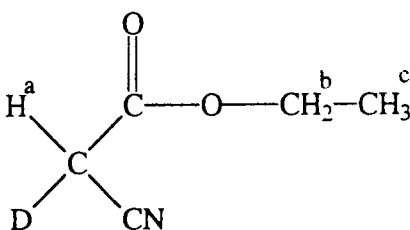


Initially the spectrum of ECA shows three peaks:



H ^a	δ=3.35ppm	singlet	2H
H ^b	δ=3.80ppm	quartet	2H
H ^c	δ=0.80ppm	triplet	3H

The methylene protons (H^a) are gradually exchanged for deuterium. This is shown by the appearance of a 1:1:1 triplet at 3.34ppm which is due to the mono-deuterated ECA {ECA(D)}. The triplet occurs due to coupling with the deuterium which has a spin quantum number of 1.



H ^a	δ=3.34ppm	1:1:1 triplet	1H
----------------	-----------	---------------	----

The protons in the ethylester group (H^b and H^c) are not exchanged for deuterium and consequently remain unchanged throughout any kinetic run. These protons can be used as a reference signal to calibrate the spectra.

From the peak integrals for H^a at 3.35ppm it is possible to determine the concentration of ECA and ECA(D) for each spectrum. The concentration of di-deuterated ECA (ECA(D₂)) can't be observed by ¹H N.M.R. but its concentration can be determined from the following mass balance equation. See equation 3.4.1.

$$[\text{ECA}]_{\text{T}} = [\text{ECA}] + [\text{ECA}(\text{D})] + [\text{ECA}(\text{D}_2)]$$

Equation 3.4.1

The effect of acidity (in the range 0.08M-0.4M) on the rate of deuterium exchange was investigated. Tables 3.4.1-3.4.3 show the concentrations of [ECA], [ECA(D)] and [ECA(D₂)] recorded as a function of time for three different acid concentrations.

Table 3.4.1

[ECA] = 0.209M [D⁺] = 0.39M T = 298K

Time/ sec	[ECA]	[ECA(D)]	[ECA(D ₂)]
0	0.209	0.00	0.00
300	0.152	0.022	0.035
900	0.120	0.046	0.043
1500	0.085	0.091	0.033
2100	0.072	0.089	0.048
2700	0.060	0.089	0.060
3300	0.039	0.102	0.068
3900	0.031	0.100	0.078
4500	0.030	0.085	0.094
5100	0.019	0.089	0.101
6000	0.013	0.076	0.120
6900	0.005	0.073	0.131
7800	0.002	0.067	0.140

Table 3.4.2

[ECA] = 0.209M [D⁺] = 0.20M T = 298K

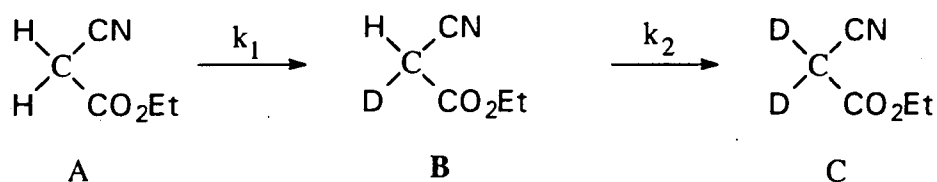
Time/ sec	[ECA]	[ECA(D)]	[ECA(D ₂)]
0	0.209	0.00	0.00
300	0.155	0.040	0.015
900	0.115	0.072	0.023
1500	0.088	0.080	0.041
2100	0.063	0.090	0.056
2700	0.0399	0.093	0.076
3300	0.0294	0.099	0.081
3900	0.0261	0.085	0.098
4500	0.0199	0.078	0.118
5100	0.0191	0.080	0.117
6000	0.0120	0.069	0.133
6900	0.0067	0.057	0.146
7800	0.0063	0.055	0.154

Table 3.4.3

[ECA] = 0.209M [D⁺] = 0.08M T = 298K

Time/ sec	[ECA]	[ECA(D)]	[ECA(D ₂)]
0	0.209	0.00	0.00
600	0.149	0.047	0.013
1200	0.098	0.077	0.034
1800	0.083	0.069	0.057
2400	0.046	0.076	0.087
3000	0.044	0.056	0.106
3600	0.025	0.072	0.112
4200	0.023	0.066	0.121
4800	0.014	0.064	0.131
5400	0.012	0.052	0.145
6300	0.0068	0.044	0.158
7200	0.0052	0.044	0.160
8100	0.000	0.041	0.168

The experimental results can be interpreted in terms of a sequential reaction. See scheme 3.4.1.



scheme 3.4.1

where k_1 and k_2 represent the rates of enolisation of ECA and ECA(D) respectively. Applying a standard sequential reaction treatment (see experimental section for a derivation) then the following expressions for ECA, ECA(D) and ECA(D₂) can be used.

$$[\text{ECA}] = [\text{ECA}]_0 e^{-k_1 t} \quad \text{Equation 3.4.2}$$

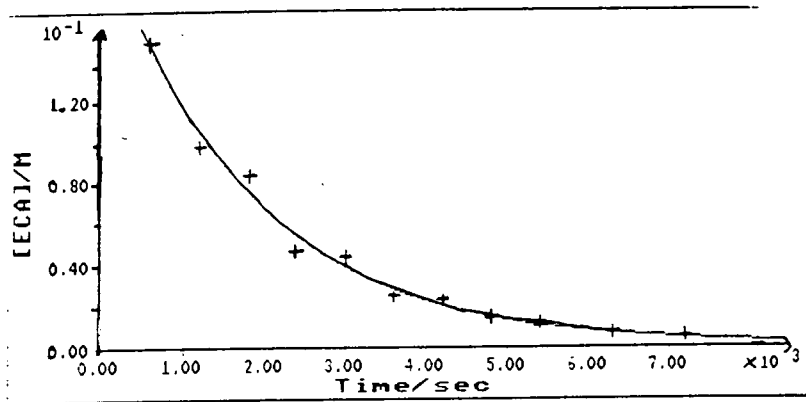
$$[\text{ECA(D)}] = k_1 [\text{ECA}]_0 \left(\frac{e^{-k_1 t} - e^{-k_2 t}}{k_2 - k_1} \right) \quad \text{Equation 3.4.3}$$

$$[\text{ECA(D}_2\text{)}] = [\text{ECA}]_0 \left[1 + \left(\frac{k_1 e^{-k_1 t} - k_2 e^{-k_2 t}}{k_2 - k_1} \right) \right] \quad \text{Equation 3.4.4}$$

A value of k_1 was determined by fitting the results to a standard exponential equation using equation 3.4.2. The value of k_1 was then used in equation 3.4.3 to obtain a value for k_2 . Figures 3.4.4-3.4.9. shows the exponential fits to obtain k_1 and the fits to equation 3.4.3. to obtain k_2 .

Figure 3.4.4

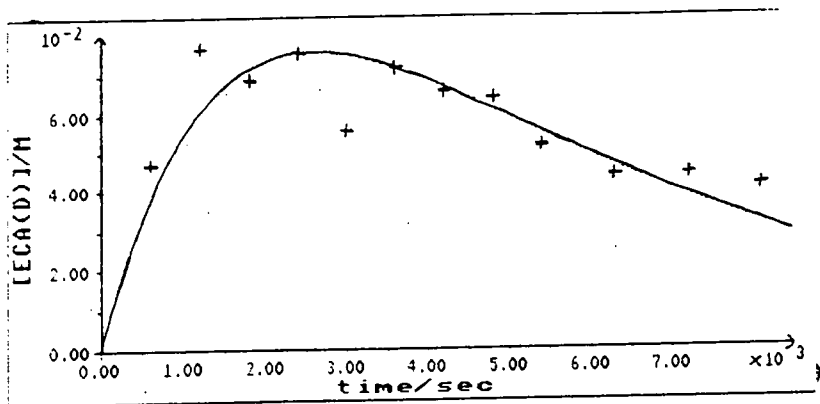
[ECA]=0.209M, [D⁺]=0.08M, T=298K



$$k_1 = 5.62 \pm 0.48 \times 10^{-4} \text{ sec}^{-1}$$

Figure 3.4.5

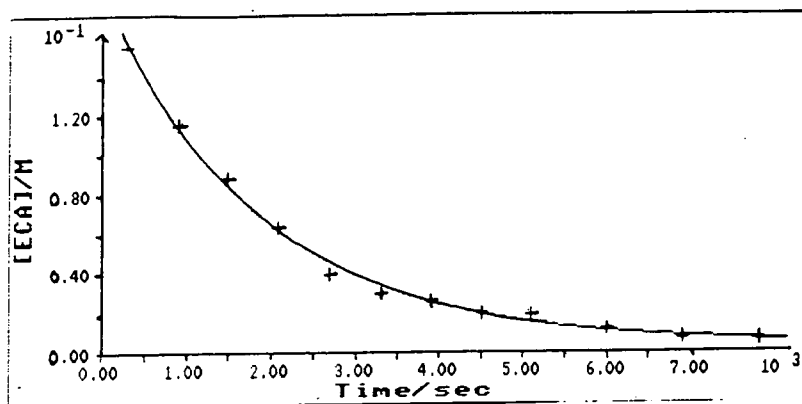
[ECA]=0.209M, [D⁺]=0.08M, T=298K



$$k_2 = 2.51 \pm 0.35 \times 10^{-4} \text{ sec}^{-1}$$

Figure 3.4.6

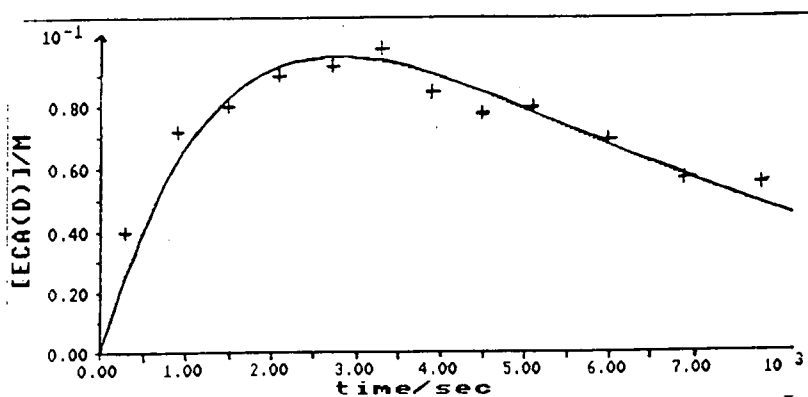
[ECA]=0.209M, [D⁺]=0.20M, T=298K



$$k_1 = 5.43 \pm 0.29 \times 10^{-4} \text{sec}^{-1}$$

Figure 3.4.7

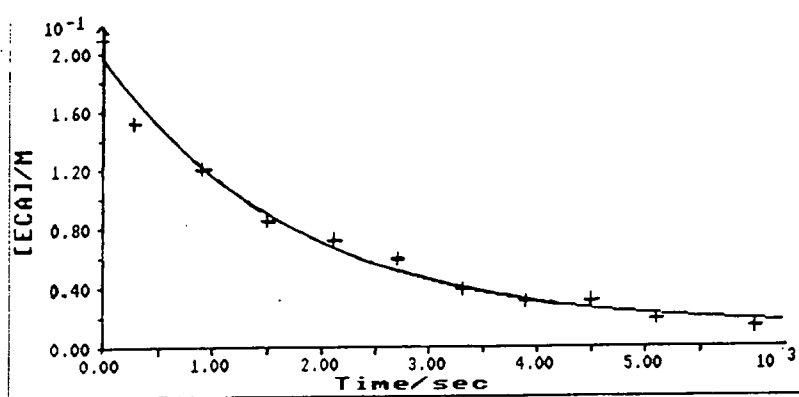
[ECA]=0.209M, [D⁺]=0.20M, T=298K



$$k_2 = 2.27 \pm 0.20 \times 10^{-4} \text{sec}^{-1}$$

Figure 3.4.8

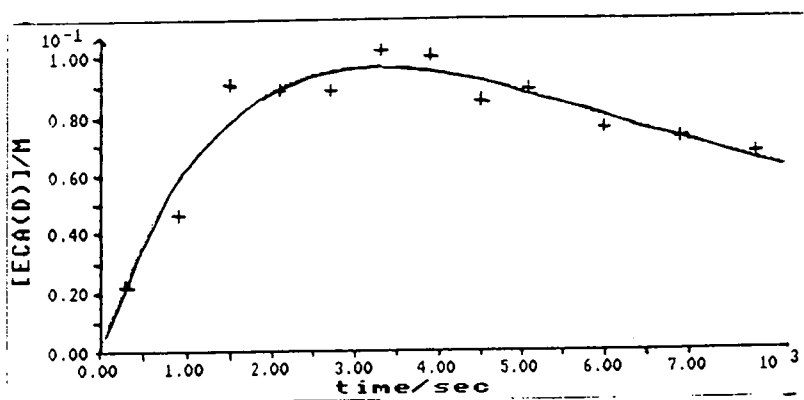
[ECA]=0.209M, [D⁺]=0.39M, T=298K



$$k_1 = 5.83 \pm 0.76 \times 10^{-4} \text{sec}^{-1}$$

Figure 3.4.9.

[ECA]=0.209M, [D⁺]=0.39M, T=298K



$$k_2 = 1.39 \pm 0.17 \times 10^{-4} \text{sec}^{-1}$$

The k_1 and k_2 values recorded are shown in table 3.4.4

Table 3.4.4

$[D^+]/M$	$k_1/10^{-4} \text{ sec}^{-1}$	$k_2/10^{-4} \text{ sec}^{-1}$
0.39	5.83 ± 0.76	1.39 ± 0.17
0.20	5.43 ± 0.29	2.27 ± 0.20
0.08	5.62 ± 0.48	2.51 ± 0.35

The k_1 values show that the reaction is *not* acid catalysed. The average value is:

$$k_1 = 5.63 \pm 0.11 \times 10^{-4} \text{ sec}^{-1}$$

This confirms the earlier work carried out by Pearson and Dillon¹ that the rate limiting step in the enolisation of ECA is the ionisation of ECA as a carbon acid, followed by rapid protonation at the oxygen to give the enol.

The rate constant for ionisation of ECA in H_2O has been calculated as;

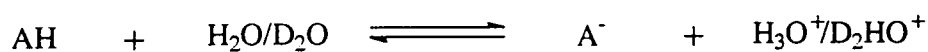
$$k_1 = 1.17 \times 10^{-3} \text{ sec}^{-1}$$

A comparison with the value calculated in D_2O gives the following value for the solvent isotope effect;

$$\frac{k_{H_2O}}{k_{D_2O}} = 2.08$$

A value of *ca* 2 is expected based on the present theory of solvent isotope effects¹⁸.

The equilibrium constants for the ionisation of carbon acids in different solvents is given by the following equation.



$$\frac{K_{H_2O}}{K_{D_2O}} = \frac{1}{l^2} = 2.10$$

where $l=0.69$ (the fractionation factor for each $+OD$ site involved in the equilibrium¹⁸). The value of the kinetic solvent isotope effect observed (2.08) is very similar to the maximum value possible (2.10), this suggests that the transition state

has a very similar structure to the carbanion. The extent of proton transfer (β) in the transition state can be calculated from the following equation¹⁸:

$$\beta = \frac{\log_{10}(k_H / k_D)}{\log_{10}(1 / I^2)}$$

This gives a value of $\beta=0.98$. This suggests almost complete proton transfer in the transition state.

The values for k_2 are less consistent than those for k_1 , this is undoubtedly due to the problems in measuring very small N.M.R. integrals. The general trend is that:

$$k_1 = 2.5k_2$$

On purely statistical grounds k_2 should be half k_1 if there was no secondary isotope effect in operation. The observed value of 2.5 shows that the secondary isotope is *ca* 1.25. The secondary isotope effect arises from a change in hybridisation at the reaction centre (in this case $sp^3 \rightarrow sp^2$) and is primarily due to a change in the out of plane bending mode¹⁹. Usually, the maximum thermodynamic secondary isotope effect observed is *ca* 1.4. The closeness of the kinetic value to 1.4 again indicates that the transition state has considerable anion character. A very similar value (1.3) has been calculated for the secondary substrate isotope effect in the enolisation of malonic acid¹⁷.

Chapter 3 References

1. R.G.Pearson and R.L.Dillon, *J. Am. Chem. Soc.*, 1953, **75**, 2439.
2. A.Graham and D.L.H.Williams, *J. Chem. Soc. Perkin Trans. 2*, 1992, 747.
3. A.R.Butler, A.M.Calsy and C.Glidewell, *J. Chem. Soc. Perkin Trans. 2*, 1988, 1179.
4. L.J.Andrew and R.M.Keefer "Molecular complexes in organic chemistry", Halden-day, 1964.
5. B.B.Bhownik and J.I.Zink, *Spectrochem., Acta.*, 1982, **38A**, 877.
6. J.Toullec and J.E.Dubois, *J. Am. Chem. Soc.*, 1981, **103**, 5393.
7. R.P.Bell and D.J.Rawlinson, *J. Chem. Soc.*, 1961, 726.
8. A.J.Kresge, *J. Am. Chem. Soc.*, 1988, **110**, 7875.
9. J.H.Ridd, *Adv. Phys. Org. Chem.*, 1978, **16**, 1.
10. C.Ainsworth and F.Chen, *J. Organomet. Chem.*, 1972, **46**, 59.
11. J.E.Dubois, M.El-Alaoui and J.Toullec, *J. Am. Chem. Soc.*, 1981, **103**, 5393.
12. H.C.Brown and Y.Okamoto, *J. Am. Chem. Soc.*, 1958, **80**, 4979.
13. S.Clementi and P.Linda, *J. Chem. Soc. Perkin Trans. 2*, 1973, 1887.
14. E.Eglesias and D.L.H.Williams, *J. Chem. Soc. Perkin Trans. 2*, 1989, 343.
15. Y.Chiang, A.J.Kresge and N.P.Schepp, *J. Am. Chem. Soc.*, 1989, **111**, 3977.
16. J.Andros, Y.Chiang, A.J.Kresge, N.P.Schepp and J.Wirz, *J. Am. Chem. Soc.*, 1994, **116**, 73.
17. E.W.Hansen and P.Ruoff, *J. Phys. Chem.*, 1988, **92**, 2641.
18. R.L.Schowen, *Prog. Phys. Org. Chem.*, 1972, **9**, 275.
19. T.H.Lowry and K.S.Richardson "mechanism and theory in organic chemistry", third ed, chap 2, P239.

Chapter 4

Halogenation of Ethylhydrogenmalonate.

4.1 Introduction

The halogenation of ethylhydrogenmalonate (EHM) was investigated to compare its mechanism to that reported for malonic acid. Malonic acid (see chapter 2) is thought to enolise via a six membered H-bonded transition state. Malonic acid has two carboxylic acid groups available to form a six membered ring whereas ethylhydrogenmalonate has only one (see figure 4.1.1). This should provide evidence as to whether the intramolecular mechanism is in operation and the effect of the ethylester group on the rate of enolisation and the enol content will be discussed.

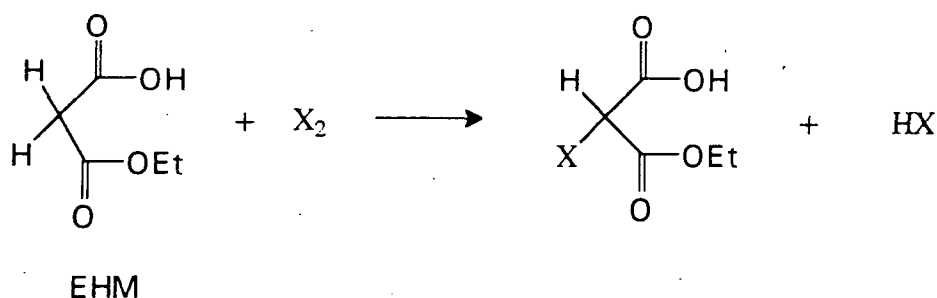


Figure 4.1.1

Diethylmalonate has been studied by many workers^{1,3,5} and the rate of enolisation and the enol content has been measured. Thus EHM is an intermediate structure between malonic acid and diethylmalonate and provides a useful comparison.

The mechanism of enolisation (under zero order halogenation conditions) was investigated. Base catalysis by the conjugate anion of EHM was measured. Kinetics were also obtained under conditions where the reaction of the halogen with the enol is rate limiting (first order in the halogen). Enolisation rate constants and enol contents are reported and a comparison with malonic acid and other related compounds is given.

4.2 Results

The bromination and iodination of EHM were carried out in water at 298K. The solubility of EHM in water is very high so there is no problem working with $[EHM] \gg [halogen]$. Every kinetic run was carried out with the concentration of EHM at least 25 times that of the halogen. The kinetics were measured by monitoring the decrease in absorbance due to the halogen (395nm for bromine and 459nm for iodine). The bromination of EHM was carried out using relatively high $[Br_2]$ where it is expected that the enolisation would be rate limiting. The iodination of EHM was studied using much lower iodine concentrations where reaction of iodine with the enol/enolate is rate limiting.

4.2.1 Zero order bromination of EHM

Using a relatively high concentration of bromine (ca $2.5 \times 10^{-3} \text{ mol dm}^{-3}$) the reaction showed good zero order dependence on bromine for approximately 80% of the reaction. Towards the end of the reaction the absorbance time plots show a slight curvature, this indicates the reaction order is changing from zero to first order. The zero order rate constants were obtained by fitting the initial part of the reaction to avoid any interference from the first order reaction. The variation of the observed zero order rate constant with $[H^+]$ and substrate concentration was investigated. The reaction was also investigated in buffered systems (using the EHM as the buffering acid) in the range $pH=2.0 - 4.5$ to examine the possibility of base catalysis by the conjugate anion of EHM. The results are shown in tables 4.2.1 - 4.2.9.

Table 4.2.1

[EHM] = 0.05M

[Br₂] = 1.01 x 10⁻³ M

[H ⁺] _T / M	k _{obs} / 10 ⁻⁵ mol l ⁻¹ sec ⁻¹
0.1	4.12
0.2	3.18
0.3	3.31
0.4	3.39
0.6	3.50

Table 4.2.2

[EHM] = 0.05M

[Br₂] = 1.80 x 10⁻³ M

[H ⁺] _T / M	k _{obs} / 10 ⁻⁵ mol l ⁻¹ sec ⁻¹
0.8	5.70
0.6	6.45
0.4	5.15
0.2	5.31

Table 4.2.3

[H⁺] = 0.1M

[Br₂] = 2.52 x 10⁻³ M

[EHM] _T / M	k _{obs} / 10 ⁻⁵ mol l ⁻¹ sec ⁻¹
0.05	4.35
0.10	8.78
0.15	12.85
0.20	19.94
0.25	24.40

Table 4.2.4

$[\text{Br}_2] = 2.5 \times 10^{-3}\text{M}$

$\text{pH} = 2.00$

$[\text{EHM}]_{\text{T}}/\text{mol l}^{-1}$	$10^4 k_{\text{obs}}/\text{mol l}^{-1} \text{sec}^{-1}$	$10^3 k_{\text{obs}}/[\text{EHM}] \text{sec}^{-1}$
0.193	2.23	1.16
0.162	1.75	1.08
0.111	1.14	1.03
0.078	0.73	0.94

Table 4.2.5

$[\text{Br}_2] = 2.5 \times 10^{-3}\text{M}$

$\text{pH} = 2.50$

$[\text{EHM}]_{\text{T}}/\text{mol l}^{-1}$	$10^4 k_{\text{obs}}/\text{mol l}^{-1} \text{sec}^{-1}$	$10^4 k_{\text{obs}}/[\text{EHM}] \text{sec}^{-1}$
0.227	4.44	19.56
0.199	3.61	18.14
0.152	2.45	16.12
0.113	1.52	13.45
0.076	0.82	10.79
0.051	0.50	9.62

Table 4.2.6 $[\text{Br}_2] = 2.4 \times 10^{-3} \text{M}$ $\text{pH} = 3.20$

$[\text{EHM}]_{\text{T}} / \text{mol l}^{-1}$	$10^4 k_{\text{obs}} / \text{mol l}^{-1} \text{sec}^{-1}$	$10^4 k_{\text{obs}} / [\text{EHM}] \text{sec}^{-1}$
0.223	7.66	34.35
0.183	5.36	29.29
0.151	3.88	25.70
0.114	2.49	21.84
0.076	1.35	17.76

Table 4.2.7 $[\text{Br}_2] = 2.5 \times 10^{-3} \text{M}$ $\text{pH} = 3.65$

$[\text{EHM}]_{\text{T}} / \text{mol l}^{-1}$	$10^4 k_{\text{obs}} / \text{mol l}^{-1} \text{sec}^{-1}$	$10^4 k_{\text{obs}} / [\text{EHM}] \text{sec}^{-1}$
0.200	5.63	28.15
0.171	4.11	24.04
0.121	2.04	16.86
0.093	1.06	11.40
0.056	0.48	8.57

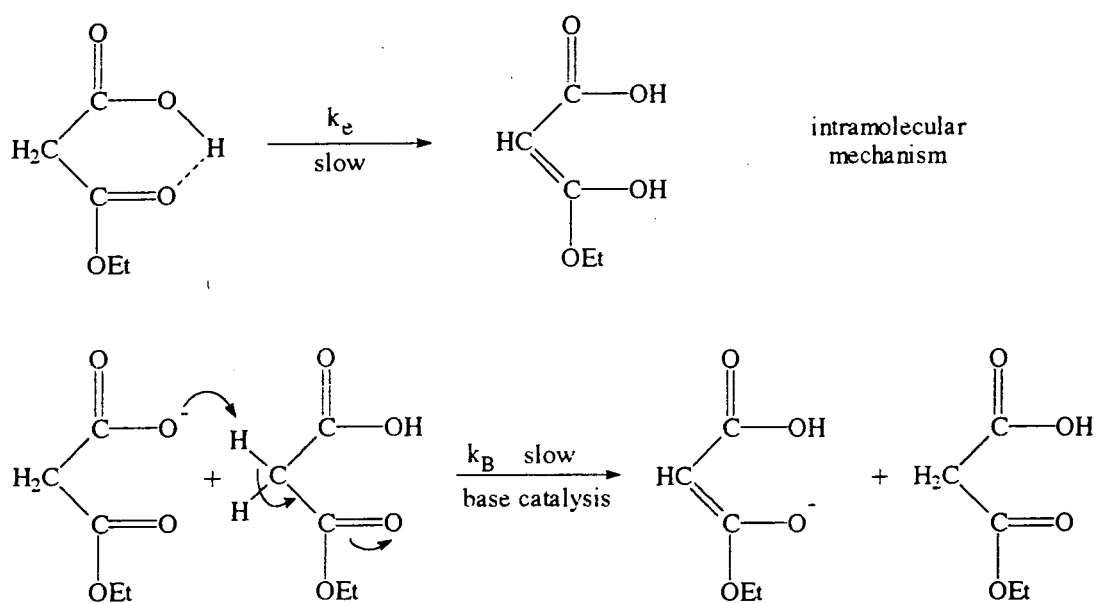
Table 4.2.8 $[\text{Br}_2] = 2.5 \times 10^{-3} \text{M}$ $\text{pH} = 3.90$

$[\text{EHM}]_{\text{T}} / \text{mol l}^{-1}$	$10^4 k_{\text{obs}} / \text{mol l}^{-1} \text{sec}^{-1}$	$10^4 k_{\text{obs}} / [\text{EHM}] \text{sec}^{-1}$
0.25	6.31	25.48
0.20	4.02	20.08
0.15	2.35	15.68
0.10	1.09	10.90
0.05	0.27	5.452

Table 4.2.9 $[\text{Br}_2] = 2.5 \times 10^{-3} \text{M}$ $\text{pH} = 4.65$

$[\text{EHM}]_{\text{T}} / \text{mol l}^{-1}$	$10^4 k_{\text{obs}} / \text{mol l}^{-1} \text{sec}^{-1}$	$10^4 k_{\text{obs}} / [\text{EHM}] \text{sec}^{-1}$
0.25	1.87	7.49
0.20	1.22	6.12
0.15	0.75	5.01
0.10	0.39	3.94
0.05	0.12	2.47

The reaction is found to be zero order in bromine up to pH=4.65. Tables 4.2.1 and 4.2.2 show that at very low pH (>0.1M HClO₄) the bromination of EHM is independent of the pH. The variation in the k_{obs} with bromine concentration shows that an increase in bromine slightly increases the rate. This suggests that the limiting condition of zero order kinetics may not be fully reached unless the concentration of bromine is *ca* $1.8 \times 10^{-3} \text{ mol l}^{-1}$ or greater. The data in table 4.2.2 may be expected to show better zero order kinetics because of the higher concentration of bromine. At pH values higher than 2 the reaction is no longer independent of acidity, this is presumably due to base catalysis by the conjugate anion of ethylhydrogenmalonate. The reaction can be analysed in terms of two parallel reactions. See scheme 4.2.1.



scheme 4.2.1

From scheme 4.2.1 the rate of the reaction is given by the following equation.

$$\text{rate} = k_{obs} = k_e[\text{EHM}]_e + k_B[\text{EHM}]_e[\text{EHM}^-]_e \quad \text{equation 4.2.1}$$

The free concentrations of EHM and EHM⁻ are given in terms of the total EHM concentration by the following expressions where K_a is the acid dissociation constant of EHM (ionising as a carboxylic acid).

$$[\text{EHM}]_e = \frac{[\text{EHM}]_T [\text{H}^+]}{[\text{H}^+] + K_a} \quad \text{equation 4.2.2}$$

and;

$$[\text{EHM}^-]_e = \frac{[\text{EHM}]_T K_a}{[\text{H}^+] + K_a} \quad \text{equation 4.2.3}$$

Substituting equations 4.2.2 and 4.2.3 into equations 4.2.1 gives the following kinetic expression.

$$k_{\text{obs}} = \frac{k_e [\text{EHM}]_T [\text{H}^+]}{[\text{H}^+] + K_a} + \frac{k_B K_a [\text{H}^+] [\text{EHM}]_T^2}{([\text{H}^+] + K_a)^2} \quad \text{equation 4.2.4}$$

At high acidity $[\text{H}^+] \gg K_a$, hence equation 4.2.4 simplifies to.

$$k_{\text{obs}} = k_e [\text{EHM}]_T + \frac{k_B K_a [\text{EHM}]_T^2}{[\text{H}^+]} \quad \text{equation 4.2.5}$$

At acid concentrations greater than 0.1 mol dm⁻³ the second term in equation 4.2.5 becomes insignificant. Thus;

$$k_{\text{obs}} = k_e [\text{EHM}]_T \quad \text{equation 4.2.6}$$

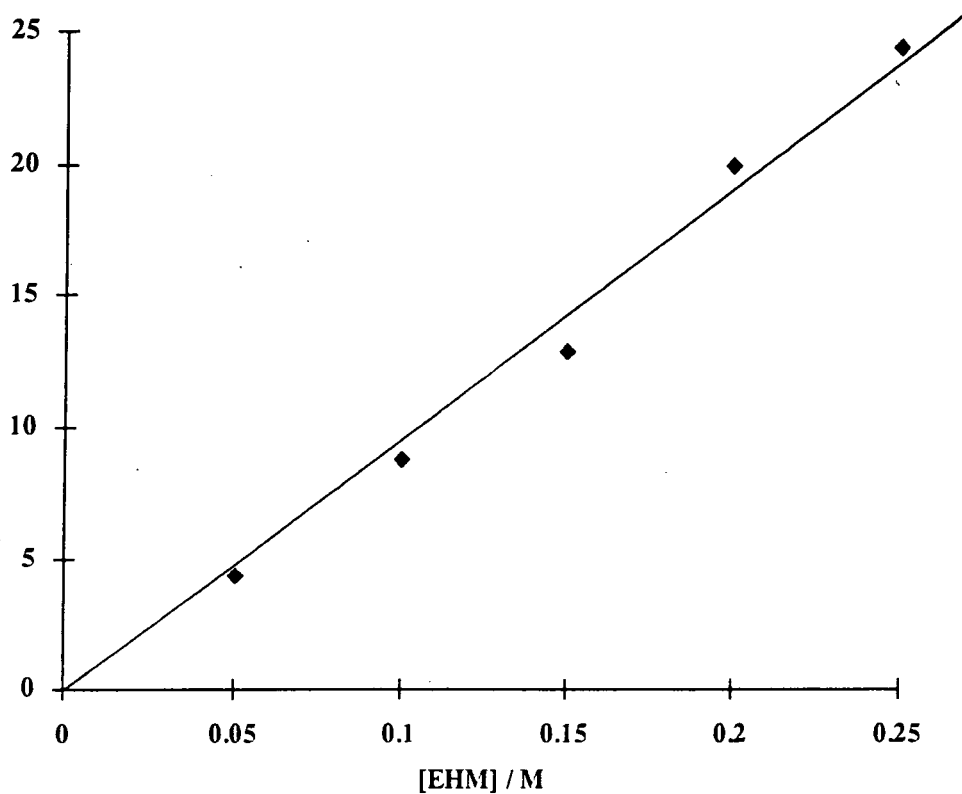
Equation 4.2.6 shows that a plot of k_{obs} against $[\text{EHM}]_T$ should be linear and from the slope a value of k_e can be calculated. Figure 4.2.1 shows a plot of the observed rate constant against total substrate concentration. Good first order dependence is observed.

Figure 4.2.1

Plot of k_{obs} vs $[\text{EHM}]_{\text{T}}$ at constant pH ($[\text{HClO}_4] = 0.1\text{M}$)

$[\text{Br}_2] = 2.5 \times 10^{-3} \text{ mol dm}^{-3}$

$10^4 k_{\text{obs}} / \text{mol l}^{-1} \text{ sec}^{-1}$



From tables 4.2.1, 4.2.2 and from the above graph values of k_e can be calculated.

See Table 4.2.10.

Table 4.2.10

$[\text{Br}_2]_0 / 10^{-3} \text{ M}$	$k_e / 10^{-3} \text{ s}^{-1}$
1.01	0.70
1.8	1.13
2.5	1.03

The values of k_e calculated are in fairly good agreement. The value calculated using lower bromine concentrations may be in error due to a small contribution from a first order reaction. Using the two values at higher bromine concentration an average value of;

$$k_e = 1.07 \pm 0.04 \times 10^{-3} \text{sec}^{-1}$$

As mentioned earlier the reaction is not independent of acidity at high pH. Under these conditions the rate of the reaction is given by the following.

$$k_{\text{obs}} = \frac{k_e[\text{EHM}]_T[\text{H}^+]}{[\text{H}^+] + K_a} + \frac{k_B K_a [\text{H}^+][\text{EHM}]_T^2}{([\text{H}^+] + K_a)^2} \quad \text{equation 4.2.7}$$

Equation 4.2.7 can be rearranged to give the following.

$$\frac{k_{\text{obs}}}{[\text{EHM}]_T} = \frac{k_e[\text{H}^+]}{[\text{H}^+] + K_a} + \frac{k_B K_a [\text{H}^+][\text{EHM}]_T}{([\text{H}^+] + K_a)^2} \quad \text{equation 4.2.8}$$

equation 4.2.8 shows that a plot of $k_{\text{obs}} / [\text{EHM}]_T$ against $[\text{EHM}]_T$ at constant acidity should be linear and from the variation of the slope with pH a value of k_B can be calculated. Figures 4.2.2 and 4.2.3 show the corresponding plots at six different pH values.

The slopes obtained from figures 4.2.1 and 4.2.2 are recorded in Table 4.2.11 for the six different pH values.

Table 4.2.11

pH	slope/ $1 \text{ mol}^{-1} \text{ sec}^{-1}$
2.00	0.00179
2.50	0.00579
3.20	0.0119
3.65	0.01415
3.90	0.00985
4.65	0.00244

Figure 4.2.2

Plot of $k_{\text{obs}}/[\text{EHM}]_{\text{T}}$ against $[\text{EHM}]_{\text{T}}$ at pH=2.0, 2.5 and 3.2

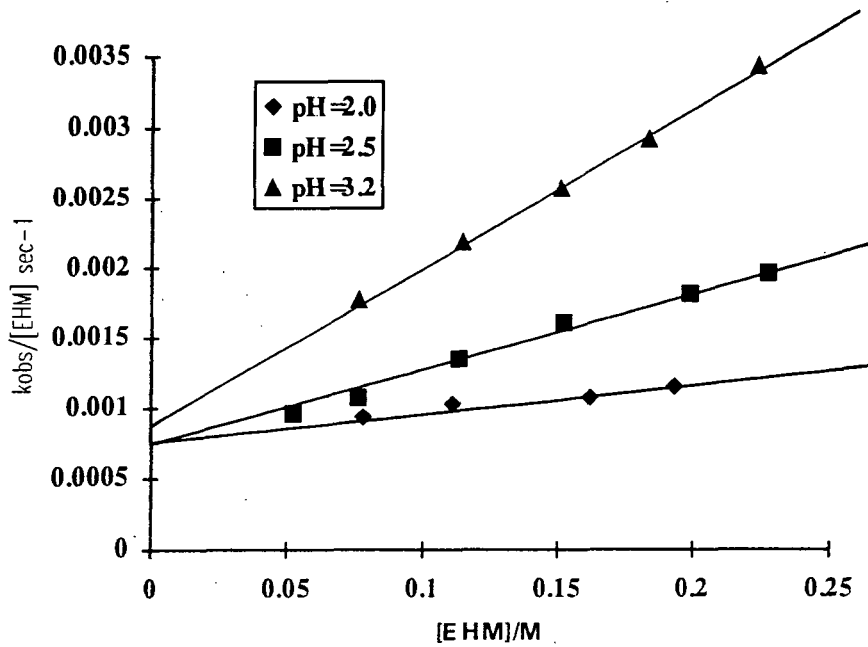
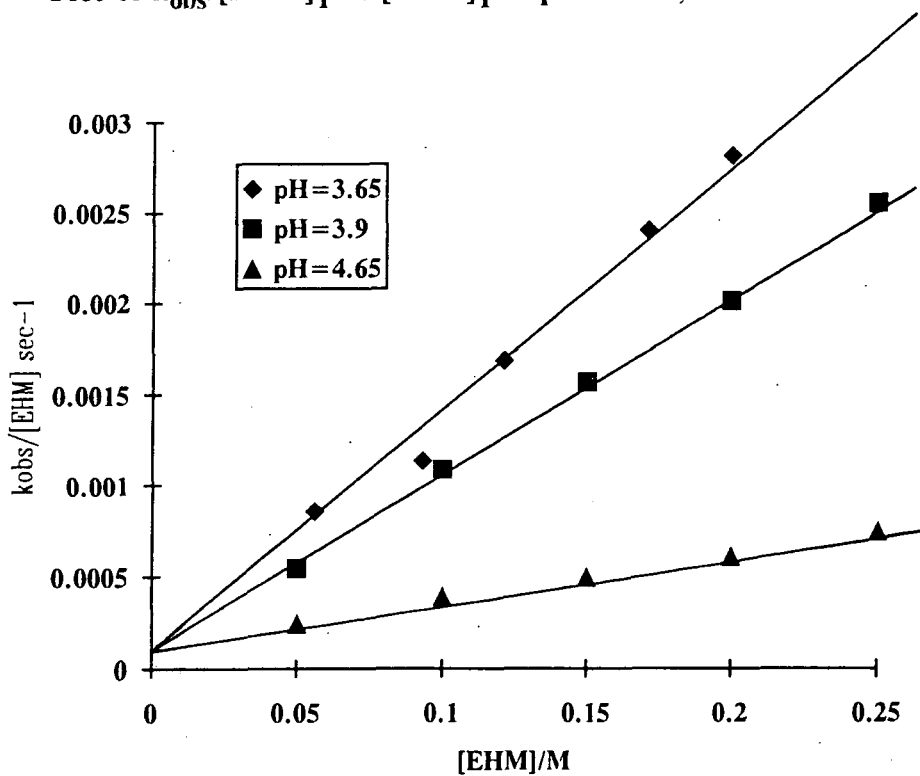


Figure 4.2.3

Plot of $k_{\text{obs}}/[\text{EHM}]_{\text{T}}$ vs $[\text{EHM}]_{\text{T}}$ at pH= 3.65, 3.90 and 4.65

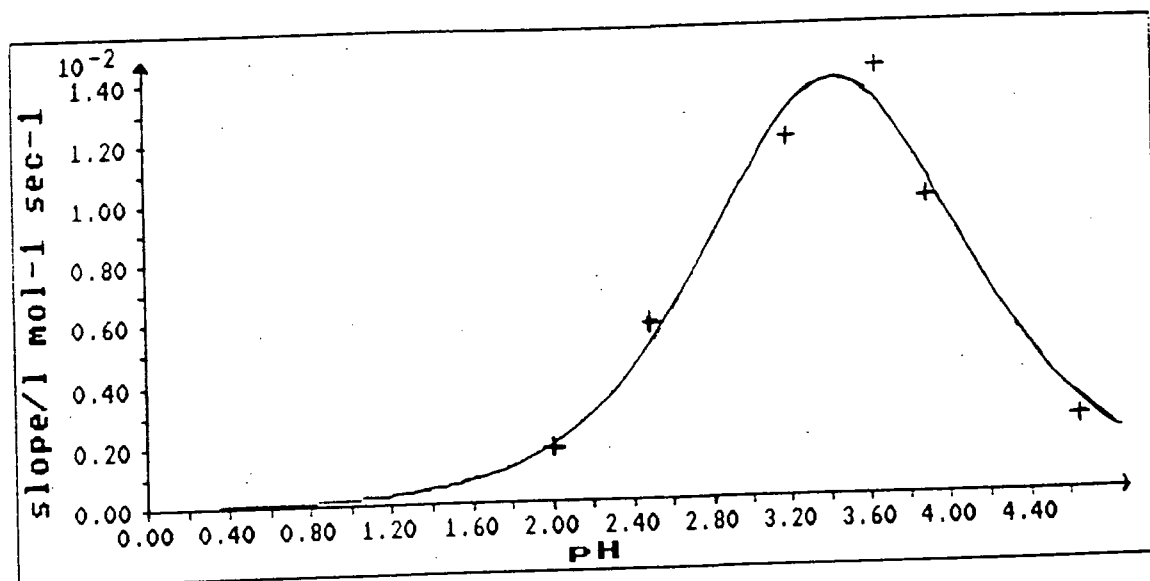


The variation of the slope with pH is given by equation 4.2.9. (taken from equation 4.2.8).

$$\text{slope} = \frac{k_B K_a [H^+]}{([H^+] + K_a)^2} \quad \text{equation 4.2.9}$$

Equation 4.2.9 can be analysed using a non linear regression program and from this values of k_B and K_a calculated. Figure 4.2.4 shows the fit to equation 4.2.9.

Figure 4.2.4



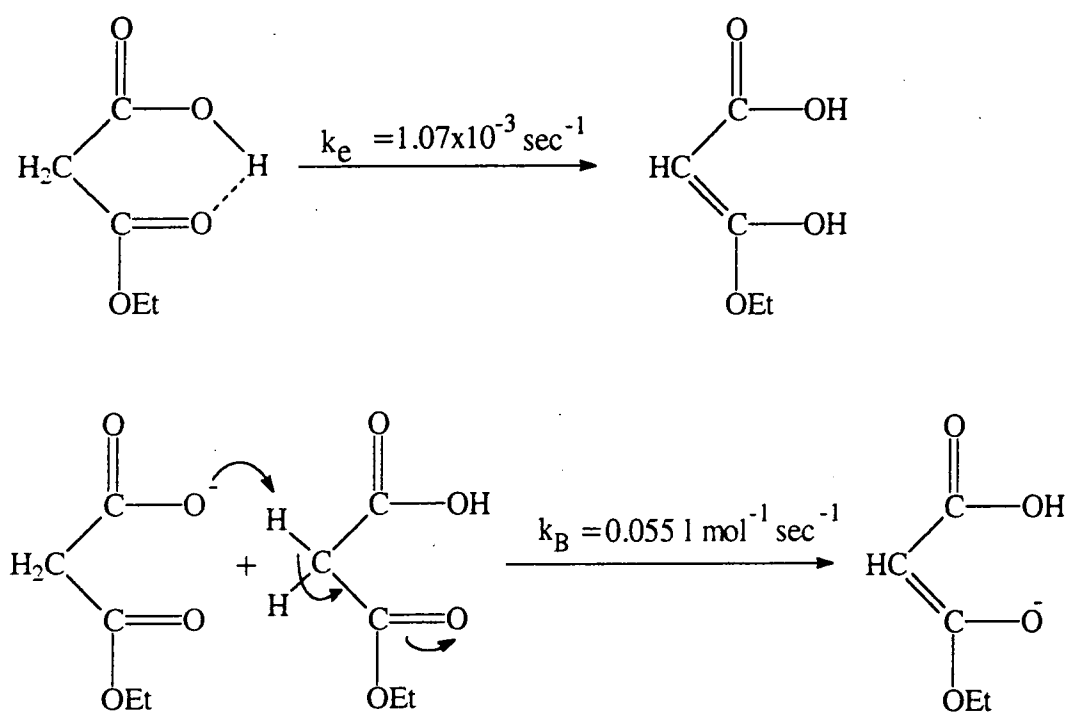
The non linear fit gives the following values for K_a and k_B .

$$k_B = 5.4 \pm 0.23 \times 10^{-2} \text{ l mol}^{-1} \text{ sec}^{-1}$$

$$K_a = 3.69 \pm 0.41 \times 10^{-4} \text{ mol l}^{-1}$$

The value of K_a calculated is very close to the literature value¹⁵ ($K_a = 4.47 \times 10^{-4} \text{ mol l}^{-1}$) reported by Vogel *et al.*

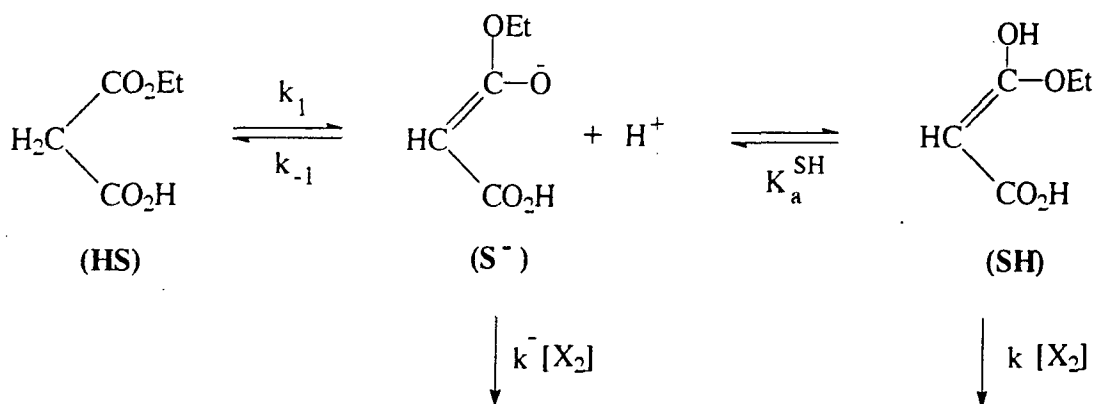
Scheme 4.2.2 shows the rate constants calculated for the kinetic scheme:



scheme 4.2.2

4.2.2 First order Halogenation

Under certain conditions the reaction of halogens with EHM can be first order in the halogen. This corresponds to the case where reaction of the halogen with the enol is the rate determining step. It was found that the concentration of halogen needed was ca 15 μM . In the case of bromine ($\epsilon = 128.5 \text{ l mol}^{-1} \text{ cm}^{-1}$ at 395nm) this concentration couldn't be observed with the available spectrophotometers. With iodine it was possible to measure these small concentrations because of the larger extinction coefficient of iodine ($\epsilon = 697 \text{ l mol}^{-1} \text{ cm}^{-1}$ at 459nm). Due to the very low absorbance changes it was necessary to average a large number of runs in order to remove the noise present in the kinetic traces. The reaction can be analysed in a similar way to malonic acid (see section 2.4). Scheme 4.2.3 shows the reaction pathway where K_a^{SH} is the ionisation constant for the enol of EHM.



scheme 4.2.3

A steady state treatment of scheme 4.2.3 gives the following equation.

$$\text{Rate} = \frac{k_1[\text{EHM}] \left(k^- [\text{X}_2] + \frac{k[\text{H}^+][\text{X}_2]}{K_a^{\text{SH}}} \right)}{k_{-1}[\text{H}^+] + \left(k^- [\text{X}_2] + \frac{k[\text{H}^+][\text{X}_2]}{K_a^{\text{SH}}} \right)} \quad \text{equation 4.2.10}$$

When the reaction is carried out with very low halogen concentrations and at high acidity the rate of halogenation of the enol ($k^- [X_2] + \frac{k[H^+][X_2]}{K_a^{SH}}$) is much less than the rate of reprotonation of the carbanion ($k_{-1}[H^+]$), thus equation 4.2.10 simplifies to the following.

$$\text{Rate} = \frac{k_1[\text{EHM}] \left(k^- [X_2] + \frac{k[H^+][X_2]}{K_a^{SH}} \right)}{k_{-1}[H^+]} \quad \text{equation 4.2.11}$$

Equation 4.2.11 can be rearranged to give the following.

$$\text{rate} = \left(\frac{k_1 k^-}{k_{-1}[H^+]} + \frac{k k_1}{k_{-1} K_a^{SH}} \right) [\text{EHM}][X_2] \quad \text{equation 4.2.12}$$

This shows that the reaction should be first order in halogen and substrate.

The variation in the observed first order rate constant is shown in tables 4.2.12 and 4.2.13.

Table 4.2.12

$[I_2] = 1.5 \times 10^{-5} \text{ mol l}^{-1}$ $[H^+] = 0.16M$ $I = 0.16M$

[EHM]/M	$k_{\text{obs}} / \text{sec}^{-1}$
0.00687	0.0612
0.0122	0.0975
0.0241	0.1935
0.0398	0.2878
0.0563	0.433

Table 4.2.13

$$[I_2] = 1.5 \times 10^{-5} \text{ mol l}^{-1} \quad I = 0.16 \text{ mol l}^{-1}$$

[EHM]/M	[H ⁺]/M	k _{obs} / sec ⁻¹	$\frac{k_{\text{obs}}}{[\text{EHM}] \text{ l mol}^{-1} \text{ sec}^{-1}}$
0.0563	0.16	0.433	7.69
0.0541	0.12	0.3915	7.24
0.0543	0.08	0.4564	8.41
0.0513	0.02	0.3268	6.38
0.0520	0.02	0.4242	8.16

Table 4.2.12 gives the variation of k_{obs} with substrate concentration, this shows a good linear dependency. See Figure 4.2.5.

Figure 4.2.5

Plot of k_{obs} against [EHM], [H⁺]=0.16M, I=0.16M

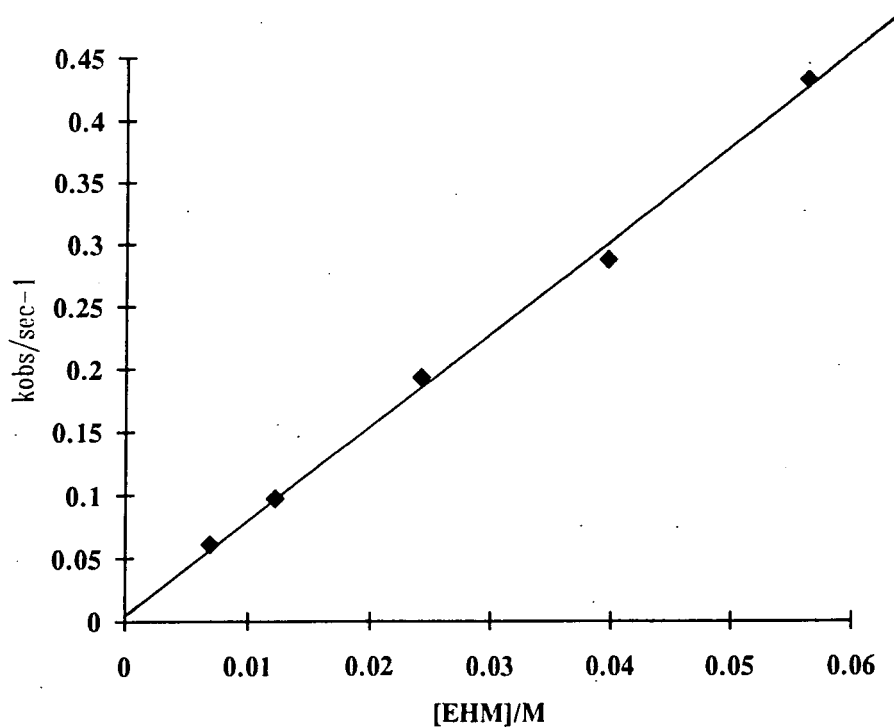
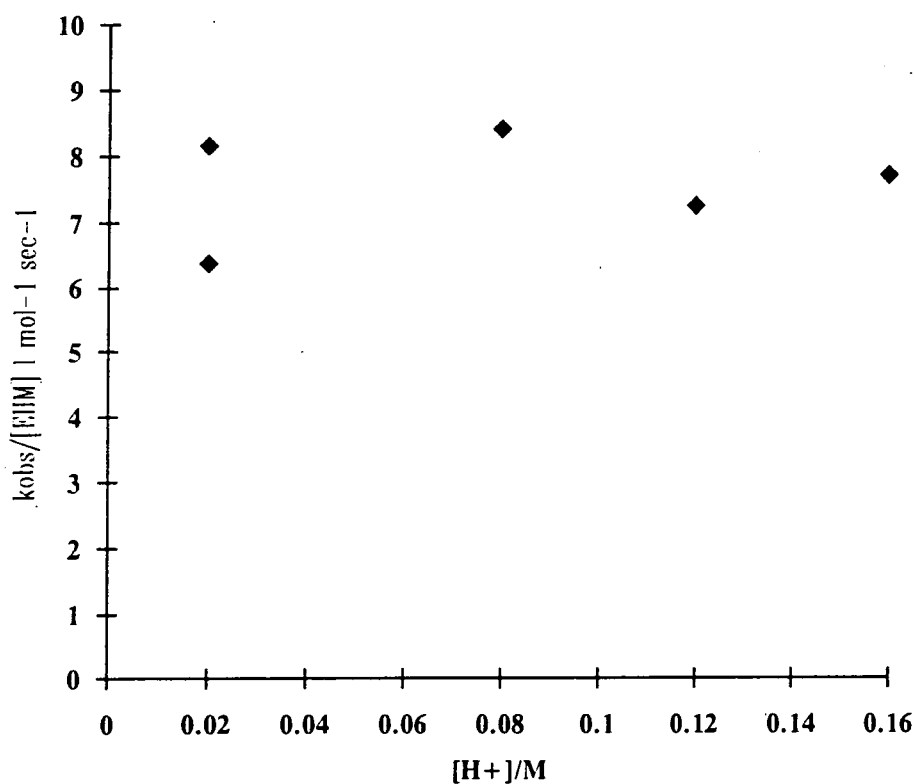


Figure 4.2.6 shows the variation of k_{obs} with acidity, At high acidity the reaction is independent of the concentration of the hydronium ion. There is a fairly large degree of scatter in figure 4.2.6. this is due to the difficulty in obtaining accurate rate constants from the very small absorbance changes measured.

Figure 4.2.6

Plot of $k_{\text{obs}}/[\text{EHM}]$, against $[\text{H}^+]$

$[\text{I}_2] = 1.5 \times 10^{-5} \text{ mol l}^{-1}$ $I = 0.16 \text{ mol l}^{-1}$



When the reaction is independent of acidity this indicates that the reaction is proceeding exclusively through the enol. Under these conditions equation 4.2.12 simplifies to the following.

$$k_{\text{obs}} = kK_{\text{E}}[\text{EHM}]_{\text{T}} \quad \text{equation 4.2.13}$$

hence a value for the product kK_E can be calculated from the substrate and acid dependencies. This gives an average of;

$$kK_E = 7.27 \pm 0.31 \text{ l mol}^{-1} \text{ sec}^{-1}$$

Assuming that reaction of iodine with the enol occurs at the diffusion limit (ie. $k=5 \times 10^9 \text{ l mol}^{-1} \text{ sec}^{-1}$) then a value for K_E can be calculated.

$$K_E = 1.45 \pm 0.06 \times 10^{-9}$$

Unlike malonic acid there are no other electrophiles that have been reacted with EHM to show that the value of kK_E obtained is the maximum value, however in all other cases the reactions have been at the diffusion limit and there is no reason to assume that EHM will be any different. Nitrosation kinetics may prove useful in confirming this assumption, however the nitrosating species used (NO^+ , NOSCN , NOCl , NOBr) in kinetic studies are often less reactive than the halogens and do not react at the diffusion limit.

Using the value of K_E calculated above an estimate of acidity of the enol can be calculated from the following equation.

$$K_a^{\text{SH}} = \frac{K_E}{K_a^{\text{HS}}} \quad \text{equation 4.2.14}$$

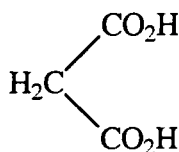
The acidity constant (K_a^{HS}) for ionisation of EHM as a carbon acid can be estimated using a rate equilibrium correlation developed by J.P. Guthrie based on Marcus theory⁴. This gives a value of ca 10^{-12} - $10^{-13} \text{ mol l}^{-1}$ for K_a^{HS} . Thus the acidity of the enol can be estimated to be ca 10^{-3} - $10^{-4} \text{ mol l}^{-1}$.

$$K_a^{\text{SH}} = 10^{-3} - 10^{-4} \text{ mol l}^{-1}$$

4.3 Discussion.

A comparison between the enolisation data for malonic acid, ethylhydrogenmalonate and diethylmalonate is shown below.

malonic acid

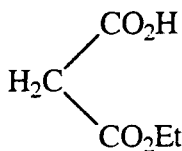


$$k_{\text{H}_2\text{O}} = 4.53 \pm 1.0 \times 10^{-3} \text{ sec}^{-1}$$

$$(\text{pK}_a = 2.85) \quad k_{\text{MAL}^-} = 0.12 \pm 0.04 \text{ l mol}^{-1} \text{ sec}^{-1}$$

$$(\text{pK}_a = 2.85) \quad k_{\text{CAA}^-} = 0.09 \pm 0.01 \text{ l mol}^{-1} \text{ sec}^{-1}$$

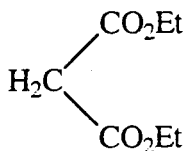
ethylhydrogenmalonate



$$k_{\text{H}_2\text{O}} = 1.07 \pm 0.04 \times 10^{-3} \text{ sec}^{-1}$$

$$(\text{pK}_a = 3.43) \quad k_{\text{EHM}^-} = 0.054 \pm 0.0023 \text{ l mol}^{-1} \text{ sec}^{-1}$$

diethylmalonate¹



$$k_{\text{H}_2\text{O}} = 2.5 \times 10^{-5} \text{ sec}^{-1}$$

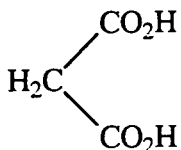
The results show that there is a difference of *ca* four between the rate constant for ionisation of malonic acid and ethylhydrogen malonate. If the intramolecular mechanism is in operation, on purely statistical grounds malonic acid should be a factor of *two* faster than EHM. Thus the chemical effect of the ester group is to reduce the rate of ionisation by two. The ethylester group and the carboxy group have very similar σ^- values ($\sigma^- = 0.68$)² hence the very small chemical effect of the ethylester group is expected. The rate of ionisation of diethylmalonate has been

calculated by Pearson and Dillon¹ as $k_{\text{H}_2\text{O}} = 2.5 \times 10^{-5} \text{ sec}^{-1}$. A comparison with EHM shows that the introduction of the first carboxy group has a *forty* fold increase on the rate of ionisation. This relatively large effect may be due to the carboxy group increasing the rate of ionisation by stabilising the negative charge developed in the transition state by a hydrogen bonding interaction. As stated earlier, the ethyl ester group and the carboxy group have very similar σ^- values ($\sigma^- = 0.68$)² hence resonance and polar effect differences should be small. This *supports* the intramolecular mechanism as the forty fold difference arises from an interaction which is absent in evaluating σ^- values i.e. hydrogen bonding. The introduction of a second carboxy group has a much smaller effect because the hydrogen bonded structure is already set up and the second carboxy group simply increases the probability of forming the six membered transition state, again this supports the intramolecular mechanism. Kirby and Lloyd¹² have calculated a value of $k_{\text{H}_2\text{O}} = 3.3 \times 10^{-4} \text{ sec}^{-1}$ for the water catalysed enolisation (in 30:70 D_2O /acetone at 29.5°C) by deuterium exchange. This is approximately three times smaller than the value calculated here, which is not unexpected considering the use of deuterium in the solvent. They argue against any assistance from the carboxy group in the enolisation of EHM, but their argument is based on a comparison with DEM enolisation which was carried out in a different solvent and at a different ionic strength.

There are many examples in the literature of intramolecular general acid catalysis in the enolisation of aldehydes and ketones. Cox and Hutchinson¹⁴ have shown that the enolisation of 2-oxocyclohexanecarboxylic acid is ca 500-1000 times faster than for the corresponding methyl ester. Bell and Page¹³ have measured the rate constant for the enolisation of 7,7-dimethyl-2-oxobicycloheptane-1-carboxylic acid and found it to be *ca* 2000 times greater than for corresponding alkyl esters.

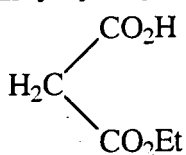
The enol contents calculated for malonic acid, ethylhydrogenmalonate and diethylmalonate are discussed below.

malonic acid



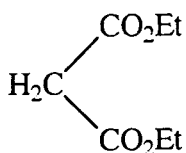
$$pK_E = 8.13 \pm 0.05$$

ethylhydrogenmalonate



$$pK_E = 8.84 \pm 0.03$$

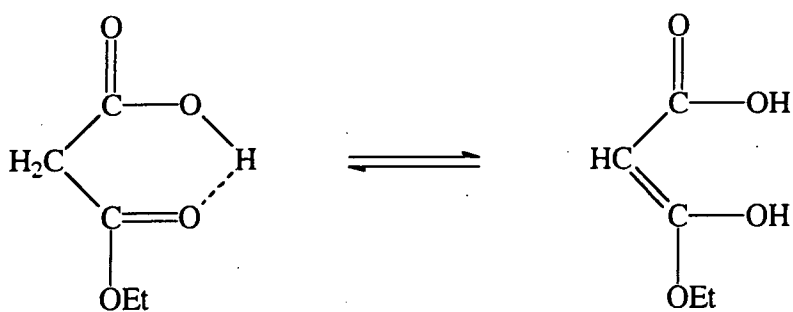
diethylmalonate⁵



$$pK_E = 10.70$$

The enolisation of diethylmalonate was studied by Bell^{3,7} in the fifties who calculated a pK_E value of ca 6.22 this was based on the assumption that carboxylic acid enols have a similar acidity constants to simple enols, this has now been shown to be untrue⁶. The value quoted above for diethylmalonate is calculated from nitrosation studies by assuming the reaction of nitrosylthiocyanate (NOSCN) occurs at the diffusion limit which is probably not fully the case.

The enol formed from diethyl malonate and ethylhydrogenmalonate can exist in cis and trans forms but it is impossible from this analysis to say which isomer is favoured. In The case of EHM the enol may be formed from the ester group or the acid group. Then enol formed from the ester group may be expected to be the major intermediate as this will be formed via the intramolecular H-bonding mechanism. See below.



enol formed in the ester group

The enol contents observed for malonic acid and EHM show that the enol content for malonic acid is approximately 4 times larger than that for EHM. The higher enol content of malonic acid (the enol of a carboxylic acid) may be due to the two hydroxy groups (as opposed to one in the enol form of EHM) which are better able to stabilise the enolic double bond through direct resonance¹¹ σ^+ (OMe)=-0.79 and σ^+ (OH)=-0.91. Recently⁸, a value of $pK_E=20\pm 2$ for the enol content of acetic acid has been calculated using thermodynamic cycles. A comparison with the above values shows that effect of a carboxy or ethylester group is to increase the enol content by *ca* 12 orders of magnitude. This massive effect may be due to hydrogen bonding stabilisation (*cf.* 6 orders of magnitude difference between the enol content in acetone⁹ and ethylacetoacetate¹⁰) or charge separation in the enol (see discussion chapter 3) which accentuates the effect of strong electron withdrawing groups on the enol contents of carboxylic acid derivatives.

Chapter 4 References

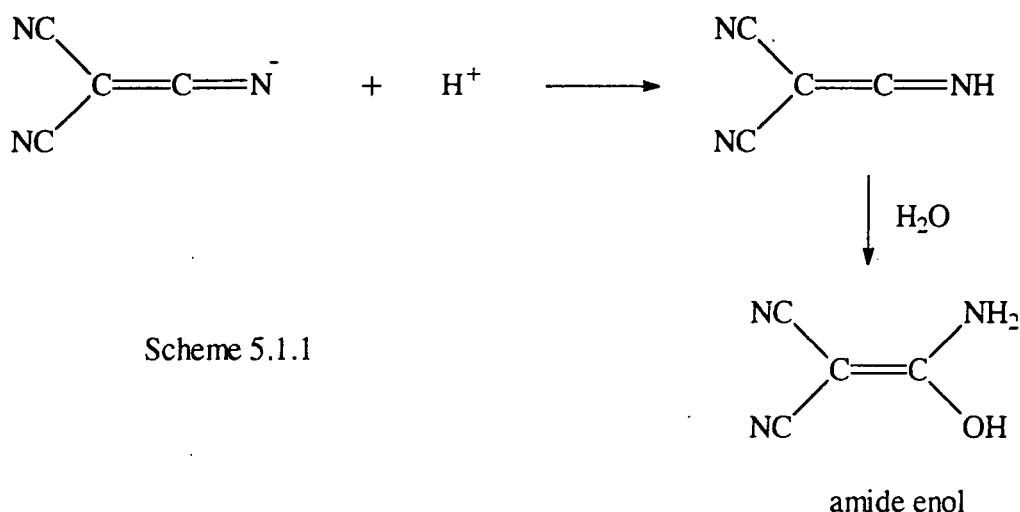
1. R.G. Pearson and R.L. Dillon, *J. Am. Chem. Soc.*, 1953, **75**, 2439.
2. C.D. Ritchie and W.F. Sager, *Prog. Phys. Org. Chem.*, 1964, **2**, 323.
3. R.P. Bell and K. Yates, *J. Chem. Soc.*, 1962, 2285.
4. J.P. Guthrie, *Can. J. Chem.*, 1979, **57**, 1177.
5. A. Graham and D.L.H. Williams, *J. Chem. Soc., Perkin Trans. 2*, 1992, 747.
6. J. Andros, Y. Chiang, C.G. Huang, A.J. Kresge and J.C. Scaiano, *J. Am. Chem. Soc.*, 1993, **115**, 10605.
7. R.P. Bell and M. Spiro, *J. Chem. Soc.*, 1953, 429
8. J.P. Guthrie, *Can. J. Chem.*, 1993, **71**, 2123.
9. A.J. Kresge, R.H. Hochstrasser, N.P. Schepp and J. Wirz, *J. Am. Chem. Soc.*, 1988, **110**, 7875.
10. A.S.N. Murthy, A. Balasubramanian, C.N.R. Rao and T.R. Kasturi, *Can. J. Chem.*, 1962, **40**, 2267.
11. A.J. Hoefnagel and B.M. Wepster, *J. Am. Chem. Soc.*, 1973, **95**, 5357.
12. A.J. Kirby and G.J. Lloyd, *J. Chem. Soc., Perkin Trans. 2*, 1976, 1763.
13. R.P. Bell and M.I. Page, *J. Chem. Soc.*, 1973, 1681.
14. B.G. Cox and R.E.J. Hutchinson, *J. Chem. Soc., Perkin Trans. 2*, 1974, 613
15. G. Kostum, W. Vogel and K. Andersson, "Dissociation constants of Organic Acids and Bases", Butterworth, London, 1961.

Chapter 5

Enolisation studies of Amides

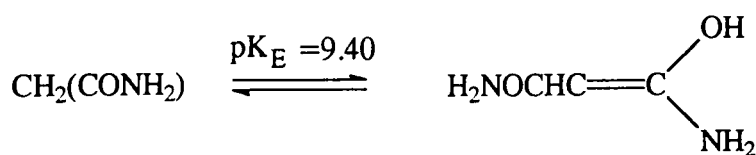
5.1 Introduction

Reports of enols formed from amides are very rare in the literature. The first identification of an amide enol was made by Trofimenko¹ who found that protonation of tricyanomethylanion occurs at the nitrogen atom which leads to the formation of the dicyanoketenimine which can be hydrolysed by water to give dicyanoacetamide enol (1-amino-2,2-dicyanoethene-1-ol). See scheme 5.1.1.



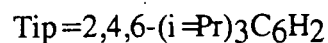
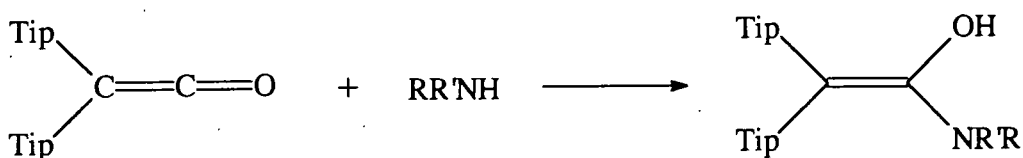
Scheme 5.1.1

The only kinetic investigation into amide enols was carried out by Williams and Xia² who measured the enol content and enolisation rate constants for malonamide [CH₂(CONH₂)]. The nitrosation and halogenation kinetics, under conditions where enolisation was the rate determining step gave a value of $k_e^{\text{H}^+} = 3.3 \times 10^{-3} \text{ l mol}^{-1} \text{ sec}^{-1}$ for the acid catalysed enolisation of malonamide. It is interesting that the enolisation is acid catalysed in the case of malonamide but none of the carboxylic acids and esters studied are acid catalysed. (see chapter 5 discussion). The enol content for malonamide was estimated to be *ca* 4×10^{-10} see scheme 5.1.2. This was calculated from the reactions of BrNO, NCSNO, I₂ and Br₂ with the enol form of malonamide which were assumed to be at the diffusion limit.



scheme 5.1.2

Recently, Rappoport³ has attempted to isolate amide enols by the addition of amines to sterically hindered ketenes.



scheme 5.1.3

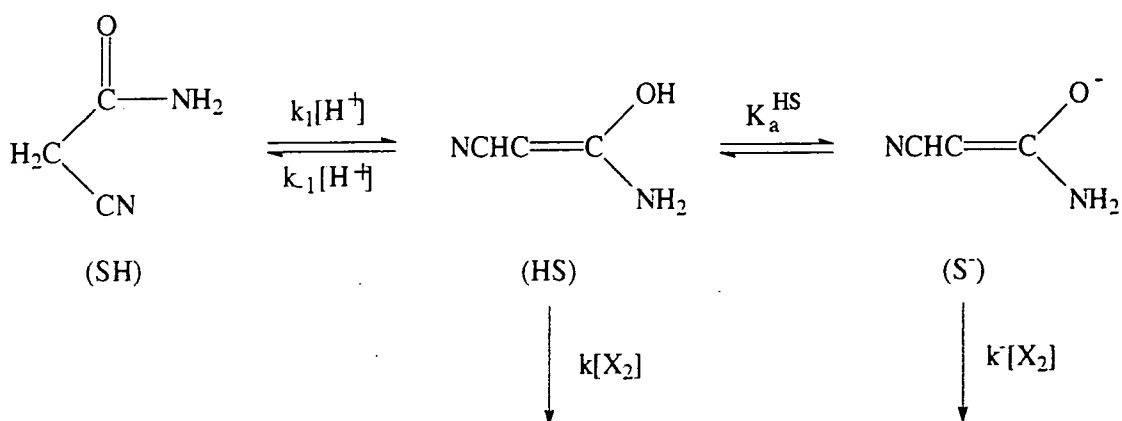
Proton N.M.R. studies indicate the initial formation of an amide enol but the amide enols appear to be unstable with respect to oxidation.

Kresge⁴ et al have studied the reactions of 30 amine bases with diphenylketene. Kinetic and product studies have shown that the amines are acting as nucleophiles (rather than as general bases assisting the attack of water on the ketene) in these reactions and that amides are observed as products. This suggests that amides enol may be formed as intermediates, but no direct observations have been made.

The present study aims to extend the kinetic and equilibrium data for amide enols by studying the halogenation and deuterium exchange reactions for 2-cyanoacetamide and 2-carboxyacetamide. Buffer catalysis and metal ion catalysis in the enolisation of malonamide was also investigated.

5.2 Halogenation of 2-cyanoacetamide

The bromination and iodination of 2-cyanoacetamide (CA) was carried out in aqueous solution at 298K. The reactions were monitored in the usual way by following the change in the absorbance due to the halogen. All the reactions were carried with the CA in at least 25 fold excess over the halogen. Experimentally, it was found to be very difficult to obtain the condition where the rate of enolisation was the rate limiting step. The possible explanation for this is that in the case of amides the ketonisation of the amide enol is an acid catalysed process so it is very difficult to obtain conditions where the rate of ketonisation is much slower than the rate of halogenation of the enol (a pre-requisite for obtaining good zero order kinetics). Scheme 5.2.1 and equation 5.2.1 illustrate this point.



Scheme 5.2.1

In scheme 5.2.1 the enol is shown as the first intermediate rather than the enolate anion. The enol is expected to be the first intermediate as the enolisation of cyanoacetamide is an acid catalysed process (see section 5.3).

A steady state treatment on scheme 5.2.1 with the enol and enolate anion as reactive intermediates gives rise to the following equation (Equation 5.2.1).

$$\text{Rate} = \frac{k_1[\text{SH}][\text{H}^+] \left(k[\text{X}_2] + \frac{k^- K_a^{\text{SH}}[\text{X}_2]}{[\text{H}^+]} \right)}{k_{-1}[\text{H}^+] + \left(k[\text{X}_2] + \frac{k^- K_a^{\text{SH}}[\text{X}_2]}{[\text{H}^+]} \right)} \quad \text{equation 5.2.1}$$

Equation 5.2.1 shows that the enolisation step is rate limiting when;

$$k[\text{X}_2] + \frac{k^- K_a^{\text{SH}}[\text{X}_2]}{[\text{H}^+]} \gg k_{-1}[\text{H}^+]$$

This condition can only be met when the acid concentration is *low* and the halogen concentration is *high*. To obtain zero order kinetics the reactions have to be carried out in buffer solutions with pH values greater than *ca* 3.5, this creates another problem in that the enolisation and ketonisation steps are catalysed by buffer acids and bases, so it is still difficult to obtain good zero order kinetics. In the case of CA zero order conditions could only be obtained in acetic acid buffer at pH values greater than 4 (see section 5.2.2).

5.2.1 First order kinetics

To obtain first order kinetics the converse of the above applies and *high* acidity and *low* halogen concentrations are required. To obtain zero order kinetics in strongly acidic solutions it is necessary to measure the rate of enolisation by deuterium exchange (see section 5.3).

Good first order kinetics were obtained by using low halogen concentrations (*ca* 2.5×10^{-4} M for bromine and 7×10^{-5} M for iodine) and relatively high acidity ($[\text{H}^+] > 0.1\text{M}$). The variation in the observed first order rate constant with acidity and substrate concentration was investigated. The results are shown in tables 5.2.1 to 5.2.4.

Table 5.2.1 $[I_2] = 7 \times 10^{-5} \text{ M},$ $[H^+] = 0.25 \text{ M}$

$[CA]_T / \text{M}$	$k_{\text{obs}} / \text{sec}^{-1}$
0.198	0.522
0.149	0.389
0.124	0.308
0.050	0.143
0.025	0.083

Table 5.2.2 $[I_2] = 7 \times 10^{-5} \text{ M},$ $[CA] = 0.15 \text{ M}$

$[H^+]_T / \text{M}$	$k_{\text{obs}} / \text{sec}^{-1}$
0.500	0.378
0.375	0.379
0.125	0.325
0.063	0.264
0.025	0.210

Table 5.2.3 $[Br_2] = 2.5 \times 10^{-4} \text{ M},$ $[H^+] = 0.5 \text{ M}$

$[CA]_T / \text{M}$	$k_{\text{obs}} / \text{sec}^{-1}$
0.150	0.220
0.125	0.196
0.100	0.173
0.050	0.103
0.025	0.066

Table 5.2.4 $[\text{Br}_2]=2.5 \times 10^{-4} \text{ M},$ $[\text{CA}]=0.05 \text{ M}$

$[\text{H}^+]_{\text{T}}/\text{M}$	$k_{\text{obs}}/\text{sec}^{-1}$
1.000	0.0933
0.875	0.0825
0.750	0.0754
0.625	0.0770
0.500	0.0740

The results show that the reaction is first order in CA (tables 5.2.1 and 5.2.3) and approximately independent of acidity at values of $[\text{H}^+] > 0.1$. Figures 5.2.1 and 5.2.2 show the variation of k_{obs} with the concentration of CA for the bromination and iodination reactions.

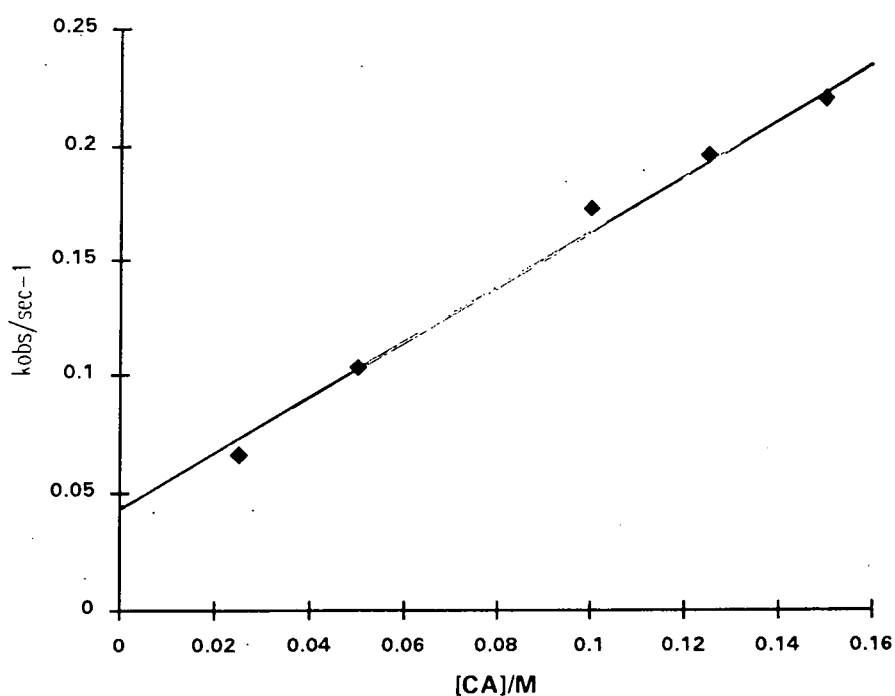
Figure 5.2.1**Plot of k_{obs} versus $[\text{CA}]_{\text{T}}$** $[\text{Br}_2]=5 \times 10^{-4} \text{ mol l}^{-1},$ $[\text{H}^+]=0.5 \text{ mol l}^{-1}$ 

Figure 5.2.2

Plot of k_{obs} versus $[\text{CA}]_{\text{T}}$

$$[\text{I}_2] = 7 \times 10^{-5} \text{ mol l}^{-1}, [\text{H}^+] = 0.25 \text{ mol l}^{-1}$$

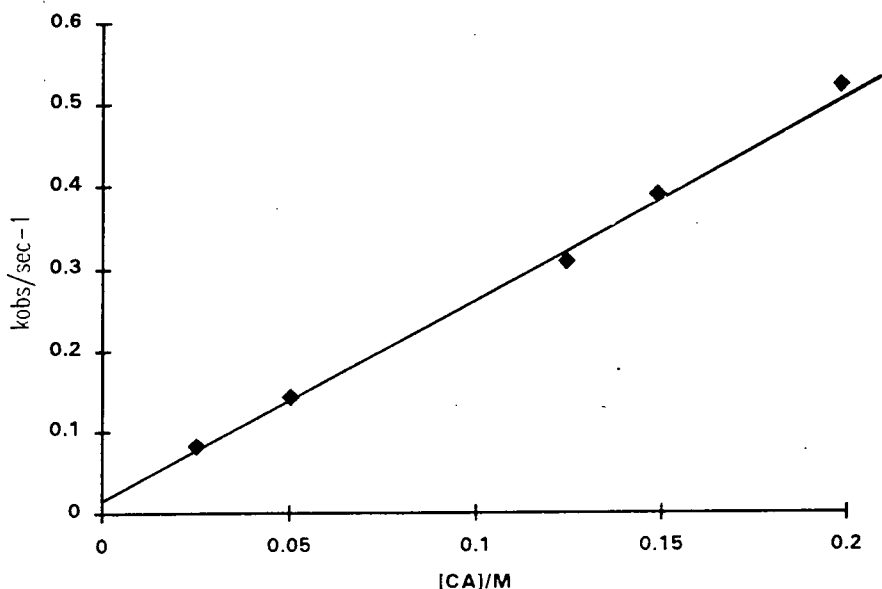
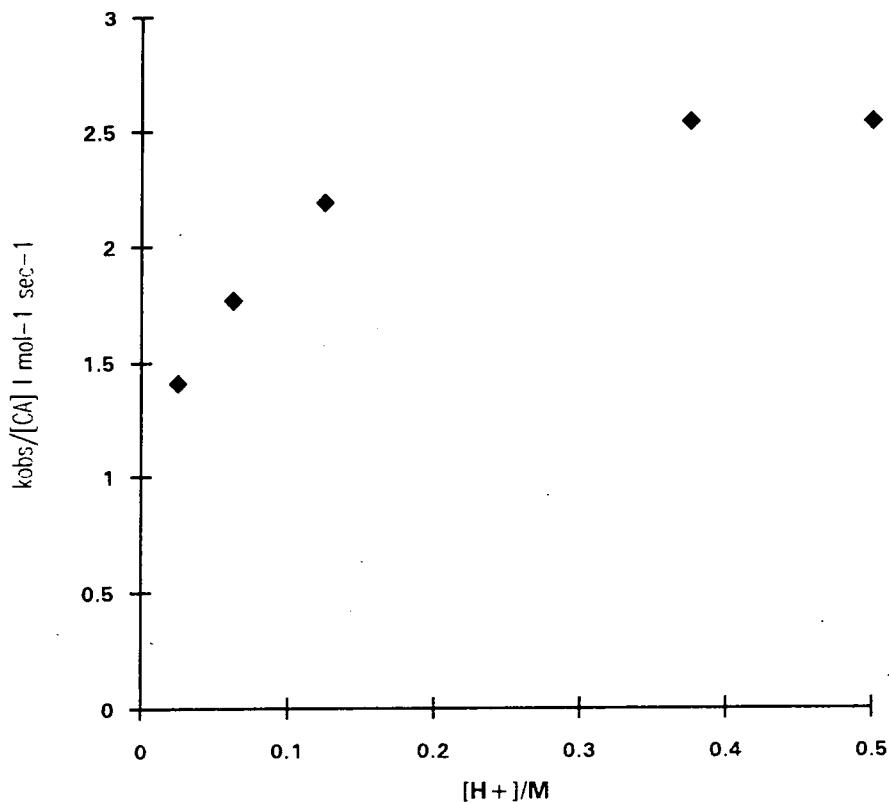


Figure 5.2.1 shows a reasonable straight line with a fairly large positive intercept, this is unusual for bromination reactions because the bromide ion generated in the reaction is a weak nucleophile (in water). Figure 5.2.2 shows a better straight line with an almost zero intercept. Tables 5.2.2 and 5.2.4 show that in highly acidic solutions $k_{\text{obs}}/[\text{CA}]$ reaches a limiting value of *ca* 1.5-2.5. The bromination results are less consistent than the iodination ones, this is usually the case and is due to the smaller extinction coefficient for bromine (*ca* one fifth that of iodine) which makes it difficult to measure very low concentrations accurately. A plot of $k_{\text{obs}}/[\text{CA}]$ versus $[\text{H}^+]$ (figure 5.2.3) shows clearly the levelling off that occurs at high acidity.

Figure 5.2.3
Plot of $k_{\text{obs}}/[\text{CA}]_{\text{T}}$ versus $[\text{H}^+]$

$[\text{I}_2] = 7 \times 10^{-5} \text{ mol l}^{-1}$,



These results can be interpreted in terms of the reaction scheme shown on page 139, a steady state approximation treating the enol and enolate as reactive intermediates gives the following expression.

$$\text{Rate} = \frac{k_1[\text{CA}][\text{H}^+] \left(k[\text{X}_2] + \frac{k^- K_a^{\text{SH}}[\text{X}_2]}{[\text{H}^+]} \right)}{k_{-1}[\text{H}^+] + \left(k[\text{X}_2] + \frac{k^- K_a^{\text{SH}}[\text{X}_2]}{[\text{H}^+]} \right)} \quad \text{equation 5.2.3}$$

Under conditions where the rate of ketonisation ($k_{-1}[H^+]$) is much greater than the rate of halogenation ($k[X_2] + \frac{k^- K_a^{SH}[X_2]}{[H^+]}$) then equation 5.2.3 simplifies to the following.

$$\text{rate} = \frac{k_1[CA][H^+] \left(k[X_2] + \frac{k^- K_a^{SH}[X_2]}{[H^+]} \right)}{k_{-1}[H^+]} \quad \text{equation 5.2.4}$$

Equation 5.2.4 can be rearranged to the following:

$$\text{Rate} = K_E[CA][X_2] \left(k + \frac{k^- K_a^{SH}}{[H^+]} \right) \quad \text{equation 5.2.5}$$

In highly acidic media the contribution from the enolate is very small and can be neglected, this gives rise to the simple expression.

$$\text{Rate} = kK_E[CA][X_2] \quad \text{equation 5.2.6}$$

Thus, from the slopes of k_{obs} against $[CA]$ and from the pH dependency, values for kK_E can be calculated. Table 5.2.5 shows the values obtained.

Table 5.2.5

		$kK_E / \text{l mol}^{-1} \text{sec}^{-1}$
IODINATION	acid dependency	2.54 ± 0.01
	substrate dependency	2.50 ± 0.08
BROMINATION	acid dependency	1.61 ± 0.07
	substrate dependency	1.24 ± 0.06

Table 5.2.5 shows that there is very little difference between the four values of kK_E determined, an average value is:

$$kK_E = 1.97 \pm 0.33 \text{ l mol}^{-1} \text{ sec}^{-1}$$

These results suggest that the reaction of the halogen is independent of the halogen used, this suggests that the reaction is at the diffusion limit (ie $k=5 \times 10^9 \text{ l mol}^{-1} \text{ sec}^{-1}$). Using this value for k gives the following value for the keto \rightleftharpoons enol equilibrium constant of.

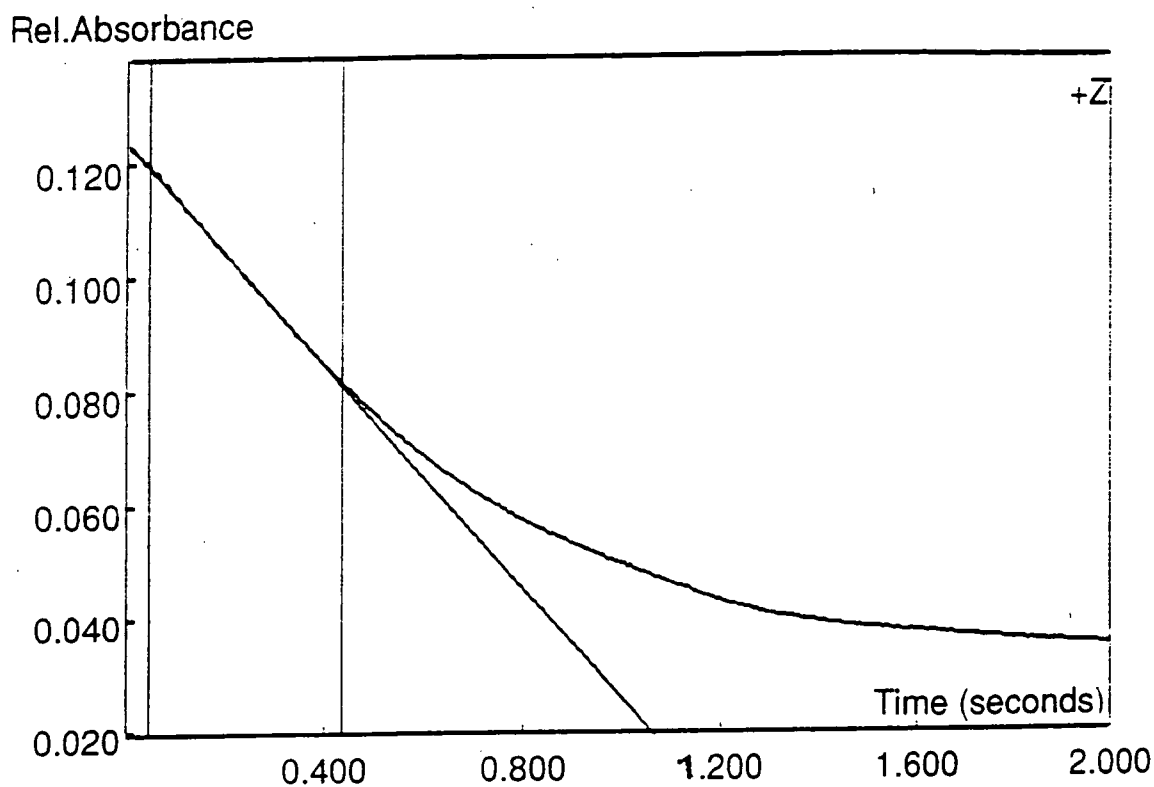
$$K_E = 3.94 \pm 0.66 \times 10^{-10}$$

This K_E value will be discussed along with other K_E values at the end of the chapter (see section 5.5).

5.2.2 Zero order kinetics

It is very difficult to obtain good zero order kinetics for the halogenation of cyanoacetamide. Using acetic acid buffer solutions at relatively high pH (>4) it was possible to obtain plots that showed a zero order dependency for the first 20% of the reaction some absorbance/time plots also exhibited a slight curvature at the beginning of the reaction. Figure 5.2.4 shows a typical plot.

Figure 5.2.4



Zero order rate constants were obtained from these plots with a relatively large degree of uncertainty. The effect of buffer concentration and substrate on the reaction was investigated. Tables 5.2.6 to 5.2.8 show the dependency of the observed zero order rate constant on CA concentration at three different pH values.

Table 5.2.6

$[\text{Br}_2] = 2.5 \times 10^{-3} \text{ M}$, $\text{pH} = 4.12$ 0.2M acetic acid buffer

[CA]/mol l ⁻¹	10 ⁴ k _{obs} / mol l ⁻¹ sec ⁻¹
0.125	6.71
0.100	5.49
0.075	4.31
0.050	3.34

Table 5.2.7

$[\text{Br}_2] = 1.4 \times 10^{-3} \text{ M}$, $\text{pH} = 4.65$ 0.2M acetic acid buffer

[CA]/mol l ⁻¹	10 ⁴ k _{obs} / mol l ⁻¹ sec ⁻¹
0.125	12.58
0.100	9.32
0.075	7.86
0.050	5.05

Table 5.2.8

$[\text{Br}_2] = 1.33 \times 10^{-3} \text{ M}$, $\text{pH} = 5.27$ 0.2M acetic acid buffer

$[\text{CA}]/\text{mol l}^{-1}$	$10^4 k_{\text{obs}}/\text{mol l}^{-1} \text{ sec}^{-1}$
0.125	22.86
0.100	19.18
0.075	14.52
0.050	11.90

The plots of k_{obs} against $[\text{CA}]$ at the three different pH values are shown in figure 5.2.5

Figure 5.2.5

Plot of k_{obs} against $[\text{CA}]/\text{M}$ at $\text{pH} = 4.12, 4.65$ and 5.27

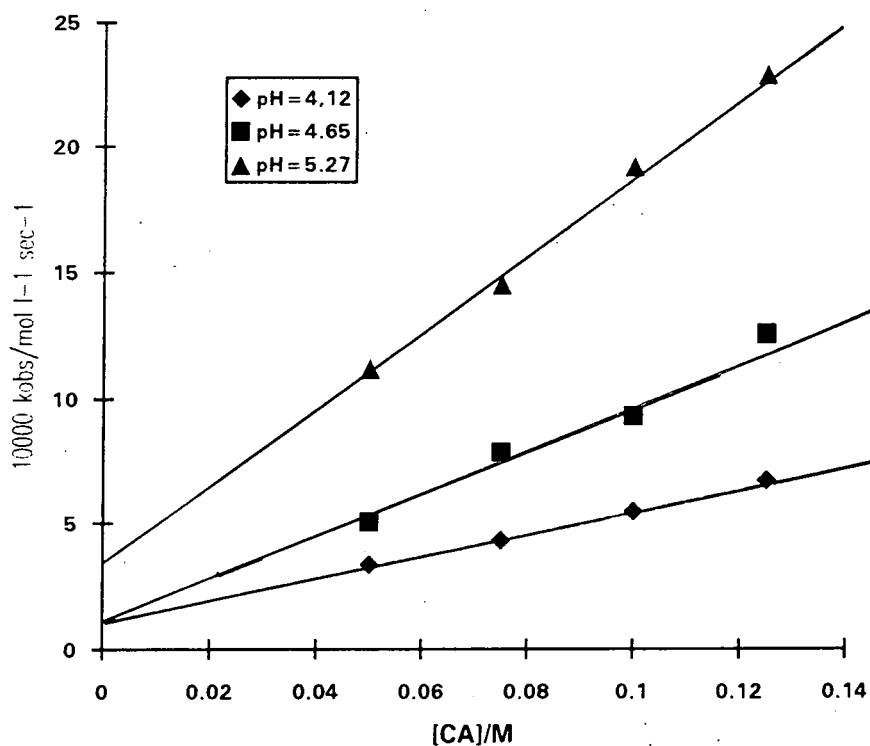
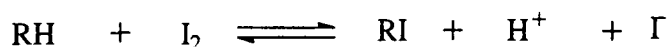


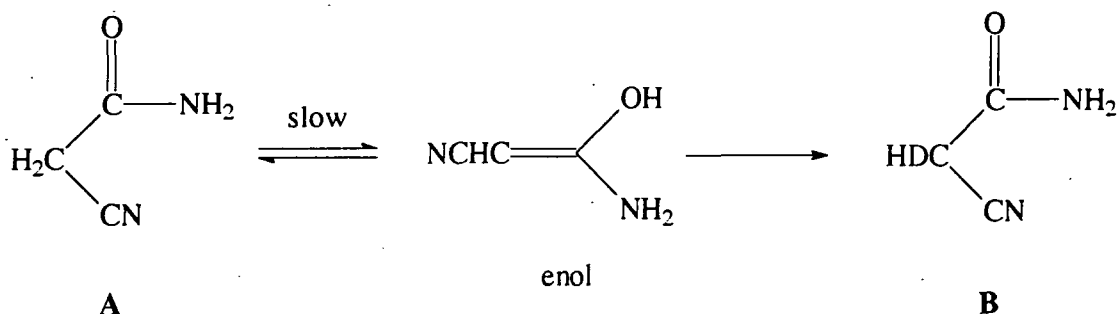
Figure 5.2.5 shows that there is a reasonable linear dependency of k_{obs} on the concentration of CA. The unusual feature of figure 5.2.5 is the large positive intercept which is observed. It appears that the intercept is larger at higher pH values this is the opposite effect usually observed for the iodination of the ketones⁵ (see below).



The large intercepts observed in figure 5.2.5 make it impossible to determine accurate values for the enolisation rate constant. These intercepts probably arise from the relatively poor zero order plots which are only linear for the initial part and consequently contain a large proportion of a first order reaction. These problems make this a very poor method for determining enolisation rate constants and as is the case with α -cyanoethylacetate (see chapter 3) the deuterium exchange method described in section 3.3 provides a better method.

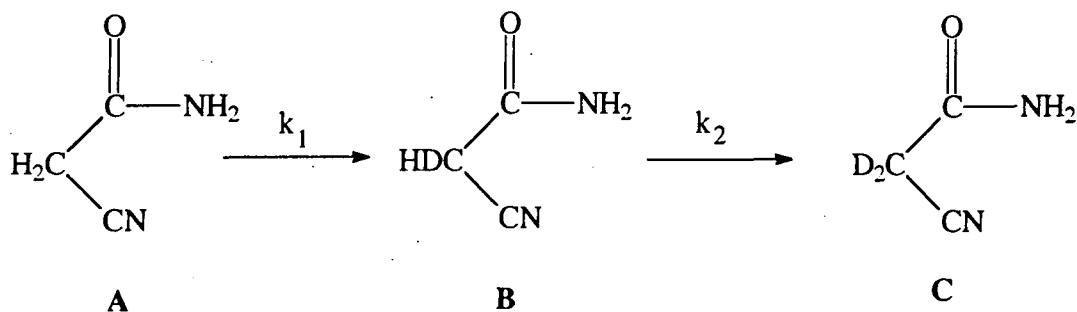
5.2.3 deuterium exchange in Cyanoacetamide

The rate of enolisation of CA was measured by monitoring the rate of exchange of the methylene protons for deuterium (see chapter 6 for experimental details). When CA is placed in an acidic solution of deuterium oxide (D_2O) exchange of the two methylene protons occurs probably via the enol intermediate (see scheme 5.2.2).



Scheme 5.2.2

If the reaction is carried out in pure D_2O the conversion to the enol is effectively irreversible because of the small amount of H_2O that is present. In scheme 5.2.2 the rate of ketonisation of the enol is much faster than the rate of enolisation, thus the rate of deuterium exchange corresponds to the rate of enolisation. If the reaction is left long enough then both methylene protons can be replaced and the reaction can be represented as an irreversible consecutive reaction, see scheme 5.2.3.



Scheme 5.2.3

The rate constants k_1 and k_2 can be measured and from these information pertaining to the secondary substrate isotope effect can be extracted.

The kinetics of deuterium exchange were measured by monitoring the change in the ^1H N.M.R. spectrum of CA as function of time. The N.M.R. samples were prepared by dissolving a small amount of CA (*ca* 0.02g) in a standard $\text{D}_2\text{O}/\text{D}_2\text{SO}_4$ solution which was thermostatted at 298K. No temperature control was employed once the samples were inside the spectrometer. Figure 5.2.6 shows an initial spectrum of CA (recorded in dimethylsulphoxide) and figure 5.2.7 shows a typical kinetic run with the change in the methylene proton peaks with time.

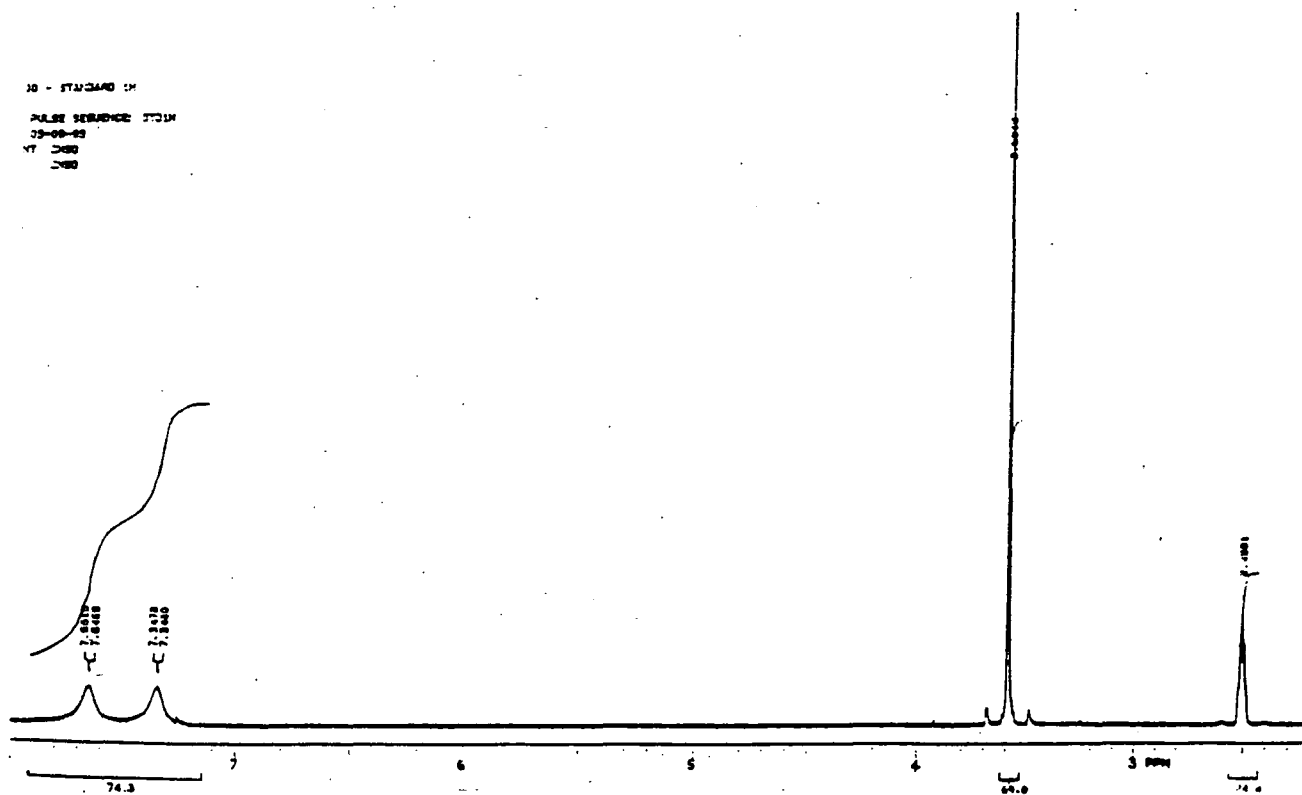


Figure 5.2.6

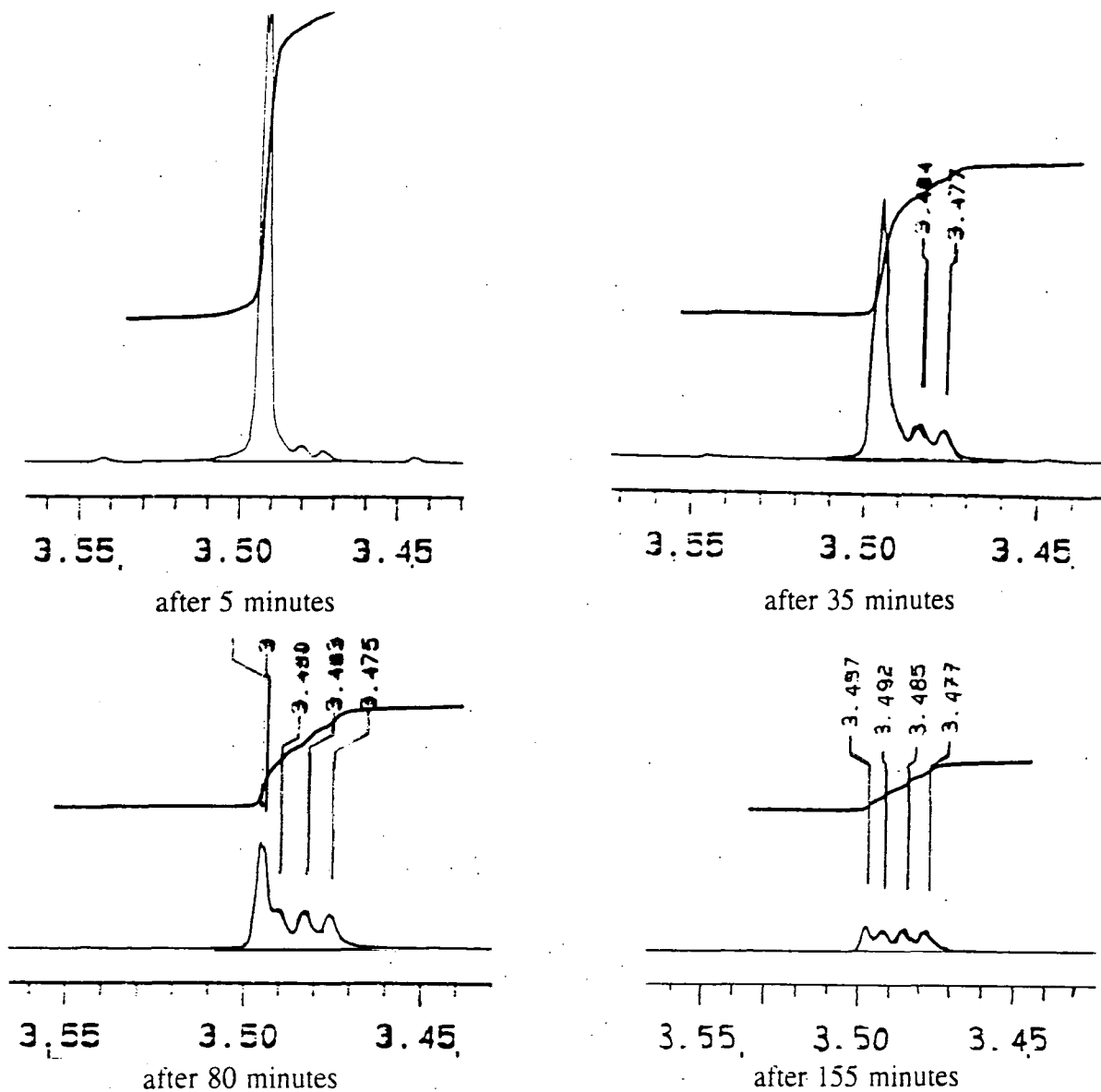
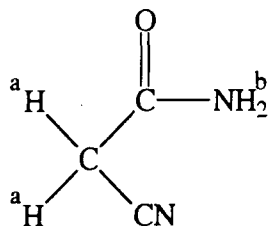


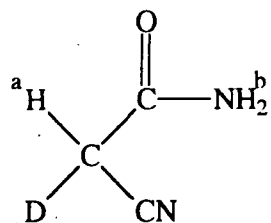
Figure 5.2.7

Initially the spectrum of CA shows the following peaks:



H ^a	δ = 3.50ppm	singlet	2H
H ^b	δ = 3.13ppm	singlet	2H

The methylene protons H^a are gradually exchanged for deuterium, this is observed by the appearance of a triplet at 3.45ppm which is due to the mono-deuterated cyanoacetamide {CA(D)}. This triplet occurs due to coupling with the deuterium atom which has a spin quantum number of I=1.



H^a $\delta = 3.45\text{ppm}$ 1:1:1 triplet 1H

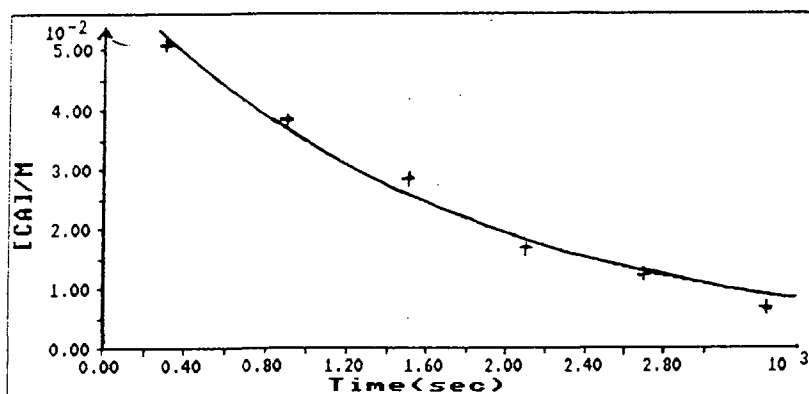
From the peak integrals for H^a it is possible to determine the concentration of CA and CA(D) as a function of time. In the case of ECA (see chapter 3) it was possible to determine the concentration of the monodeuterated species (ECA(D)) fairly accurately, unfortunately in the case of cyanoacetamide it was only possible to measure CA accurately (this was due to the very broad CA(D) peak) thus only k_1 could be measured. The kinetics were carried out in acidic solutions in the range 0.1M-0.3M D₂SO₄. Methanol was added to the kinetic runs to act as a standard (the protons in methanol will not be exchanged in the time period of the experiments) in order to calibrate the spectra. The results are shown in tables 5.2.9-5.2.11 along with the first order fits for the disappearance of cyanoacetamide.

Table 5.2.9

[CA]=0.06M, [D₂SO₄]=0.20M, [MeOH]=0.10M

time/ sec	[CA]/ mol l ⁻¹
300	0.0508
900	0.0385
1500	0.0285
2100	0.0168
2700	0.0123
3300	0.00675

plot of [CA] versus time



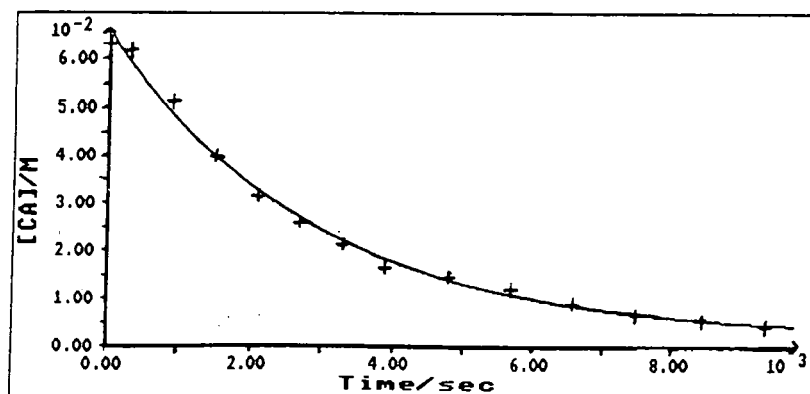
$$k_{\text{obs}} = 5.87 \pm 0.43 \times 10^{-4} \text{sec}^{-1}$$

Table 5.2.10

[CA]=0.0636M, [D₂SO₄]=0.10M, [MeOH]=0.05M

time/sec	[CA]/M
300	0.0616
900	0.0515
1500	0.0396
2100	0.0313
2700	0.0255
3300	0.0213
3900	0.0166
4800	0.0146
5700	0.0119
6600	0.0090
7500	0.0064

plot of [CA] versus time



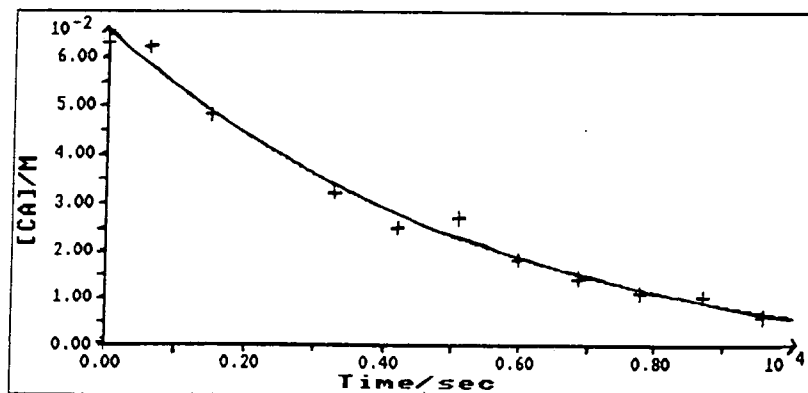
$$k_{\text{obs}} = 3.53 \pm 0.24 \times 10^{-4} \text{sec}^{-1}$$

Table 5.2.11

[CA]=0.0636M, [D₂SO₄]=0.05M, [MeOH]=0.05M

time/sec	[CA]/M
600	0.062
1500	0.048
2400	0.062
3300	0.032
4200	0.025
5100	0.027
6000	0.018
6900	0.014
7800	0.011
8700	0.010
9600	0.006

plot of [CA] versus time



$$k_{\text{obs}} = 1.76 \pm 0.34 \times 10^{-4} \text{sec}^{-1}$$

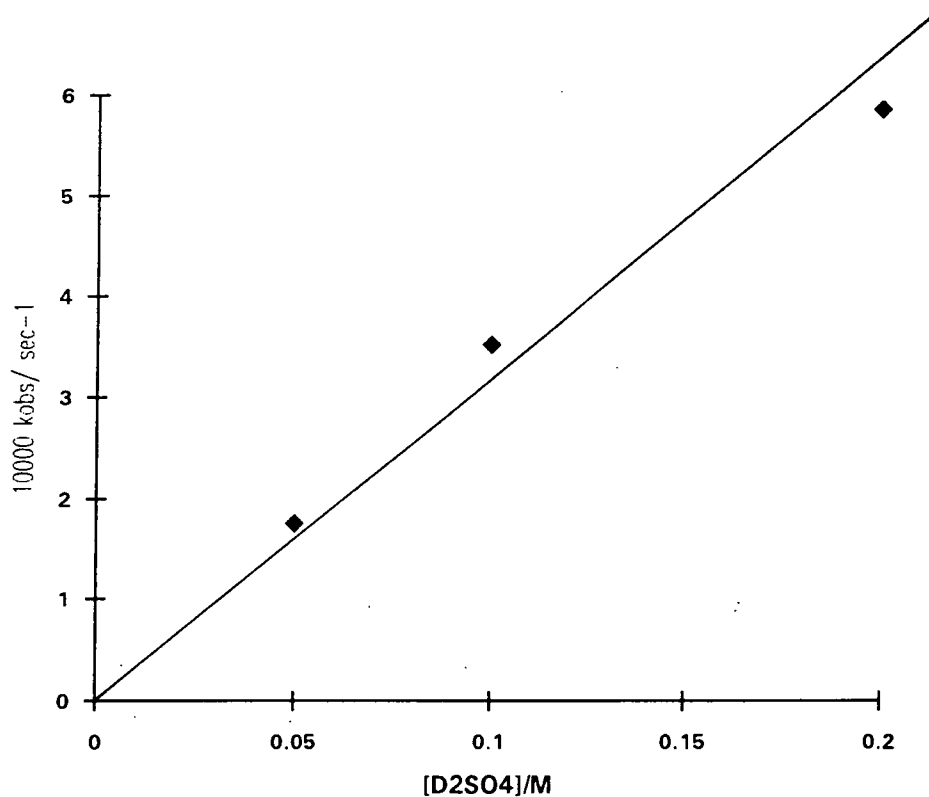
The first order fits obtained are fairly good. With the faster reaction carried out in 0.2M D₂SO₄ it was only possible to measure the reaction for one hour (corresponding to six spectra). The first order rate constants measured are reported in Table 5.2.12

Table 5.2.12

[D ₂ SO ₄]/ mol l ⁻¹	10 ⁴ k _{obs} /sec-1
0.20	5.87±0.43
0.10	3.53±0.15
0.05	1.76±0.34

Figure 5.2.8 shows a plot of k_{obs} versus [D₂SO₄]

Figure 5.2.8
Plot of k_{obs} against [D₂SO₄]



The graph shows clearly that the reaction is acid catalysed. Under the concentrations used D_2SO_4 should behave approximately as a monobasic acid (pK_a of $HSO_4^- = 1.9$)⁶. Figure 5.2.8 gives a slope of $2.68 \pm 0.29 \times 10^{-3} \text{ l mol}^{-1} \text{ sec}^{-1}$ thus the rate constant for the acid catalysed enolisation of cyanoacetamide is:

$$k_e^{H^+} = 2.68 \pm 0.29 \times 10^{-3} \text{ l mol}^{-1} \text{ sec}^{-1}$$

5.3 Enolisation of malonamide

The enolisation mechanism of malonamide has been studied by Williams and Xia², who reported an acid catalysed mechanism involving rate limiting proton abstraction from the oxonium ion intermediate. See figure 5.3.1.

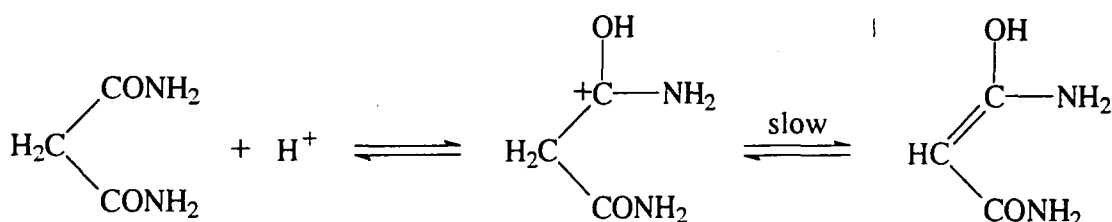


Figure 5.3.1

A value of $3.3 \times 10^{-3} \text{ l mol}^{-1} \text{ sec}^{-1}$ is reported for the acid catalysed enolisation rate constant. Deuterium isotope effects using $\text{CD}_2(\text{COND}_2)_2$ have shown that C-H/D bond fission is occurring in the rate determining step although a relatively low primary isotope effect of *ca* 2.2 is found. No measurements have been carried out in buffer solutions to investigate the possibility of general/specific acid or base catalysis. The present work aims to investigate buffer catalysis and compare the results with those previously determined for malonic acid (see chapter 2).

5.3.1 Iodination in chloroacetic acid buffers

The iodination of malonamide was carried out in mono-chloroacetic acid (MCAA) buffers in the pH range 2-3. The reaction was followed by monitoring the decrease in iodine absorbance at 459nm. In all kinetic runs the malonamide was present in at least 25 fold excess over the iodine. The absorbance time plots showed good zero-order behaviour and from the slopes of these traces zero-order rate constants were measured. The variation of k_{obs} with buffer concentration at three different pH values were measured. Tables 5.3.1 to 5.3.3 show the results recorded.

table 5.3.1

$[I_2]=2.45 \times 10^{-4} \text{M}$ $\text{pH}=2.22$ $[\text{malonamide}]=0.025 \text{M}$

$[\text{MCAA}]_T / \text{mol l}^{-1}$	$10^6 k_{\text{obs}} / \text{mol l}^{-1} \text{sec}^{-1}$
0.16	3.31
0.12	2.50
0.08	1.98
0.04	1.24
0.02	0.85

table 5.3.2

$[I_2]=2.45 \times 10^{-4} \text{M}$ $\text{pH}=2.67$ $[\text{malonamide}]=0.025 \text{M}$

$[\text{MCAA}]_T / \text{mol l}^{-1}$	$10^6 k_{\text{obs}} / \text{mol l}^{-1} \text{sec}^{-1}$
0.16	1.48
0.12	1.25
0.08	0.997
0.06	0.936
0.04	0.717

table 5.3.3

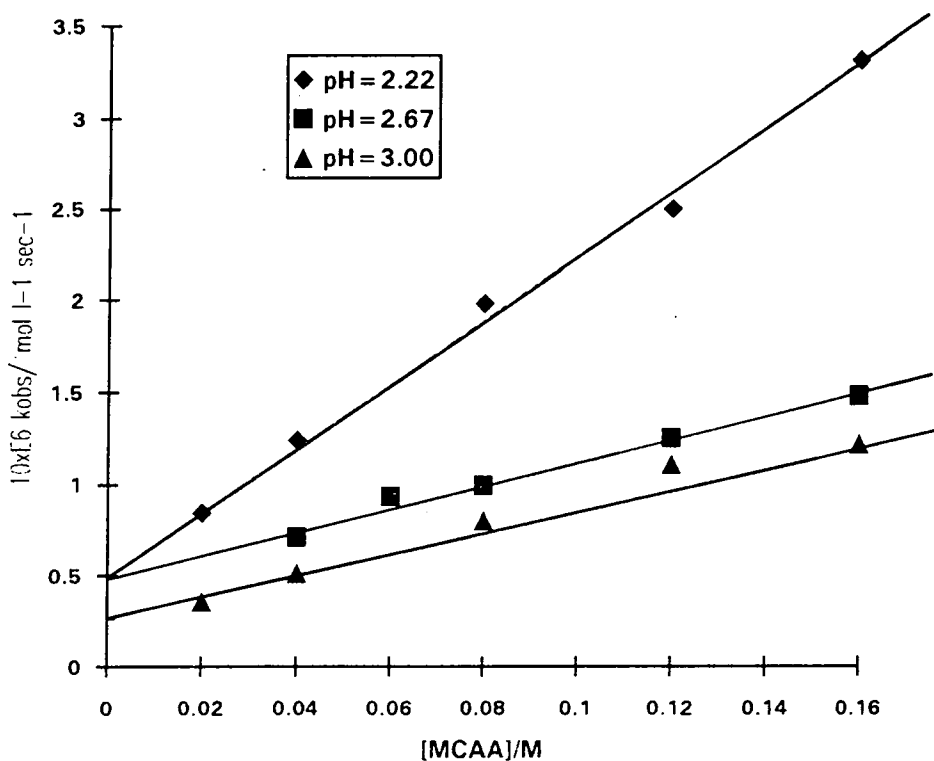
$[I_2]=2.45 \times 10^{-4} \text{M}$ $\text{pH}=3.00$ $[\text{malonamide}]=0.025 \text{M}$

$[\text{MCAA}]_T / \text{mol l}^{-1}$	$10^6 k_{\text{obs}} / \text{mol l}^{-1} \text{sec}^{-1}$
0.16	1.22
0.12	1.11
0.08	0.805
0.04	0.516
0.02	0.358

Figure 5.3.2 shows the plots of k_{obs} versus $[\text{MCAA}]_T$ at the three different pH values.

Figure 5.3.2

Plot of k_{obs} versus $[\text{MCAA}]/M$ at pH=2.22, 2.67, 3.00



From figure 5.3.2 the following rate equation can be derived:

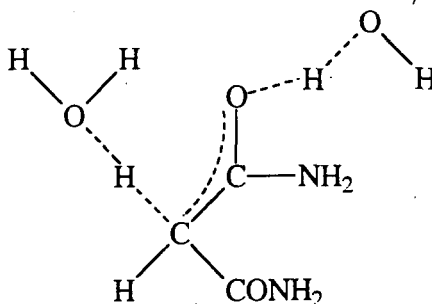
$$\text{Rate} = (k' + k[\text{MCAA}])[\text{Malonamide}]$$

The experimental intercept values (k') represent reaction by the proton catalysed and uncatalysed mechanisms. Values of k' can be calculated from the known rate constants². These k' values are shown in table 5.3.4 along with the slopes and intercepts calculated from figure 5.3.2.

Table 5.3.4

pH	slope/sec ⁻¹	Int (obs) /mol l ⁻¹ sec ⁻¹	Int (calc) /mol l ⁻¹ sec ⁻¹
2.22	1.72x10 ⁻⁵	5.3x10 ⁻⁷	1.15x10 ⁻⁶
2.67	6.05x10 ⁻⁶	5.0x10 ⁻⁷	8.0x10 ⁻⁷
3.00	7.55x10 ⁻⁶	2.0x10 ⁻⁷	7.1x10 ⁻⁷

The experimental intercept values are significantly lower than the calculated values, this is very unusual and may suggest that the actual pH in the reaction may be different to that measured initially. Many of the k_{obs} values reported in tables 5.3.1-5.3.3 are smaller than the expected values, this could be due to errors in the known value of the rate constant for the uncatalysed reaction which is calculated from a very small intercept on a plot of k_{obs} versus $[\text{H}^+]$. The slopes recorded in table 5.3.4 are very small and indicate that catalysis by MCAA is very slight. It appears from these results that at relatively high pH values (greater than *ca* 2) the dominant enolisation mechanism is that involving water molecules. Figure 5.3.3 shows the transition state for the concerted water catalysed mechanism.

Figure 5.3.3

transition state

A comparison between the hydronium catalysed and uncatalysed rate constants previously calculated² (see below)

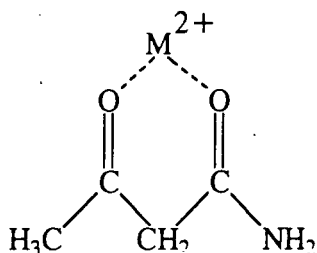
$$k_e^{H^+} = 3.3 \times 10^{-3} \text{ l mol}^{-1} \text{ sec}^{-1}$$

$$k_{H_2O} = 2.5 \times 10^{-5} \text{ sec}^{-1}$$

shows that at H^+ concentrations smaller than *ca* 0.01M the dominant mechanism is the uncatalysed one. Due to the lack of any significant buffer catalysis observed with monochloroacetic acid it was decided that further studies with other carboxylic acid buffers would not be very informative.

5.3.2 Metal ion catalysis in malonamide

Metal ion catalysis (by Zn^{2+} and Ni^{2+}) has been observed in the enolisation of β -ketoamides⁷ and has been attributed to a complexation of the type shown below.



It is reported that Ni^{2+} is a slightly better catalyst than Zn^{2+} (*ca* 3 fold in the enolisation of acetoacetamide and *ca* 1.4 fold in acetoacetanilide). Metal ion catalysis has also been observed in the enolisation of β -ketoesters⁸ and again has been attributed to a small degree of complexation with the keto tautomer of the ester. Catalysis by Zn^{2+} , Ni^{2+} and Cu^{2+} in the enolisation of 2-acetylpyridine⁹ leads to rate enhancements of *ca* 2×10^5 . In the case of 2-acetylpyridines their is extensive complexation, sufficient for the complexes to be observed by U.V./Vis spectrophotometry.

The present work aims to investigate the effect of Cu^{2+} , Ni^{2+} , Zn^{2+} and Co^{2+} on the enolisation of malonamide. The iodination of malonamide was carried out in acid solutions (0.1M $HClO_4$) at one concentration for each metal ion. The kinetics were monitored by following the disappearance at 459nm due to the iodine. In all kinetic

runs the malonamide was in at least 100 fold excess over the iodine. The absorbance time plots showed good zero order behaviour indicating that the rate determining step was the enolisation of malonamide. The zero order rate constants measured are reported in table 5.3.5 along with the expected rate constant (without any metal ions added).

Table 5.3.5

$[I_2]=4.30 \times 10^{-4} \text{ mol l}^{-1}$ $[H^+]=0.10 \text{ mol l}^{-1}$ $[\text{malonamide}]=0.052\text{M}-0.0125\text{M}$

metal Ion	concentration/mol l ⁻¹	k _{obs} / mol l ⁻¹ sec ⁻¹	k _{calc} /mol l ⁻¹ sec ⁻¹
Co ²⁺	4.77x10 ⁻³	6.03x10 ⁻⁵	4.44x10 ⁻⁵
Ni ²⁺	5.71x10 ⁻³	2.42x10 ⁻⁵	1.88x10 ⁻⁵
Cu ²⁺	7.39x10 ⁻³	2.58x10 ⁻⁵	1.88x10 ⁻⁵
Zn ²⁺	8.34x10 ⁻³	2.02x10 ⁻⁵	1.73x10 ⁻⁵

The results show that the observed rate constants are all slightly higher than the expected values, considering the relatively high concentrations of metal ions present the differences are very small. Cobalt ion shows the greatest increase (over 40%). The effect of pH on the metal ion catalysis was not investigated but malonamide is a very weak carbon acid so no significant concentration of the anion will be present until the pH is very high (> 12).

5.4 Enolisation studies on malonamic acid

As further evidence for the intramolecular mechanism (see chapter 2) proposed for malonic acid it was decided to study the enolisation mechanism of malonamic acid (2-carboxyacetamide). This compound may be expected to exhibit the intramolecular mechanism (see figure 5.4.1) because of the greater basicity of the amide group (see chapter 5 discussion) over the carboxylic acid and ester groups.

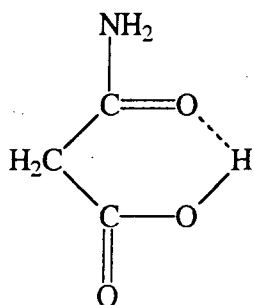


Figure 5.4.1

5.4.1 Kinetic studies on malonamic acid

The bromination of malonamic acid (see experimental section for preparation) was carried out in aqueous solution by monitoring the decrease in absorbance due to the halogen. The kinetics were measured with the malonamic acid (MA) in at least 20 fold excess over the bromine. The absorbance time plots observed showed an initial curved decrease followed by a slower decrease which was linear for the majority of the reaction. Figure 5.4.2 shows a typical kinetic trace.

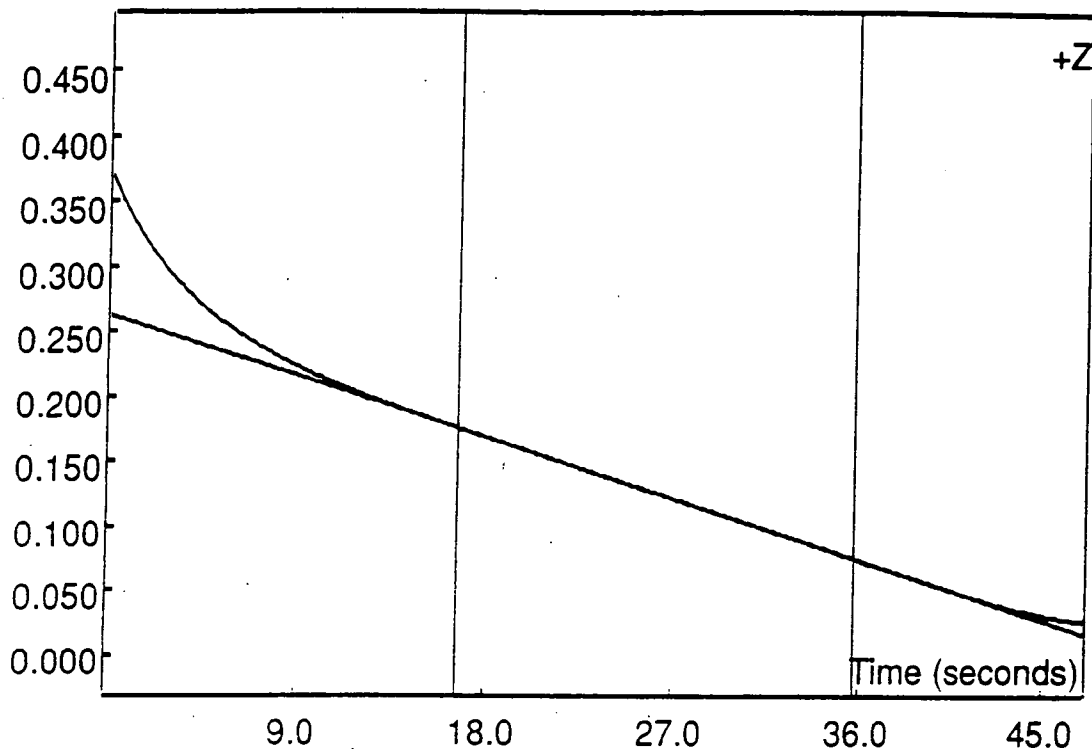
Figure 5.4.2

$[H^+] = 0.1M$

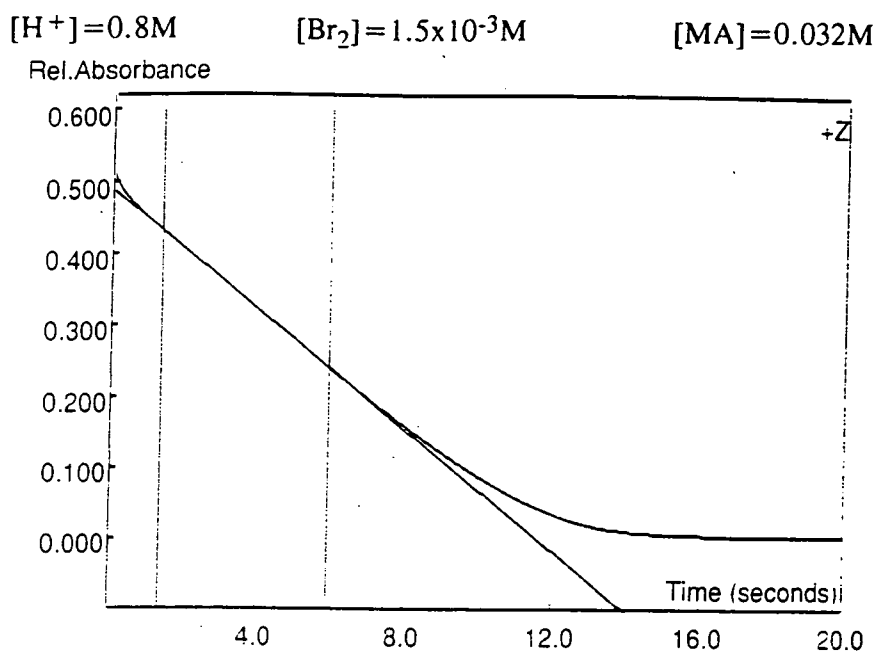
$[Br_2] = 1.5 \times 10^{-3}M$

$[MA] = 0.032M$

Rel.Absorbance



Under the above conditions the reaction is complete after *ca* 50 seconds. The initial drop takes place over the first 10 seconds and after this a much slower linear decrease in absorbance is observed. The effect of acidity on the shape of the plots was investigated. It was found that at higher acidity (*ca* 0.8M) the initial drop was reduced and the rate of decrease of the linear section of the curve was increased. Figure 5.4.3 shows an absorbance time plot obtained at higher acidity.

Figure 5.4.3

It was also noted that at any given acid concentration the initial drop was greater the higher the concentration of malonamic acid employed. The absorbance time plots obtained at high acidity show a reasonable zero order dependency (ignoring the initial and final sections) and from these, values of the zero order rate constant can be calculated. The variation of the zero order rate constant with acidity and substrate was investigated. The results are shown in tables 5.4.1 and 5.4.2

Table 5.4.1

$[MA] = 0.032M$ $[Br_2] = 1.5 \times 10^{-3}M$ Ionic strength = 0.8M

$[HCl]/mol\ l^{-1}$	$10^4 k_{obs} / mol\ l^{-1}\ sec^{-1}$
0.8	3.58
0.6	2.66
0.5	2.10
0.4	1.86
0.3	1.39
0.2	0.78
0.1	0.41
0.05	0.30

Table 5.4.2

$[H^+] = 0.8M$ $[Br_2] = 1.5 \times 10^{-3}M$ Ionic strength = 0.8M

$[MA]/\text{mol l}^{-1}$	$10^4 k_{\text{obs}}/\text{mol l}^{-1} \text{sec}^{-1}$
0.196	18.5
0.147	14.2
0.100	9.10
0.048	4.30
0.037	3.38

The plots of k_{obs} against $[H^+]$ and $[MA]$ are shown in figures 5.4.4 and 5.4.5

Figure 5.4.4

Plot of k_{obs} versus $[H^+]$

$[MA] = 0.032M$ $[Br_2] = 1.5 \times 10^{-3}M$ Ionic strength = 0.8M

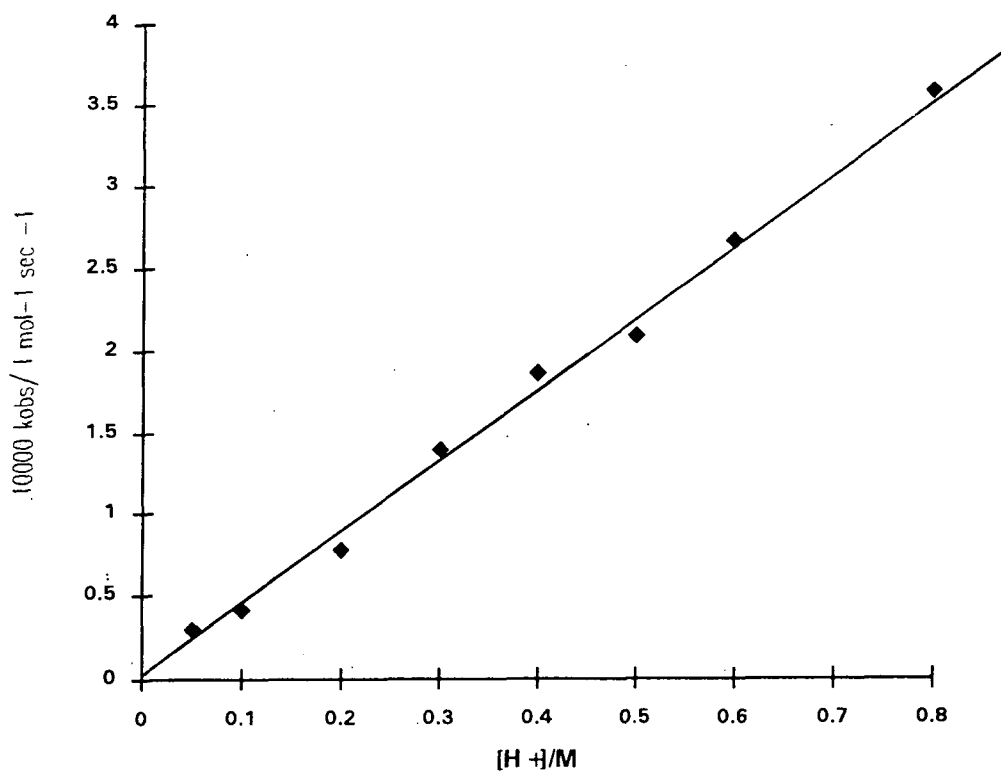
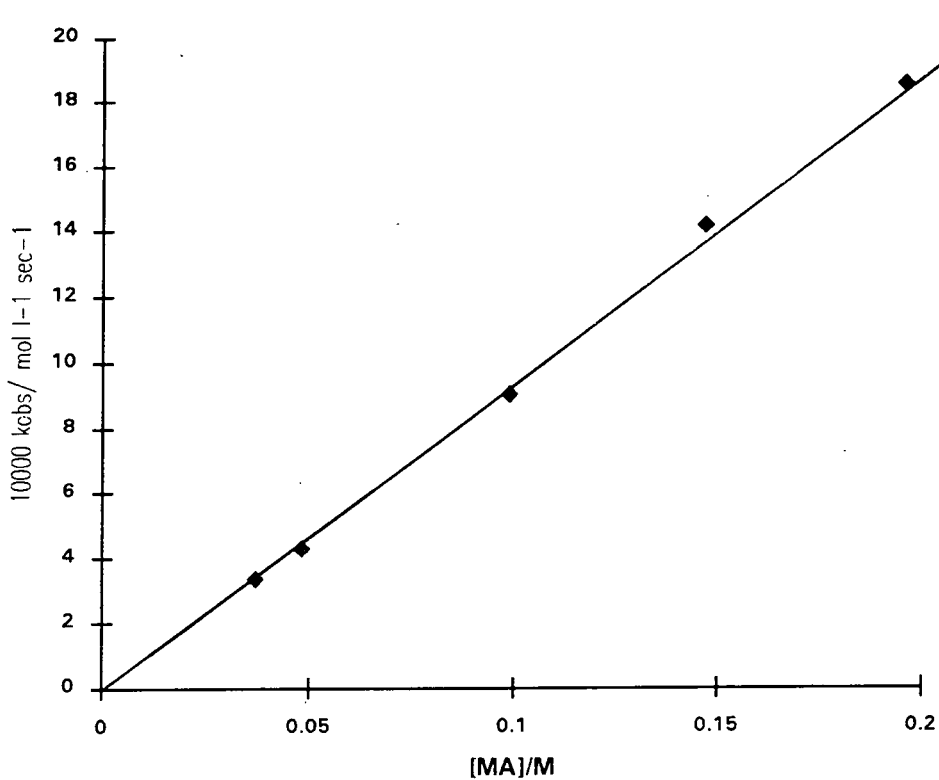


Figure 5.4.5

Plot of k_{obs} versus [MA]

[H⁺]=0.8M [Br₂]=1.5x10⁻³M Ionic strength=0.8M



Both plots show good linearity, thus the following simple rate equation can be established.

$$k_{\text{obs}} = k_e[\text{H}^+][\text{MA}]$$

Values of k_e can be calculated from the acid and substrate dependencies:

Substrate: $k_e = 1.20 \pm 0.10 \times 10^{-2} \text{ l mol}^{-1} \text{ sec}^{-1}$

Acid: $k_e = 1.37 \pm 0.03 \times 10^{-2} \text{ l mol}^{-1} \text{ sec}^{-1}$

The results are in fairly good agreement and give the following average value.

$$k_e = 1.29 \pm 0.09 \times 10^{-2} \text{ l mol}^{-1} \text{ sec}^{-1}$$

The results are reasonably consistent given the procedure employed to calculate the zero order rate constants.

Other halogenation reactions were not studied due to the problems in obtaining "good quality" starting material (malonamic acid being very susceptible to CO₂ loss). The initial curvature observed in these plots could be due to an impurity in the synthesised malonamic acid which reacts rapidly with bromine. At higher acidity the initial drop is reduced which may suggest that protonation of the impurity may reduce its reactivity, strangely the N.M.R. spectrum of malonamic acid didn't show any impurity peaks and the elemental analysis was reasonably consistent with that expected. The initial drop could result from enol already present in the malonamic acid solution, this seems unlikely as the N.M.R. should have shown a peak for the enol and the concentration of enol required to cause this relatively large drop would be *ca* 10⁻⁴M which is far greater than the enol content measured for similar compounds². Further halogenation and nitrosation studies on malonamic acid would be useful in order to confirm the enolisation rate constant reported here and also to determine the enol content (K_E) and confirm that the initial drop is not due to enol present in the system. In order to do this preparative problems need to be overcome possibly by the use of a different purification technique.

5.5 Discussion

5.5.1 Enolisation mechanisms

Up until the 1990's very little was known about the enolisation mechanisms of carboxylic acids, esters and amides. A breakthrough was made in 1990 when Kresge¹¹ made the first quantitative investigation into a carboxylic acid enol (enol formed from mandelic acid generated by flash photolysis). Since then Kresge *et al* have prepared a variety of carboxylic acid enols^{12,13} and have studied the ketonisation mechanisms. Most of the work carried out by Kresge has focused on carboxylic acid enols, but very little is known about amide or ester enols.

All the studies carried out so far suggest that ketonisation of carboxylic acid enols is not an acid catalysed process, but occurs by carbon protonation of the enolate anion (see figure 5.5.1 taken from ref 2).

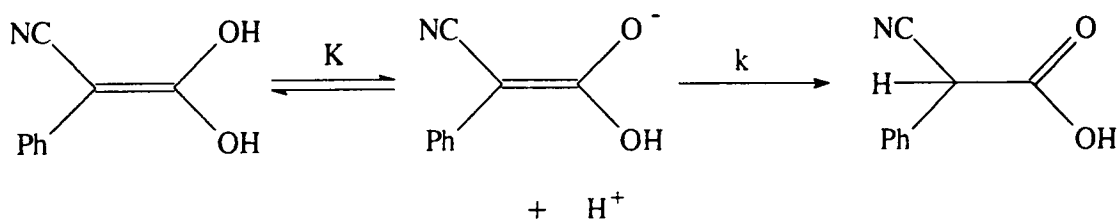


figure 5.5.1

This implies that the enolisation must occur via the same mechanism i.e. no acid catalysis should be observed in the enolisation of carboxylic acids. Table 5.5.1 shows rate constants reported for the enolisation of carboxylic acids esters where no acid catalysis has been observed. It was proposed by Leopold and Haim¹⁶ that the lack of acid catalysis in the enolisation of malonic acid was due to intramolecular acid catalysis (see chapters 2 and 4) but results from this work show that no acid catalysis is observed even when intramolecular catalysis is impossible.

Results obtained on the enolisation of malonic acid and ethylhydrogenmalonate (EHM) provide support for the intramolecular mechanism proposed by Leopold and Haim. A comparison between the rates of ionisation of diethylmalonate (DEM), EHM

and malonic acid show that there is a relatively large increase, *ca* 40 times in the ionisation of EHM compared to that of DEM. This is unexpected given the very similar σ^- values²⁴ for the ethylester and carboxy groups ($\sigma^- = 0.74$) and suggests that an extra interaction not present in the determination of σ^- values may be operating, presumably *hydrogen bonding*.

Table 5.5.1

compound	k_p/sec^{-1}
$\begin{array}{c} \text{CO}_2\text{H} \\ \diagdown \\ \text{H}_2\text{C} \\ \diagup \\ \text{CO}_2\text{H} \end{array}$	4.5×10^{-3} (ref 14)
$\begin{array}{c} \text{CO}_2\text{Et} \\ \diagdown \\ \text{H}_2\text{C} \\ \diagup \\ \text{CO}_2\text{H} \end{array}$	1.1×10^{-3} (this work)
$\begin{array}{c} \text{CO}_2\text{Et} \\ \diagdown \\ \text{H}_2\text{C} \\ \diagup \\ \text{CN} \end{array}$	5.5×10^{-4} (in D_2O this work) 1.17×10^{-3} (in H_2O , ref 15)

In the case where no hydrogen bonding is possible i.e) 2-cyanoethylacetate The lack of acid catalysis is probably due to the relatively high carbon acidity of the above compounds ($\text{pK}_a = \text{ca } 13$) compared with acetone ($\text{pK}_a = 20$) rather than any particular feature of the carboxylic acid group or ester group. The uncatalysed mechanism can be favoured in the enolisation of ketones if the carbon acidity is relatively high such as in acetylacetone and 1,3-dichloroacetone¹⁷.

It may be informative to investigate the enolisation/ketonisation mechanism of carboxylic acids with lower carbon acidity (i.e.without any strong electron withdrawing groups in the 2-position) to try and observe an acid catalysed mechanism. The obvious problem with this is the very slow rates of enolisation and

the instability of carboxylic acid enols¹⁸ not stabilised by electron withdrawing groups.

The only kinetic investigation into the enolisation mechanisms of amides is that carried out by Williams and Xia², who reported an acid catalysed process. Further studies carried out in this work also observed an acid catalysed reaction. Table 5.5.2 shows the acid catalysed rate constants reported.

Table 5.5.2

compound	$k_e^{H^+} / \text{l mol}^{-1} \text{sec}^{-1}$
malonamide $\begin{array}{c} \text{CONH}_2 \\ \\ \text{H}_2\text{C} \\ \\ \text{CONH}_2 \end{array}$	3.3×10^{-3} (ref 2)
cyanoacetamide $\begin{array}{c} \text{CONH}_2 \\ \\ \text{H}_2\text{C} \\ \\ \text{CN} \end{array}$	2.7×10^{-3} (this work)
malonamic acid $\begin{array}{c} \text{CONH}_2 \\ \\ \text{H}_2\text{C} \\ \\ \text{CO}_2\text{H} \end{array}$	1.3×10^{-2} (this work)

The observed acid catalysis in the enolisation of amides is presumably due to the increased basicity (for protonation at oxygen) of the amide group relative to that of carboxylic acids and esters. The acidity constant (pK_{BH^+}) for acetamide¹⁹ is ca -0.7 compared with pK_{BH^+} values of -6 to -8 for carboxylic acids²⁰ and esters²⁰. This 10^6 fold difference in basicity is sufficient to favour the acid catalysed mechanism.

Accurate values of pK_{BH^+} for the compounds in table 5.5.2 would allow the evaluation of rate constants for proton abstraction from the oxonium ion. See figure 5.5.2.

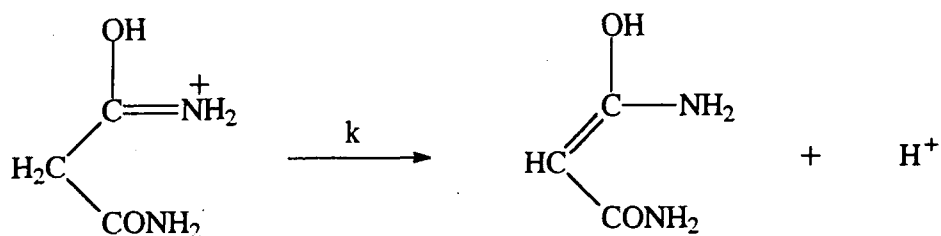


figure 5.5.2

Unfortunately pK_{BH^+} values for these compounds are not known, it may be possible to measure these using the same techniques (1H or ^{13}C N.M.R) employed by Cox¹⁹ *et al* . If it is assumed that the pK_{BH^+} values are similar to that of acetamide (*ca* -0.7) then values of k in the range $1-6 \times 10^{-2} \text{ sec}^{-1}$ can be calculated. The lack of any correlation between $k_e^{H^+}$ and σ^- or σ values again suggests that hydrogen bonding effects may operate, with stabilisation of the oxonium ion favoured in the cases of malonamide and malonamic acid.

No studies on the ketonisation of amides have been reported. It would be very interesting to study the ketonisation of amides to confirm the acid catalysed pathway proposed and investigate the interesting basic properties (protonation at carbon or nitrogen?) of amide enols²¹.

5.5.2 Enol contents of carboxylic acids, esters and amides.

Carboxylic acid enol contents have generally been determined by two methods:

- 1) Direct measurement of enolisation and ketonisation rate constants.
- 2) Indirect kinetic determination using the assumption of diffusion controlled reactivity.

The enol contents measured in this work are calculated by the second method and enol contents quoted from Kresge are calculated using the first method. Table 5.5.3 shows the enol contents reported in this work along with those for acetone²² and acetic acid¹⁸.

Table 5.5.3

compound	$pK_E = -\log_{10}K_E$
malonic acid $\begin{array}{c} \text{CO}_2\text{H} \\ \diagup \\ \text{H}_2\text{C} \\ \diagdown \\ \text{CO}_2\text{H} \end{array}$	8.22
ethylhydrogenmalonate $\begin{array}{c} \text{CO}_2\text{Et} \\ \diagup \\ \text{H}_2\text{C} \\ \diagdown \\ \text{CO}_2\text{H} \end{array}$	8.85
α -cyanoethylacetate $\begin{array}{c} \text{CO}_2\text{Et} \\ \diagup \\ \text{H}_2\text{C} \\ \diagdown \\ \text{CN} \end{array}$	9.69
malonamide $\begin{array}{c} \text{CONH}_2 \\ \diagup \\ \text{H}_2\text{C} \\ \diagdown \\ \text{CONH}_2 \end{array}$	9.40
cyanoacetamide $\begin{array}{c} \text{CONH}_2 \\ \diagup \\ \text{H}_2\text{C} \\ \diagdown \\ \text{CN} \end{array}$	9.30
$\begin{array}{c} \text{O} \\ \parallel \\ \text{C} \\ \diagup \quad \diagdown \\ \text{H}_3\text{C} \quad \text{OH} \end{array}$	21 (reference 18)
$\begin{array}{c} \text{O} \\ \parallel \\ \text{C} \\ \diagup \quad \diagdown \\ \text{H}_3\text{C} \quad \text{CH}_3 \end{array}$	8.2 (reference 22)

A comparison between the enol contents of malonic acid, ethylhydrogenmalonate(EHM) and acetic acid shows that exchanging one of the hydrogen atoms for a carboxylic acid or ester group has a massive effect (ca 10^{13}) on the enol content. This can be explained by the hydrogen bonding interactions in malonic acid and EHM which can stabilise the enol. see figure 5.5.3.

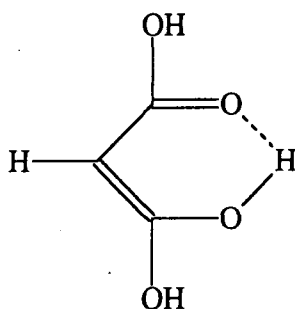
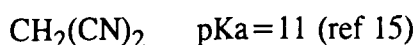
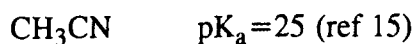


figure 5.5.3

This effect is the same as that observed with acetylacetone²³, in this case exchanging one hydrogen in acetone for an acetyl group increases the enol content by a factor of 10^8 .

The large increase in the enol content for α -cyanoethylacetate(ECA) cannot be explained in this way because the cyano group is unable to bend round and form a hydrogen bond (this may explain the smaller enol content in ECA than malonic acid and EHM). Assuming the enol content of ethylacetate is similar to that for acetic acid then the *ca* 10^{11} fold increase in the enol content of ECA is presumably due to a very strong interaction between the enol double bond and the cyano group. It is interesting to compare the effect of a cyano group on carbon acidity; the effect of changing one hydrogen in acetonitrile for a cyanide group decreases the pK_a by *ca* 14 units, see below:



The closeness of these two effects may suggest that the enol has a significant contribution from a charge separated canonical form, see figure 5.5.4.

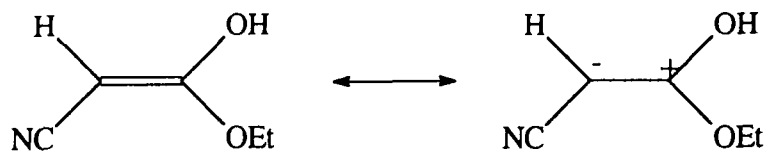
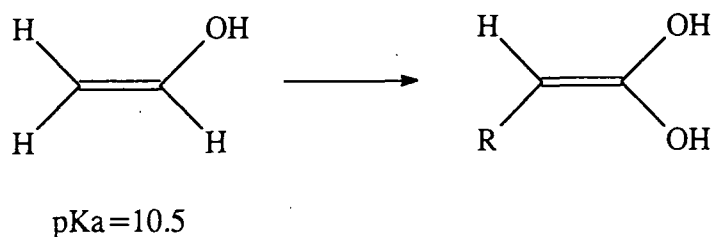


figure 5.5.4

The enol contents observed for cyanoacetamide (9.30) and ethylcyanoacetate (9.69) are not vastly different, the slight effect is probably due to the greater ability of the NH_2 group over the OEt to stabilise the positive charge in the enol.

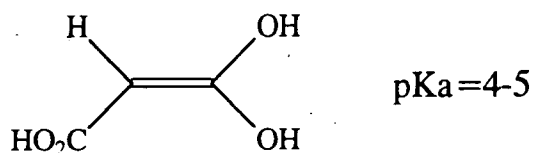
Kresge¹³ has used a simple formula to estimate the effect of substituents on the acidity of carboxylic acid enols. Starting with acetaldehyde enol as a standard for which the pK_a is known²⁴, $\text{pK}_a=10.5$ and then assessing the effect of the other substituents see below.



The effect of an α -OH group is estimated to be ca 2 pK_a units by comparison with the difference in acidity between alcohols and gem diols²⁵. The effect of the R group is approximated to the effect on the pK_a of acetaldehyde enol. Kresge has found that the acidifying effects of Ph and CN are 1 and 6 pK_a units respectively. The effect of other groups can be estimated by comparison with σ_n values²⁶, i.e the effect of a carboxy group is midway between that of CN and Ph.

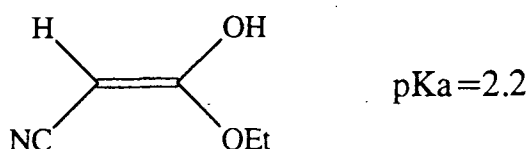
substituent	σ_n	acidifying effect (pK_a units)
CN	0.61	6
CO_2R	0.34	3-4
Ph	0.05	1

Using this value of *ca* 3-4 for the acidifying effect of a carboxy group we can estimate the pK_a of malonic acid enol.



The value of 4-5 for the pK_a of malonic acid confirms the observation that in acidic solutions ($pH < 3$) the only reactive intermediate is the enol.

The pK_a of the enol formed from 2-cyanoacetate has been estimated to be **2.2**. (see chapter 3 discussion).



This is close to value expected using the above values for the acidifying effect of CN (6 pK_a units) and OH/OEt (2 pK_a units). This confirms the results from Kresge that the cyano group has a remarkable effect on the acidity of carboxylic acid enols. It may be interesting to investigate the enolic properties of 2,2-dicyanoacetic acid and 2,2-dicyanoacetamide. It has been reported by Trofimenko¹ that 2,2-dicyanoacetamide exists almost exclusively in the enol form.

The pK_E values reported here compare very favourably with those measured by Kresge¹³ considering the completely different techniques employed. Kresge has reported a value of $pK_E = 7.22$ for α -cyanoethylacetic acid which is approximately 300 times greater than the enol content for α -cyanoethylacetate, this difference reflects the double bond stabilising ability of the phenyl group.

The synthetic problems encountered in the preparation of malonamic acid (see section 5.4.1) may provide a possible route to the preparation of a simple amide enol. Loss of carboxylic acid occurs readily from malonamic acid producing acetamide, this reaction may proceed via the enol of acetamide, see figure 5.5.5.

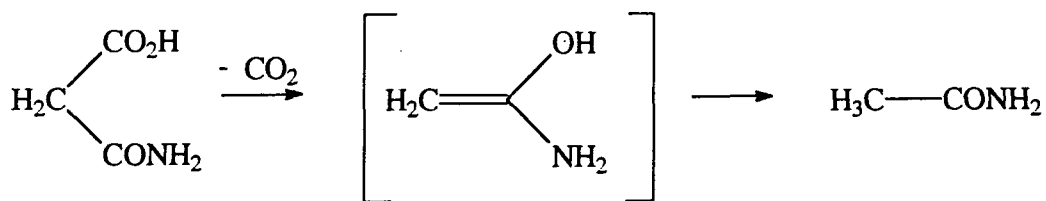


figure 5.5.5

If the decarboxylation reaction could be carried out in a "perfectly" dry aprotic solvent (ketonisation of the enol requires water or a protic solvent) it may be possible to reduce the rate of ketonisation sufficiently for the enol to be detected.

References

1. S.Trofimenko, E.L.Little and H.F.Mower, *J.Org. Chem.*, 1962, **27**, 433.
2. L.Xia and D.L.H.Williams, *J.Chem.Soc., Perkin Trans 2.*, 1993, 1429.
3. Z.Rappoport. "Simple stable enediols and derivatives". seminar, 12th I.U.P.A.C conference on physical organic chemistry, Padova, Italy, August, 1994.
4. J.Andraos and A.J.Kresge, *J.Am. Chem. Soc.*, 1992, **114**, 5643.
5. J.Toullec and J.E. Dubois, *J.Am. Chem. Soc.*, 1981, **103**, 5393.
6. "Handbook of chemistry and physics", 63rd edition, CRC press, 1982, D-171.
7. M.J.Hynes and E.M. Clarke, *J.Chem.Soc., Perkin Trans 2.*, 1994, 901.
8. K.J. Pederson, *Acta, Chem.Scand.*, 1948, **2**, 252.
9. B.G.Cox, *J.Am. Chem. Soc.*, 1974, **96**, 6823.
10. A.I.Vogel and J.H.George, *J.Chem.Soc.*, 1934, 1101.
11. Y.Chiang, A.J.Kresge, P.Pruszynski, N.P.Schepp and J.Wirz, *Angew. Chem. Int. Ed.*, 1990, **29**, 792.
12. J.Andraos, Y.Chiang, C.G.Huang, A.J.Kresge and J.C. Scaiano, *J.Am. Chem. Soc.*, 1993, **115**, 10605.
13. J.Andraos, Y.Chiang, A.J.Kresge, I.G.Pojarlieff, N.P.Schepp and J.Wirz, *J.Am. Chem. Soc.*, 1994, **116**, 73.
14. A.Graham and D.L.H.Williams, *Tetrahedron*, 1992, **48**, 7973.
15. R.G.Pearson and R.L.Dillon, *J.Am. Chem. Soc.*, 1953, **75**, 2439.
16. K.R.Leopold and A.Haim, *Int. J. Chem. Kinet*, 1977, **9**, 83.
17. J.R.Leis, M.E.Pena, D.L.H.Williams, *J.Chem.Soc., Perkin Trans 2.*, 1988, 157.
18. P.J. Guthrie, *Can.J. Chem.*, 1993, **71**, 2123.
19. R.A. Cox, L.M.Druet, A.E. Klausner, T.A. Modro, P.Wan and K. Yates, *Can. J. Chem.*, 1981, **59**, 1568.
20. E.W. Arnett, *Prog. Phys. Org. Chem.*, 1963, **1**, 223.
21. A.J. Kresge, private communication, Durham University, 1995.

22. A.J.Kresge, J.R. Keefe and J.Wirz, *J.Am.Chem.Soc.*, 1988, **110**, 7875.
23. J. Emsley and N.J. Freeman, *J. Mol. Struct.*, 1987, **161**, 193.
24. Y.Chiang, A.J.Kresge, P.A.Walsh, Y. Yin, *J.Chem. Soc., Chem Commun.* 1989, 869.
25. R.Stewart, "The Proton: Applications to Organic Chemistry: Academic Press: New York, 1985, p44.
26. J.Hine, "Structural Effects on Equilibria in Organic Chemistry", Wiley-Interscience, New York, 1975, p72.

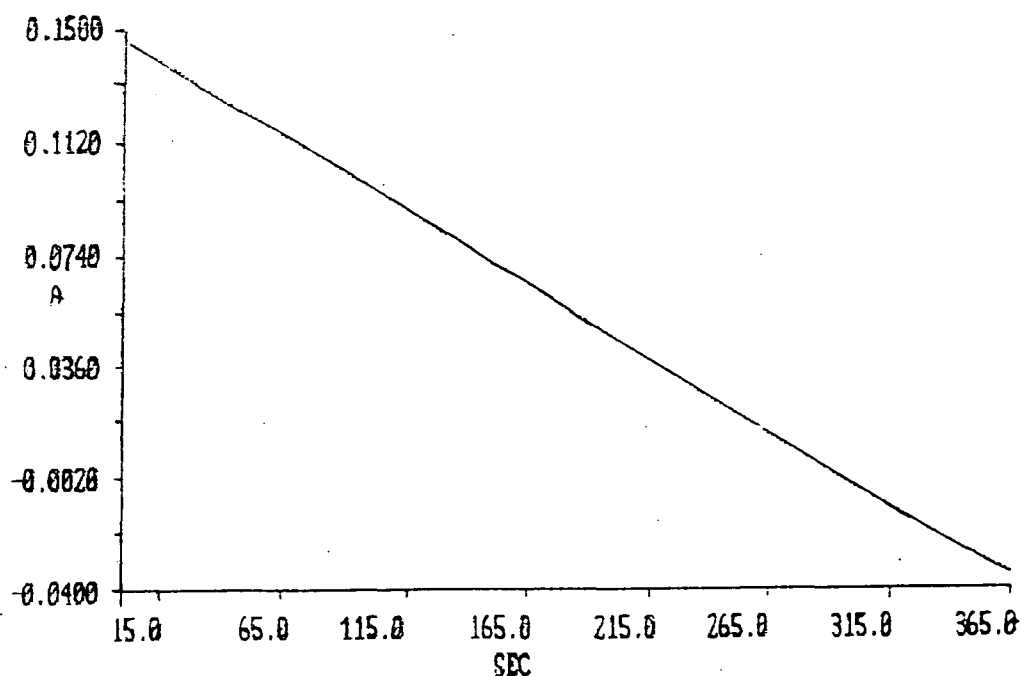
Chapter 6

Experimental details

6.1. U.V./Visible Spectrophotometry.

All u.v./vis spectra were obtained from solutions in 1cm path length quartz cells on either a Perkin-Elmer Lambda 2 or a Shimadzu 2102-PC instrument. The Perkin-Elmer Lambda 2 was used when measuring the kinetics of slow reactions ($t_{1/2} > 20$ seconds). For rapid reactions ($t_{1/2} \leq 20$ seconds) a stopped flow technique was used (section 6.1.2). All kinetics were carried out at 298K, the solutions were thermostatted in a water bath at 298k prior to mixing and The cell holder was thermostatted using water from the water bath. The kinetics were analysed using a computer fitting program (PECSS-Perkin Elmer computerised spectroscopy software). Figure 6.1.1 shows a typical kinetic trace obtained.

Figure 6.1.1



6.2 Stopped flow Spectrophotometry.

Reactions with half lives less than 20 seconds were measured on a Hi-Tech Scientific SF-3 series stopped flow spectrophotometer and with a modern Applied Photophysics DX.17MV sequential stopped flow spectrophotometer. Both machines work on the same principal but the Applied Photophysics machine had the option of a 0.4cm or 1 cm path length whereas the Hi-Tech machine only had a 0.2 cm path length. The longer path length enabled low absorbances to be measured in the Applied Photophysics machine, this was particularly useful when using very low halogen concentrations. A schematic diagram of a stopped flow machine is shown in Figure 6.2.1.

The two solutions to be reacted, A and B, are stored in reservoirs and are drawn into two identical syringes so that equal volumes are mixed. The syringes are compressed simultaneously, either manually (in the case of the Hi-Tech machine) or using a compressed air supply (in the case of the Applied Photophysics machine), and mixing occurs at point M extremely rapidly ($< 1\text{ms}$). Both stopped flow machines have a dead time of approximately 0.8ms, thus reactions that have half lives smaller than this cannot be measured by stopped flow methods. The mixture flows into a thermostatted 4mm or 10mm path length quartz cell at point O. The plunger of the third syringe will hit a stop and the flow of solution will be stopped. Hitting the stop also triggers the acquisition of data from the reaction. The reaction is observed by passing a beam of monochromatic light of the appropriate wavelength through the cell by fibre optic cable. The light is passed through a photomultiplier and the change in voltage measured due to a change in absorbance of the solution is observed. The voltage/time signal is converted into absorbance/time automatically using the computer Software available.

Schematic Diagram of a Stopped-Flow Spectrophotometer

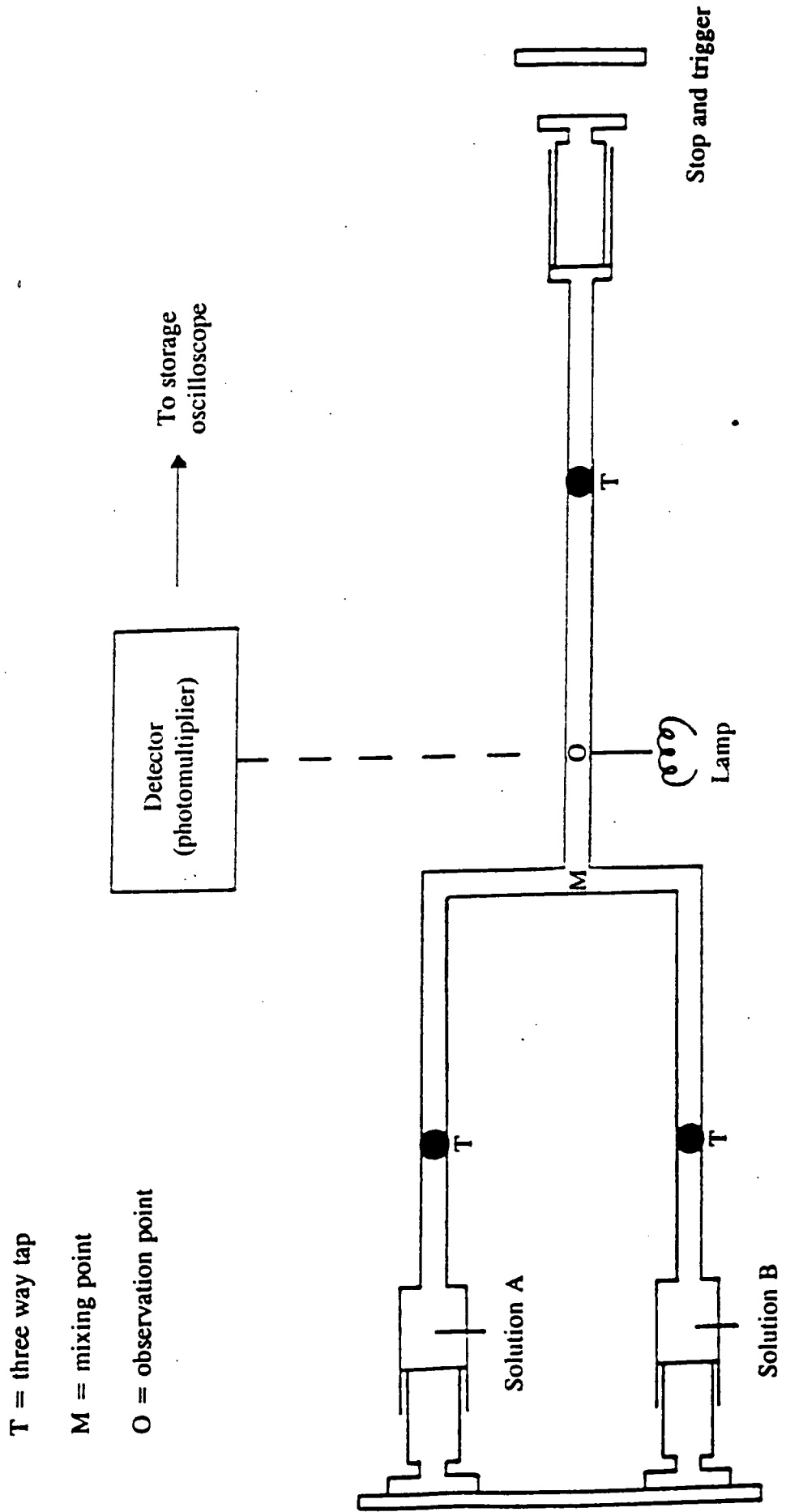


Figure 6.2.1.

6.3 Kinetic analysis

The halogenation kinetics were measured at a single wavelength by monitoring the absorbance due to the halogen. All reactions were carried out under conditions where the halogen was the limiting reagent. For halogenation reactions two kinetic scenarios were observed, first order and zero order. Sections 6.3.1 and 6.3.2 show the derivations of the kinetic equations used to analyse the kinetics. For the deuterium exchange experiments these were analysed using a sequential reaction scheme, section 6.3.3 shows the derived equations.

6.3.1 First order kinetics

For a first order process $A \longrightarrow B$, the rate of formation of product (B) or the disappearance of reactant (A) can be expressed by equation 6.3.1.

$$-\frac{d[A]}{dt} = \frac{d[B]}{dt} = k[A] \quad \text{Equation. 6.3.1}$$

Integration of equation 6.3.1 gives an expression for the observed first order rate constant, k_o (equation.6.3.2).

$$k_o = \frac{1}{t} \ln \frac{[A]_0}{[A]_t} \quad \text{Equation. 6.3.2}$$

Where $[A]_0$ and $[A]_t$ are the concentrations of A at times $t = 0$ and $t = t$ respectively.

Using the Beer-Lambert law ($A = \epsilon cl$, where A is the absorbance, ϵ is the molar extinction coefficient, c is the concentration and l is the path length) and assuming the path length to be 1cm expressions for the absorbance at $t = 0$ and $t = t$ can be derived (equations 6.3.3 and 6.3.4).

$$A_0 = \epsilon_A[A]_0 \quad \text{Equation. 6.3.3}$$

$$A_t = \epsilon_A[A]_t + \epsilon_B[B]_t \quad \text{Equation. 6.3.4}$$

Now as $[B]_t = [A]_0 - [A]_t$ substituting for $[B]_t$ into equation 6.3.4 gives:

$$A_t = \epsilon_A[A]_t + \epsilon_B[A]_0 - \epsilon_B[A]_t \quad \text{Equation. 6.3.5}$$

But $A_\infty = \epsilon_B[A]_0 = \epsilon_B[B]_\infty$ since $[B]_\infty = [A]_0$

Thus $(A_t - A_\infty) = \epsilon_A[A]_t - \epsilon_B[A]_t$

$$[A]_t = \frac{(A_t - A_\infty)}{(\epsilon_A - \epsilon_B)} \quad \text{Equation 6.3.6}$$

Similarly $A_0 = \epsilon_A[A]_0$, and $A_\infty = \epsilon_B[B]_\infty = \epsilon_B[A]_0$ and

$$(A_0 - A_\infty) = \epsilon_A[A]_0 - \epsilon_B[A]_0$$

$$[A]_0 = \frac{(A_0 - A_\infty)}{(\epsilon_A - \epsilon_B)} \quad \text{Equation. 6.3.7}$$

Substituting equations 6.3.6 and 6.3.7 into equation 6.3.2 gives:

$$k_0 = \frac{1}{t} \ln \frac{(A_0 - A_\infty)}{(A_t - A_\infty)} \quad \text{Equation. 6.3.8}$$

Rearranging gives:

$$\ln(A_t - A_\infty) = -k_0 t + \ln(A_0 - A_\infty) \quad \text{Equation. 6.3.9}$$

Therefore a plot of $\ln(A_t - A_\infty)$ against t is linear with a slope of $-k_0$. The infinity values A_∞ , were determined after a period of ten half lives and the change in absorbance was followed for at least two half lives.

For very rapid reactions that were followed using stopped flow spectrophotometry the software available allowed a computer fit to the data. The rate constants recorded were the average of at least ten runs (the applied photophysics machine allowed the averaging of kinetics traces so a single average rate constant could be recorded). The errors quoted on observed rate constant are the standard errors.

6.3.2 Zero order kinetics.

Under zero order conditions the rate of formation of product (B) and the rate of disappearance of reactants (A) is given by equation 6.3.10.

$$\frac{d[B]}{dt} = -\frac{d[A]}{dt} = k_0 \quad \text{Equation 6.3.10}$$

Equation 6.3.10 can be integrated to give equation 6.3.11.

$$[A]_t - [A]_0 = -k_0 t \quad \text{Equation 6.3.11}$$

using equations 6.3.6 and 6.3.7 (see first order derivation) gives the following equation.

$$k_0 t = \frac{(A_0 - A_\infty)}{(\epsilon_A - \epsilon_B)} - \frac{(A_t - A_\infty)}{(\epsilon_A - \epsilon_B)} \quad \text{Equation 6.3.12}$$

and:

$$k_0 t = \frac{(A_0 - A_t)}{(\epsilon_A - \epsilon_B)} \quad \text{Equation 6.3.13}$$

In all the kinetics studied the absorbance from the product was insignificant so that $\epsilon_A - \epsilon_B = \epsilon_A$, Hence equation 6.3.13 simplifies to equation 6.3.14.

$$k_0 t \epsilon_A = (A_0 - A_t) \quad \text{equation 6.3.13}$$

This shows that a plot of $(A_0 - A_t)$ versus time is linear with slope $\epsilon_A k_0$. The extinction coefficient is known or has been measured for all three halogen studied hence k_0 can easily be determined from the slope. For the earlier zero order results that were obtained on a Hi-Tech machine it was necessary to convert the voltage reading to absorbance using the following equations.

$$A_t = \log_{10} \left(\frac{I_0}{I_t} \right) \quad \text{equation 6.3.14}$$

and;

$$\frac{I_0}{I_t} = \frac{V_0}{V_0 - (\Delta V)_t} \quad \text{equation 6.3.15}$$

where:

I_t = Intensity of light transmitted at time = t.

I_0 = Intensity of light transmitted with no absorbing species present.

V_0 = voltage across the cell with no absorbing species present.

$(\Delta V)_t$ = voltage change in the after time = t.

Substituting 6.3.15 into 6.3.14 gives the following.

$$A_t = \log_{10} \left(\frac{V_0}{V_0 - (\Delta V)_t} \right) \quad \text{equation 6.3.16}$$

At time $t=0$ the voltage change is 0, therefore $\Delta V=0$ and $A_0=0$. Thus substituting equation 6.3.16 into 6.3.13 gives the following expression for the zero order rate constant.

$$k_o = -\frac{\log_{10}\left(\frac{V_o}{V_o - (\Delta V)t}\right)}{t \cdot \epsilon_A} \quad \text{equation 6.3.16}$$

Thus the k_o is calculated by measuring the voltage decrease over a given period of time (t).

6.3.3 Sequential reactions.

For a reaction $A \rightarrow B \rightarrow C$ the decrease in A is given by the following:

$$\frac{d[A]}{dt} = -k_1[A] \quad \text{equation 6.3.17}$$

hence:

$$\boxed{[A]_t = [A]_o e^{-k_1 t}} \quad \text{equation 6.3.18}$$

Thus the change in the concentration of A is given by a standard exponential expression (see section 6.3.1.). The rate of change of B is given by the following equation.

$$\frac{d[B]}{dt} = k_1[A] - k_2[B] \quad \text{equation 6.3.19}$$

substituting equation 6.3.18 gives the following;

$$\frac{d[B]}{dt} = k_1[A]_o e^{-k_1 t} - k_2[B]_t \quad \text{equation 6.3.20}$$

rearranging 6.3.20.

$$\frac{d[B]}{dt} + k_2[B]_t = k_1[A]_o e^{-k_1 t} \quad \text{equation 6.3.21}$$

This differential equation can be solved in the following way:

let,

$$[B] = C_1 e^{-k_1 t} + C_2 e^{-k_2 t} \quad \text{equation 6.3.22}$$

where C_1 and C_2 are constants. Differentiating 6.3.22 gives:

$$\frac{d[B]}{dt} = -k_1 C_1 e^{-k_1 t} - k_2 C_2 e^{-k_2 t} \quad \text{equation 6.3.23}$$

substituting 6.3.23 and 6.3.22 into 6.3.21 gives the following.

$$C_1 e^{-k_1 t} (k_2 - k_1) = k_1 [A]_0 e^{-k_1 t} \quad \text{equation 6.3.24}$$

thus;

$$C_1 = \frac{k_1 [A]_0}{(k_2 - k_1)} \quad \text{equation 6.3.25}$$

Substituting 6.3.23 into 6.3.21 gives the following.

$$k_2 [B] - C_1 k_1 e^{-k_1 t} - C_2 k_2 e^{-k_2 t} = k_1 [A]_0 e^{-k_1 t} \quad \text{equation 6.3.26}$$

At $t=0$, $[B]=0$, therefore equation 6.3.26 becomes;

$$-C_1 k_1 - C_2 k_2 = k_1 [A]_0 \quad \text{equation 6.3.27}$$

the known value of C_1 , equation 6.3.25 can be substituted into 6.3.27 to give the value of C_2 ;

$$C_2 = \frac{k_1 [A]_0}{k_1 - k_2} \quad \text{equation 6.3.28}$$

The values of C_1 and C_2 can be substituted back into equation 6.3.22 to give an expression for the the concentration of B at time= t .

$$\boxed{[B]_t = \frac{k_1 [A]_0}{k_2 - k_1} (e^{-k_1 t} - e^{-k_2 t})} \quad \text{equation 6.3.29.}$$

The variation in C can be calculated from the mass balance equation.

$$[A]_0 = [A]_t = [B]_t + [C]_t \quad \text{equation 6.3.30}$$

Substituting equation 6.3.18 and 6.3.29 into equation 6.3.30 gives the following expression for the variation of C with time.

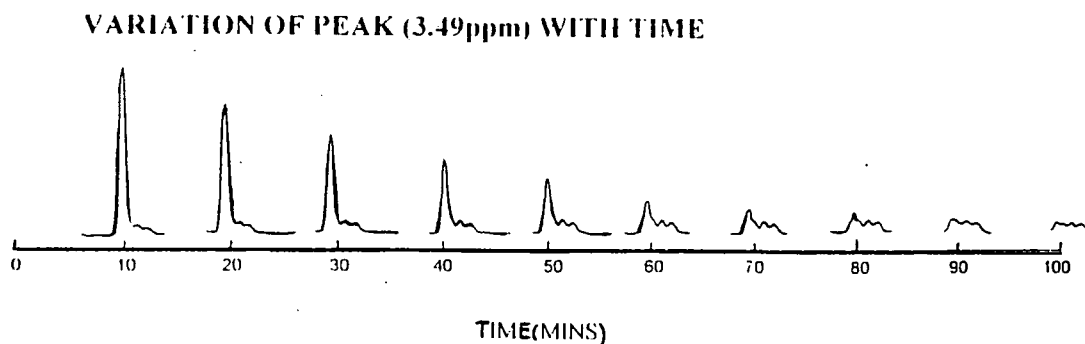
$$\boxed{[C]_t = [A]_0 \left[1 + \left(\frac{k_1 e^{-k_2 t} - k_2 e^{-k_1 t}}{k_2 - k_1} \right) \right]} \quad \text{equation 6.3.31}$$

Equation 6.3.18, 6.3.29 and 6.3.31 show the kinetic expressions for the concentrations A, B and C. These equations were used to fit the data obtained from the N.M.R. experiments which are described in section 6.4.

6.4 Nuclear Magnetic Resonance (N.M.R.)

N.M.R. kinetics were performed on a varian 400MHz spectrometer. The N.M.R. samples were prepared from thermostatted solutions immediately before the first spectrum was recorded. No temperature control was employed once the samples were in the spectrometer. The rates of reactions were too fast to allow the samples to be removed from the spectrometer and thermostatted between recording the spectra. The peak integrals were recorded for the relevant peak which composed of a signal due to $-CH_2$ and a signal due to $-CHD$. Figure 6.4.1 shows a typical kinetic run showing the variation in the methylene peak with time.

Figure 6.4.1



In most cases one peak of the CHD triplet was underneath the CH₂ singlet. In order to determine the CH₂ integral accurately it was necessary to split the integral up into a portion due to the CH₂ and a portion due to the CHD. The part of the CHD integral that was under the CH₂ was determined by dividing the separate CHD integral by two and taking this away from the CH₂ integral. The total CHD integral was calculated by multiplying the separate CHD integral by 1.5.

This kinetic N.M.R. technique is fairly inaccurate for a number of reasons:

1. The actual time at which the spectra are recorded is difficult to determine accurately.
2. The overlap between the CHD and CH₂ signals makes it necessary to extrapolate to determine the proportion of the CHD peak under the CH₂ peak.
3. The integrals have to be referenced against the ethyl ester peaks (in the case of ECA) or the methanol peak (in the case of CA) which may undergo slow exchange.
4. Slow hydrolysis of the ester group (in ECA) occurs. This is shown by the appearance of ethanol in the spectrum (this is only usually observed towards the end of a kinetic run).
5. No accurate temperature control is employed once the N.M.R. samples are in the spectrometer.

All the above factors ensure that the errors on the rate constants are relatively large.

6.5 pH Measurements

All pH measurements were carried out using a PTI-6 Universal digital pH meter (accurate to ± 0.02 pH units). The pH meter was calibrated over the range pH 4.0 to 7.0 or pH 7.0 to 10.0 depending on the solution to be measured. The pH of buffered solutions were checked before and after a reaction to ensure no change had taken place.

6.6 Diffusion controlled reactions¹

Throughout this work reference has been made to the diffusion controlled rate constant and a value of $5 \times 10^9 \text{ l mol}^{-1} \text{ sec}^{-1}$ has been used. This value is calculated in the following manner:

k_{en} for encounter of A and B is given by the following equation:

$$k_{\text{en}} = 4\pi L D_{\text{AB}}(r_{\text{A}} + r_{\text{B}}) \quad 1$$

where: D_{AB} = diffusion coefficient

L = Avogadro constant

$r_{\text{A}}/r_{\text{B}}$ = radii of A and B (treated as spheres)

The diffusion coefficient is related to the viscosity of the solvent by the following:

$$D_{\text{AB}} = \frac{kT(r_{\text{A}} + r_{\text{B}})}{6\pi\eta r_{\text{A}}r_{\text{B}}} \quad 2$$

where: η = viscosity of the solvent.

substitution of equation 2 into 1 gives the following:

$$D_{\text{AB}} = \frac{2RT(r_{\text{A}} + r_{\text{B}})^2}{3\eta r_{\text{A}}r_{\text{B}}} \quad 3$$

Using the approximation $r_{\text{A}} = r_{\text{B}}$ equation 3 simplifies to the following:

$$k_{\text{en}} = \frac{8RT}{3\eta} \quad 4$$

This very simple equation shows that the diffusion coefficient depends only on the viscosity of the solvent and the temperature, using a value of $\eta = 9 \times 10^{-4} \text{ Nm}^{-2}\text{s}$ for water at 25°C gives a value of $k_{\text{en}} = 7 \times 10^9 \text{ l mol}^{-1} \text{ sec}^{-1}$

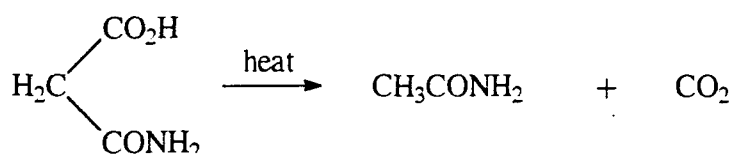
The derivation shown is only a crude approximation as no effect of molecular orientation in the collision is considered, however, k_{en} values measured are close to the value of $5 \times 10^9 \text{ l mol}^{-1} \text{ sec}^{-1}$ so it appears that the approximations are valid.

1.) J.H.Ridd, *Adv. Phys. Org. Chem.*, 1978, 16, 1.

6.7 Synthesis of malonamic acid

Malonamic acid was prepared according to the method of Vogel and Jeffries¹⁰.

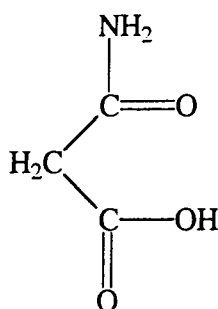
5g of ethylhydrogenmalonate (0.038M) and 8.33 cm³ of aqueous ammonia solution (d=0.89) were placed in glass stoppered flasks and cooled in a fridge at 4°C. The ammonia solution was added dropwise to the ethylhydrogenmalonate with constant stirring. The mixture was stoppered and placed in a fridge for 48 hours (at 4°C). After 48 hours the reaction was acidified dropwise with ice cold dilute sulphuric acid until the pH was *ca* 1-2. The product was extracted into 2-butanone and the solvent was dried with magnesium sulphate and evaporated under reduced pressure. White crystals formed as the final portion of the solvent was evaporated. The final product was dried on a vac line to remove the last traces of solvent. The product gave melting point 110°C (lit 121°C) after re-crystallisation from 3-pentanone. N.M.R. analysis of the re-crystallised product showed the presence of acetamide ($\delta=1.95\text{ppm}$) which was formed from the decarboxylation of malonamic acid, see below.



The method of re-crystallisation (from 3-pentanone) described by Vogel always produced significant amounts of acetamide and consequently was not used in further preparations, instead the product was simply washed with 3-pentanone (without heating) and the product was dried very slowly on an oven top. This less harsh treatment of the compound gave white crystals with mpt 116°C (lit 121°C) which showed no acetamide peak and gave the following elemental analysis.

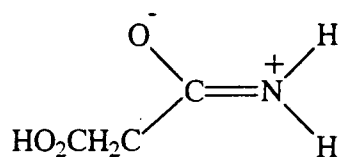
element	observed (%)	calculated(%)
carbon	13.73	13.59
hydrogen	35.32	34.95
nitrogen	4.89	4.85

Proton N.M.R. showed no acetamide impurity and gave the following peaks (see figure 6.7.1).



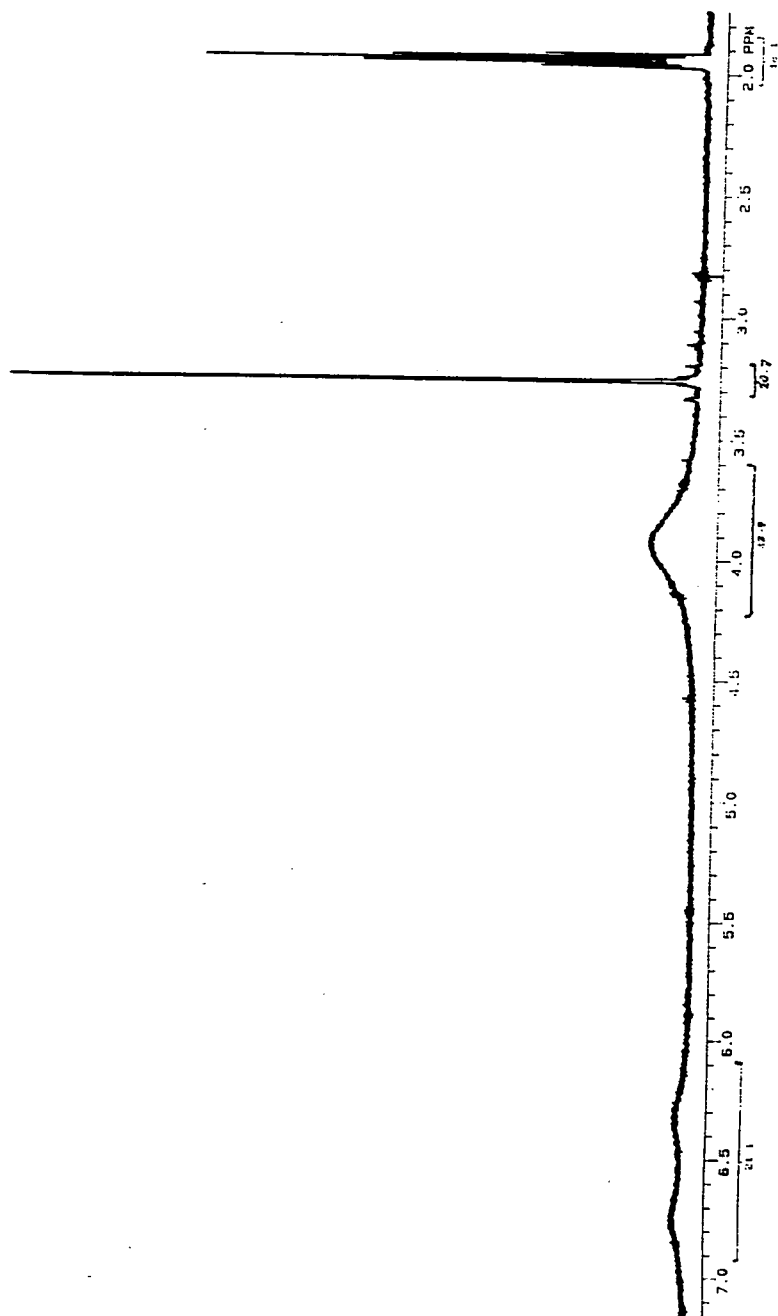
$\delta=3.27\text{ppm}$ 2H singlet
 $\delta=6.50\text{ppm}$ 2H broad doublet

The singlet at 3.27ppm is due to the methylene protons and the broad doublet at 6.50ppm is from the amide protons. The doublet arises from restricted rotation about the C-NH₂ bond caused by resonance with the C=O bond.



The carboxylic acid proton could not be observed due to exchange with water present in the N.M.R. solvent.

Figure 6.7.1
N.M.R. spectrum of malonamic acid in CD₃CN



APPENDIX

Research Colloquia, Seminars, Lectures and Conferences attended

A.1 First Year Induction Course (October 1992)

The course consists of a series of one hour lectures on the services available in the department and instruction on the use of the N.M.R. spectrometers.

1. Introduction, research resources and practicalities.
2. Safety matters.
3. Electrical appliances and hands on spectroscopic services.
4. Departmental computing.
5. Chromatography and high pressure operations.
6. Elemental analysis.
7. Mass spectrometry.
8. Nuclear magnetic resonance spectroscopy.
9. Glassblowing techniques.

A.2 Research colloquia, seminars and lectures arranged by Durham university chemistry department 1992-1995. (*denotes lectures attended)

1992

- October 15 Dr M. Glazer & Dr. S. Tarling, Oxford University & Birbeck College, London
It Pays to be British! - The Chemist's Role as an Expert Witness in Patent Litigation
- * October 20 Dr. H. E. Bryndza, Du Pont Central Research
Synthesis, Reactions and Thermochemistry of Metal (Alkyl) Cyanide Complexes and Their Impact on Olefin Hydrocyanation Catalysis
- * October 22 Prof. A. Davies, University College London
The Ingold-Albert Lecture The Behaviour of Hydrogen as a Pseudometal
- October 28 Dr. J. K. Cockcroft, University of Durham
Recent Developments in Powder Diffraction
- * October 29 Dr. J. Emsley, Imperial College, London
The Shocking History of Phosphorus
- November 4 Dr. T. P. Kee, University of Leeds
Synthesis and Co-ordination Chemistry of Silylated Phosphites
- * November 5 Dr. C. J. Ludman, University of Durham
Explosions, A Demonstration Lecture
- * November 11 Prof. D. Robins, Glasgow University
Pyrrolizidine Alkaloids: Biological Activity, Biosynthesis and Benefits
- November 12 Prof. M. R. Truter, University College, London
Luck and Logic in Host - Guest Chemistry
- November 18 Dr. R. Nix, Queen Mary College, London
Characterisation of Heterogeneous Catalysts
- * November 25 Prof. Y. Vallee, University of Caen
Reactive Thiocarbonyl Compounds
- November 25 Prof. L. D. Quin, University of Massachusetts, Amherst
Fragmentation of Phosphorous Heterocycles as a Route to Phosphoryl Species with Uncommon Bonding

- * November 26 Dr. D. Humber, Glaxo, Greenford
AIDS - The Development of a Novel Series of Inhibitors of HIV
- * December 2 Prof. A. F. Hegarty, University College, Dublin
Highly Reactive Enols Stabilised by Steric Protection
- * December 2 Dr. R. A. Aitken, University of St. Andrews
The Versatile Cycloaddition Chemistry of Bu₃P.CS₂
- * December 3 Prof. P. Edwards, Birmingham University
The SCI Lecture - What is a Metal?
- December 9 Dr. A. N. Burgess, ICI Runcorn
The Structure of Perfluorinated Ionomer Membranes

1993

- January 20 Dr. D. C. Clary, University of Cambridge
Energy Flow in Chemical Reactions
- * January 21 Prof. L. Hall, Cambridge
NMR - Window to the Human Body
- * January 27 Dr. W. Kerr, University of Strathclyde
Development of the Pauson-Khand Annulation Reaction : Organocobalt
Mediated Synthesis of Natural and Unnatural Products
- * January 28 Prof. J. Mann, University of Reading
Murder, Magic and Medicine
- February 3 Prof. S. M. Roberts, University of Exeter
Enzymes in Organic Synthesis
- February 10 Dr. D. Gillies, University of Surrey
NMR and Molecular Motion in Solution
- * February 11 Prof. S. Knox, Bristol University
The Tilden Lecture Organic Chemistry at Polynuclear Metal Centres
- February 17 Dr. R. W. Kemmitt, University of Leicester
Oxatrimethylenemethane Metal Complexes
- February 18 Dr. I. Fraser, ICI Wilton
Reactive Processing of Composite Materials
- February 22 Prof. D. M. Grant, University of Utah
Single Crystals, Molecular Structure, and Chemical-Shift Anisotropy

- * February 24 Prof. C. J. M. Stirling, University of Sheffield
Chemistry on the Flat-Reactivity of Ordered Systems
- * March 10 Dr. P. K. Baker, University College of North Wales, Bangor
'Chemistry of Highly Versatile 7-Coordinate Complexes'
- March 11 Dr. R. A. Y. Jones, University of East Anglia
The Chemistry of Wine Making
- March 17 Dr. R. J. K. Taylor, University of East Anglia
Adventures in Natural Product Synthesis
- * March 24 Prof. I. O. Sutherland, University of Liverpool
Chromogenic Reagents for Cations
- * May 13 Prof. J. A. Pople, Carnegie-Mellon University, Pittsburgh, USA
The Boys-Rahman Lecture Applications of Molecular Orbital Theory
- May 21 Prof. L. Weber, University of Bielefeld
Metallo-phospha Alkenes as Synthons in Organometallic Chemistry
- * June 1 Prof. J. P. Konopelski, University of California, Santa Cruz
Synthetic Adventures with Enantiomerically Pure Acetals
- June 2 Prof. F. Ciardelli, University of Pisa
Chiral Discrimination in the Stereospecific Polymerisation of Alpha Olefins
- June 7 Prof. R. S. Stein, University of Massachusetts
Scattering Studies of Crystalline and Liquid Crystalline Polymers
- June 16 Prof. A. K. Covington, University of Newcastle
Use of Ion Selective Electrodes as Detectors in Ion Chromatography
- June 17 Prof. O. F. Nielsen, H. C. Orsted Institute, University of Copenhagen
Low-Frequency IR - and Raman Studies of Hydrogen Bonded Liquids
- * September 13 Prof. Dr. A.D. Schlüter, Freie Universität Berlin, Germany
Synthesis and Characterisation of Molecular Rods and Ribbons
- September 13 Dr. K.J. Wynne, Office of Naval Research, Washington, USA
Polymer Surface Design for Minimal Adhesion
- September 14 Prof. J.M. DeSimone, University of North Carolina, Chapel Hill, USA
Homogeneous and Heterogeneous Polymerisations in Environmentally Responsible Carbon Dioxide
- September 28 Prof. H. Ila, North Eastern Hill University, India
Synthetic Strategies for Cyclopentanoids via Oxoketene Dithioacetals

- October 4 Prof. F.J. Feher, University of California, Irvine, USA
Bridging the Gap between Surfaces and Solution with Sessilquioxanes
- * October 14 Dr. P. Hubberstey, University of Nottingham
Alkali Metals: Alchemist's Nightmare, Biochemist's Puzzle and
Technologist's Dream
- * October 20 Dr. P. Quayle, University of Manchester
Aspects of Aqueous ROMP Chemistry
- * October 21 Prof. R. Adams, University of South Carolina, USA
Chemistry of Metal Carbonyl Cluster Complexes : Development of
Cluster Based Alkyne Hydrogenation Catalysts
- October 27 Dr. R.A.L. Jones, Cavendish Laboratory, Cambridge
Perambulating Polymers
- * November 10 Prof. M.N.R. Ashfold, University of Bristol
High Resolution Photofragment Translational Spectroscopy : A New
Way to Watch Photodissociation
- November 17 Dr. A. Parker, Rutherford Appleton Laboratory, Didcot
Applications of Time Resolved Resonance Raman Spectroscopy to
Chemical and Biochemical Problems
- * November 24 Dr. P.G. Bruce, University of St. Andrews
Structure and Properties of Inorganic Solids and Polymers
- November 25 Dr. R.P. Wayne, University of Oxford
The Origin and Evolution of the Atmosphere
- * December 1 Prof. M.A. McKervey, Queen's University, Belfast
Synthesis and Applications of Chemically Modified Calixarenes
- * December 8 Prof. O. Meth-Cohn, University of Sunderland
Friedel's Folly Revisited - A Super Way to Fused Pyridines
- * December 16 Prof. R.F. Hudson, University of Kent
Close Encounters of the Second Kind

1994

- * January 26 Prof. J. Evans, University of Southampton
Shining Light on Catalysts
- February 2 Dr. A. Masters, University of Manchester
Modelling Water Without Using Pair Potentials

- February 9 Prof. D. Young, University of Sussex
Chemical and Biological Studies on the Coenzyme Tetrahydrofolic Acid
- February 16 Prof. K.H. Theopold, University of Delaware, USA
Paramagnetic Chromium Alkyls: Synthesis and Reactivity
- February 23 Prof. P.M. Maitlis, University of Sheffield
Across the Border: From Homogeneous to Heterogeneous Catalysis
- * March 2 Dr. C. Hunter, University of Sheffield
Noncovalent Interactions between Aromatic Molecules
- March 9 Prof. F. Wilkinson, Loughborough University of Technology
Nanosecond and Picosecond Laser Flash Photolysis
- * March 10 Prof. S.V. Ley, University of Cambridge
New Methods for Organic Synthesis
- March 25 Dr. J. Dilworth, University of Essex
Technetium and Rhenium Compounds with Applications as Imaging Agents
- * April 28 Prof. R. J. Gillespie, McMaster University, Canada
The Molecular Structure of some Metal Fluorides and Oxofluorides: Apparent Exceptions to the VSEPR Model
- * May 12 Prof. D. A. Humphreys, McMaster University, Canada
Bringing Knowledge to Life
- * October 5 Professor N. L. Owen, Brigham Young University, Utah
Determining Molecular Structure - the INADEQUATE NMR Way.
- * October 19 Professor N. Bartlett, University of California
Some Aspects of (AgII) and (AgIII) Chemistry.
- October 26 Dr. G. Rumbles, Imperial College
Real or Imaginary 3rd Order Non-Linear Optical Materials.
- November 2 Dr. P. G. Edwards, University of Wales, Cardiff
The Manipulation of Electronic and Structural Diversity in Metal Complexes - New Ligands for New Properties.
- * November 9 Dr. G. Hogarth, University College, London
New Vistas in Metal Imido Chemistry.
- * November 16 Professor M. Page, University of Huddersfield
Four Membered Rings and B-Lactamase.

- * November 23 Dr. J. Williams, University of Loughborough
New Approaches to Asymmetric Catalysis.

- November 30 Professor P. Parsons, University of Reading
Applications of Tandem Reactions in Organic Synthesis.

- December 7 Professor D. Briggs, ICI and University of Durham
Surface Mass Spectrometry.

- * January 25 Dr. D. A. Roberts, Zeneca Pharmaceuticals
The Design and Synthesis of Inhibitors of the Renin-Angiotensin System.

- February 1 Dr. T. Cosgrove, Bristol University
Polymers do it at Interfaces.

- February 8 Dr. D. O'Hare, Oxford University
Synthesis and Solid State Properties of Poly- Oligo- and Multidecker Metallocenes.

- * February 15 Professor W. Motherwell, University College, London
New Reactions for Organic Synthesis.

- February 22 Professor E. Schaumann, University of Clausthal
Silicon- and sulphur-mediated ring opening reactions of epoxide.

- * March 1 Dr. M. Rosseinsky, Oxford University
Fullerene Intercalation Chemistry.

- April 26 Dr. M. Schroder, University of Edinburgh
Redox Active Macrocyclic Complexes: Rings, Stacks and Liquid Crystals.

- May 3 Professor E. W. Randall, Queen Mary and Westfield College
New Perspectives in NMR imaging.

- May 24 Dr. P. Beer, Oxford University
Anion Complexation Chemistry.

A.3 Conferences attended

International Union of Pure and Applied Chemistry

12th conference on physical organic chemistry, Padova, Italy, Aug 28- Sept 2, 1994

Poster presented: "Enol intermediates derived from carboxylic acid derivatives"

Third winter school in organic reactivity (WISOR-III), Bressanone, Italy, Jan 7-15, 1994.

Poster presented: "Enol intermediates derived from carboxylic acid derivatives"

Royal Society of Chemistry Organic reaction mechanisms Seminars:

SmithKline Beecham, Welwyn Garden City, September, 1993

Zeneca, Huddersfield, Yorkshire, September, 1994

Merck Sharp and Dohme, Harlow, Essex, September, 1995

